EARLINET:
A European Aerosol Research Lidar Network to Establish an Aerosol Climatology.

Contract EVR1-CT1999-40003

Scientific Report for the period February 2001 to January 2002.

April 2, 2002

Compiled by:

Jens Bösenberg
Max-Planck-Institut für Meteorologie
Bundesstr. 55
D-20146 Hamburg

Contents

Chapter 1

Management report

See separate report, e.g. at *http://lidarb.dkrz.de/earlinet*

Chapter 2

Executive summary

2.1 Objectives

The main objectives of EARLINET are the establishment of a comprehensive and quantitative statistical data base of the horizontal and vertical distribution of aerosols on the European scale using a network of advanced laser remote sensing stations, and the use of these data for studies related to the impact of aerosols on a variety of environmental problems. The main objectives for the reporting period were to complete data quality assurance, to operate the network to the largest possible extent, to establish a common data base, and to start data analysis.

2.2 Scientific achievements

The quality assessment has been completed with good success, as documented in detail in a special quality assessment report. This required a greater effort as initially foreseen, but all partners have provided the extra resources as required. The extra effort was necessary because several initial results showed clearly that better performance could be achieved by improving either the lidar system, the adjustment procedures, or the retrieval algorithm. Substantial progress was made by all groups on one or more of these areas. This is considered a great success of the exercise bringing EARLINET participants clearly ahead of other lidar groups.
An additional action has been launched and almost completed regarding the intercomparison of extinction retrieval algorithms. This was done to assure that results from different groups would be comparable, and to optimize the existing retrieval schemes. As for the other intercomparisons this turned out to be very useful and served to produce more homogeneous data sets.
The regularly scheduled measurements have been continued in a very satisfactory way, the number of profiles has increased substantially to about 3500 for this category at the end of the reporting period. The total number of files in the data base has increased to almost 9000, so the basis for more detailed statistical investigations is actually being established. Besides the climatological data set the special observations on Saharan dust outbreaks and on studies of the diurnal cycle are highly valuable and unique material for studies of the associated processes.
A data base structure that is suitable for automated processing has been established. A common platform independent file format is used, the files containing either profiles or time series of profiles are prepared and made accessible by the individual institutions. These files are collected in a common data base which is automatically updated every night. Automatic check procedures are installed to increase data consistency and compatibility. Controlled access to these data by all participants and

by approved external users is provided.
First data analysis demonstrates that the data are very useful and suitable for the intended purposes. Basic statistical properties like aerosol optical depth for selected layers, mean backscatter and extinction profiles and the boundary layer height can be derived for many stations. It is also possible to derive distribution functions and the annual cycle for these parameters. For selected stations statistical distributions for the extinction to backscatter ratio have been derived, a quantity that is important both for aerosol characterization and for future retrievals from spaceborne backscatter lidars.
Studies of Saharan dust outbreaks have been performed on the basis of selected cases, but the number of events with associated lidar measurements has increased substantially so that statistical investigations become possible as well. A true monitoring scheme has been established, including forecast and hence early warning, data collection from lidar stations and other relevant sources, and post-event data analysis based on satellite images, backtrajectories, meteorological fields, and lidar observations. The results show very clearly that Saharan dust is not constrained to the Mediterranean, long range transport e.g. across the Alps occurs more often than expected. It is only with height resolved measurements from lidar that unambiguous identification of corresponding dust layers is possible.
The data set for studies of the diurnal cycle of the aerosol distribution and controlling processes has been greatly extended, in particular by coordinated measurements at several stations. Standard patterns are recognized, apparently with some differences between urban and rural stations. This analysis will be refined, more observations will be made to increase the statistical significance of the results.
A first attempt has been made to study the modification of the aerosol load for air passing from the Atlantic Ocean over Britain and Northern Europe, based on a statistical approach using lidar profiles combined with trajectory analysis. The results show significant uptake of aerosol particles between the Atlantic and Central Europe, e.g. the aerosol optical depth increases from 0.05 to 0.3 on the way from the coast of Wales to east Germany. Details like the influence of ship traffic on the North Sea are likely to be identified from such studies. The method looks very promising, the data material appears very suitable for this purpose.
The development of methods to retrieve microphysical aerosol parameters from lidar observations has made very good progress. Algorithms are available that have been used successfully for the inversion of selected data sets. However, routine operation is not yet possible, because excellent data quality is necessary, and both backscatter and extinction measurements have to be provided for a large wavelength range. This is more than standard stations presently provide, but studies are being performed regarding the minimum requirements for a standard microphysical inversion. With the results from these studies it will be possible to define an ”optimized” lidar system. It is likely that this can be based on the use of a single laser source including frequency doubler and triplers, and on elastic plus Raman detection channels.
All other work packages are making good progress as well. However, results are still preliminary because it is only now that sufficient data become available.

2.3 Socio-economic relevance and policy implications

The main achievement so far is the installation of a network providing the aerosol vertical distribution based on homogeneous, quality controlled procedures. It is for the first time worldwide that such a network is established, and this contributes significantly to enhanced understanding of the aerosol distribution, the processes controlling it, and the impact of aerosol on human life.

Because aerosol plays a role in many atmospheric processes there is a large number of research areas that need to be addressed by special studies, not all of which are actually covered within EARLINET. To mention just a few:

- observations of the aerosol distribution allows to retrieve boundary layer characteristics, which in turn are most important for the distribution of pollutants.
- Studies of Saharan dust outbreaks allow to address directly the mechanisms of mineral dust formation, long range transport, and impact on solar radiation and climate. Using the particles as tracers also serves to study long range transport of many other pollutants.
- Observations of the modification of aerosol properties when air masses pass over Europe provide excellent material to improve air pollution and climate prediction models, and thus help to develop abatement strategies.
- Observations of elevated aerosol layers in combination with trajectory analysis permit to study long range transport of pollutants on a hemispherical scale. Again this is important material to improve air pollution and climate prediction models.
- The development of methods to retrieve microphysical properties of aerosol will lead to a much better characterization of the aerosol distribution, providing additional information about the composition and origin of the particles. This will help to identify major sources of aerosol and hence support the develpment of suitable abatement strategies.

Apart from the individual studies that have been initialized on the basis of the growing data set, an important achievement of the project is the establishment of a real network with fairly homogeneous operation and evaluation procedures and with comparable and well assessed data quality, despite of the different starting conditions for the participating groups. It also has to be emphasized that very good cooperation has been achieved. It is now standard that several groups perform coordinated measurements for special purposes, and that data from several groups are used for joint analyses. Thus a new community has been formed that is truly European, spanning a major part of the continent. It is particularly encouraging to see a large number of young scientists involved, demonstrating the transfer of know-how between different groups as well as between generations. EARLINET has turned out as an excellent training ground for the application of high-tech methodology to environmental prblems.

2.3.1 Plan for the next period

The last year of the current project will see continuous efforts to increase the data base by both regularly scheduled and special measurements. The routine and increased experience that has been achieved for all groups now will help to increase the number of measurements in parallel to the data analysis. Particular emphasis will be put on data interpretation in terms of the quantification of the aerosol load in different areas, identification of source regions, studies of long range transport, changes in aerosol load during the overpass over Europe, and Saharan dust impact in the Mediterranean and other European regions.
In case that the proposed extension of EARLINET to NAS-countries will be approved, three more stations will become operational which will follow the same measurement and evaluation procedures. This would enhance the value of EARLINET data in particular for the Eastern and South-Eastern regions, which are mostly downstrem from the industrialized areas of Europe, but are also

close to probably important source regions in Eastern Europe. In addition a modelling group would participate for further enhancing the analysis capabilities for Saharan dust outbreaks and possibly serving to generalize the results.

2.4 Conclusions

The project has made very good progress in many areas of research. An infrastructure has been developed that is truly unique worldwide. The selection of measurement methods, the extensive quality control, and the establishment of a common data base served to create an excellent basis for a wide range of scientific studies related to the vertical distribution of aerosols.
The strategy for setting up the network operation has proven successful, only minor modifications were necessary. The suitability of the collected data for the intended studies has been demonstrated. New methodology for the using the unique data set is being developed, first preliminary results have become available.
EARLINET and the institutions that are active within this project have contributed significantly to the making Europe the leader in a broad and important area of aerosol studies and related applications. The project has also contributed to strengthen the European capabilities in the trendsetting area of laser remote sensing of the atmosphere.
From development of the project in the first two years of operation it is expected that most of its goals can be reached and that important additional aspects can be treated.

2.5 List of publications

2.5.1 Peer reviewed articles:

Bösenberg, J., Ansmann, A., Baldasano, J., Balis, D., Böckmann, C., Calpini, B., Chaikovsky, A., Flamant, P., Hågård, A., Mitev, V., Papayannis, A., Pelon, J., Resendes, D., Schneider, J., Spinelli, N., Vaughan, T. T. G., Visconti, G., and Wiegner, M. (2000). EARLINET: A European Aerosol Research Lidar Network. In Dabas, A., Loth, C., and Pelon, J., editors, *Laser Remote Sensing of the Atmosphere. Selected Papers of the 20^{th} International Laser Radar Conference*, pages 155–158. Edition Ecole Polytechnique, Palaiseau.

Böckmann, C. (2001a). Hybrid regularization method for the ill-posed inversion of multi-wavelength lidar data in the retrieval of aerosol size distributions. *Appl. Opt.* , 40:1329–1342.

Chourdakis, G. and Papayannis, A. (2001). Analysis of the receiver response for a non-coaxial lidar system with fiber-optic output. *Applied Optics*, in press. Larchevque, G., I. Balin, R. Nessler, P. Quaglia, V. Simeonov,

H. van den Bergh, and B. Calpini (2002) Development of a multiwavelength aerosol and water vapor lidar at the Jungfraujoch Alpine Station (3580m ASL) in Switzerland *Appl. Optics*, in press.

Eixmann, R., Böckmann, C., Fay, B., Matthias, V., Mattis, I., Müller, D., Kreipl, S., Schneider, J., and Stohl, A. (2002). Tropospheric aerosol layers after a cold front passage in January 2000 as observed at several stations of the German Lidar Network. *Atmos. Res.*, in press.

Mattis, I., Ansmann, A., Müller, D., Wandinger, U., and Althausen, D. (2002). Dual–wavelength Raman lidar observations of the extinction–to–backscatter ratio of Saharan dust. *Geophysical Research Letters*, in press.

Papayannis, A., V. Amoiridis, J. Baldasano, J. Balin, D. Balis, A. Boselli, A. Chaikovsky, B. Chatenet, G. Chourdakis, V. Freudenthaler, M. Frioux, J. Herman, M. Iarlori, S. Kreipl, G. Larcheveque, R. Matthey, I. Mattis, D. Müller, M. Pandolfi, G. Pappalardo, J. Pelon, M.R. Perrone, V. Rizi, A. Rodriguez, L. Sauvage, P. Sobolewski, N. Spinelli F. de Tomasi, T. Trickl and M. Wiegner (2002) Continental–scale vertical profile measurements of free tropospheric Saharan dust particles performed by a coordinated ground–based European Aerosol Research Lidar Network (EARLINET project) *J. Geophys. Res.*, submitted.

Rocadenbosch, F., A. Comeron, and L. Albiol (2000) Statistics of the slope-method estimator. *Appl. Opt.* 39:6049–6057.

2.5.2 Others:

Balis, D., Zerefos, C., Amoiridis, V., Meleti, C., Bais, A., Kazantzidis, A., Papayannis, A., Chourdakis, G., Tsaknakis, G., and Trickl, T. (2001). Study of the aerosol effect on the UV-B irradiance at the Earths surface. Cases studies selected from urban sites in the frame of the EARLINET project. *Journal of Aerosol Science*, 32:391–392.

Barun, V., Bril, A., Kabashnikov, V., Popov, V., and Chaikovsky, A. (2001). Optimal regressions to estimate aerosol parameters by data of two- and three-wavelength laser sounding. In *Proceedings of SPIE, Eighth Joint International Symposium on Atmospheric and Ocean Optics. Atmospheric Physics, Irkutsk, 2001*.

Böckmann, C. (2001c). Runge-Kutta type methods for ill-posed problems. In *Proceedings of the International Conference on Mathematical Modeling and Scientific Computing, Ankara 2001*.

Böckmann, C., Müller, D., and Wandinger, U. (2001a). Microphysical Particle Properties from 3-Wavelength Raman Lidar. *Journal of Aerosol Science*, 32:393–394.

Böckmann, C., Wandinger, U., Ansmann, A., Bösenberg, J., Amiridis, V., Boselli, A., Delaval, A., Tomasi, F. D., Frioud, M., Iarlori, M., Komguem, L., Kreipl, S., Larcheveque, G., Matthias, V., Papayannis, A.,

Rocadenbosch, F., Schneider, J., Shcherbakov, V., and Wiegner, M. (2001b). EARLINET-Lidar Algorithm Intercomparison. *Journal of Aerosol Science*, 32:433–434.

Böckmann, C. and Wauer, J. (2001). The influence of spheroids on the inversion in the retrieval of microphysical particle parameters from lidar data. In *Proc. SPIE Intern. Soc. Opt. Eng., Japan, 2000*, volume 4015, pages 283–289.

Böckmann, C. (2002). Runge–Kutta–Type Methods for Ill-posed Problems and the Retrieval of Aerosol Size Distributions. *Proceedings in Applied Mathematics and Mechanics*, 1, in press.

A.Boselli, Ambrico, P. F., Amodeo, A., Amoruso, S., Armenante, M., Girolamo, P. D., Pandolfi, M., Pappalardo, G., Perrone, M. R., Serio, C., Spinelli, N., and Velotta, R. (2000). The INFM contribution to EARLINET, the European Aerosol Research Lidar Network. In *Abstracts of the INFMeeting 2000, Genova-Italy, July 2000*, page 242.

Chaikovsky, A., Dubovik, O., Holben, B., and Bril, A. (2001). Methodology to retrieve atmospheric aerosol parameters by combining ground-based measurements of multi-wavelength lidar and sun sky-scanning radiometer. In *Proceedings of SPIE, Eighth Joint International Symposium on Atmospheric and Ocean Optics. Atmospheric Physics, Irkutsk, 2001*.

De Tomasi, F., Guido, D., Pompa, P., Frassanito, M. C., Protopapa, M. L., and Perrone, M. R. (2001a). Simultaneous Measurements of Tropospheric aerosols and water vapor vertical profiles. *Journal of Aerosol Science*, 32:441–442.

De Tomasi, F., Perrone, M. R., Pompa, P. P., and Protopapa, M. L. (2001b). Lidar monitoring of tropospheric aerosols over the Sallentum peninsula (Italy). In *Proceedings of the Int. Symposium on Optical Science and Technology, San Diego (USA), 2001*.

Matthias, V., Bösenberg, J., Freudenthaler, V., Amodeo, A., Balis, D., Chourdakis, G., Comeron, A., Delavel, A., Tomasi, F. D., Eixmann, R., A. Hågård, A. H., Kreipl, S., Matthey, R., Mattis, I., Rizi, V., and Wang, X. (2001). Intercomparison of 15 aerosol lidar systems in the frame of EARLINET. *Journal of Aerosol Science*, 32:397–398.

Mattis, I., Müller, D., Ansmann, A., Wandinger, U., Forster, C., and Stohl, A. (2001). Major Saharan-dust outbreak observed with Raman lidar over Leipzig (Germany). *Journal of Aerosol Science*, 32:389–390.

Papayannis, A., Boselli, A., Calpini, B., Chaikovsky, A., Chourdakis, G., Cuomo, V., Frioux, M., Iarlori, M., Kreipl, S., Larcheveque, G., Matthey, R., Pappalardo, G., Pelon, J., Perrone, M., Rizi, V., Rocadenbosch, F., Sauvage, V., Sobolewski, P., Soriano, C., Spinelli, N., Tomasi, F. D., Amoiridis, V., Balis, D., and Trickl, T. (2001). Simultaneous observations of free tropospheric Saharan dust layers over Europe monitored by a co-ordinated ground-based lidar network in frame of the EARLINET project. *Journal of Aerosol Science*, 32:389–390.

Papayannis, A. et al. (2001). One-year observations of the vertical structure of Saharan dust over Athens, Greece monitored by NTUA's lidar system in the frame of EARLINET. In *Remote Sensing of Clouds and the Atmosphere VI, SPIE, Toulouse, France, 2001*, volume 4539.

Rocadenbosch, F., Soriano, C., Comeron, A., Baldasano, J. M., Rodriguez, A., Muñ oz, C., and Garcia–Vizcaino, D. (2001) 3D scanning portable backscatter lidar platform for atmospheric remote sensing: performance and architecture overview. *In Proceedings of the SPIE, Remote Sensing of Clouds and the Atmosphere V, Barcelona 2000.* 4168:158-169

Soriano, C., Rocadenbosch, F., Rodriguez, A., Muñ oz, C., Garcia–Vizcaino, D., Baldasano, J.M., and Comeron, A. (2001). Barcelona atmospheric monitoring with lidar: first measurements with the UPC's scanning portable lidar. *In Proceedings of the SPIE, Remote Sensing of Clouds and the Atmosphere V, Barcelona 2000.* 4168:170–181

Schneider, J., Balis, D., Böckmann, C., Bösenberg, J., Calpini, B., Chaikovsky, A. P., Comeron, A., Flamant, P., Freudenthaler, V., gård, A. H., Mattis, I., Mitev, V., Papayannis, A., Pappalardo, G., Pelon, J., Perrone, M. R., Resendes, D. P., Spinelli, N., Trickl, T., Vaughan, G., and Visconti, G. (2000). A European Aerosol Research Lidar Network to Establish an Aerosol climatology (EARLINET). *J. Aerosol Sci.*, 31:592–593.

Schneider, J. and Eixmann, R. (2000). Subvisible aerosol layers in the free troposphere: Lidar measurements and trajectory analysis.

Bösenberg, J. (ed.) (2000). EARLINET: Handbook of Instruments Internet publication on project page

C. Böckmann, D. Müller, and A. Chaikovsky (2001) Operational microphysical inversion algorithm Internet publication on project page

V. Matthias, C. Böckmann, V. Freudenthaler, G. Pappalardo, and J. Bösenberg (ed.) (2001). EARLINET: Quality Assurance Report Internet publication on project page

H. Linné (ed.) (2002) CD-ROM with aerosol data

I. Mattis (ed.) (2002) CD-ROM with trajectory data

Chapter 3

Progress of Work

Introduction

This chapter is organised strictly according to the structure of work packages as defined in the statement of work. No individual group reports are included. It is emphasized that all work package reports have been compiled using the input of a large number of individuals including all groups. It is considered a great advantage of this project that the work is performed in very close cooperation between many groups, with mutual benefits from the work of other partners. The disadvantage of course is that not always proper credit can be given to the individuals that have contributed. However, all these contributions are explicitly acknowledged here.

3.1 WP1, Hardware setup

by Jens Bösenberg

3.1.1 Objective

The main goal of this work package, the preparation of lidar systems at all sites for regularly scheduled operation as well as for special observations has already been reached about three months after the beginning of the project. However, to achieve a very early start for establishing an aerosol climatology over a long period of time some compromises had to be made regarding the technical properties of the systems which were quite different when the project was initialized. This was due to the fact that only previously existing systems were used. In the course of the project opportunities were taken to install a number of important upgrades.

3.1.2 Achievements

At almost all stations the lidar systems were ready for operation as scheduled. The details of the used instruments are described in the handbook of instruments which has been published in September 2000 and which is available at *http://lidarb.dkrz.de/earlinet*. Table 3.1 provides an overview over the present status of the hardware at the individual stations. Comparison with the status at the beginning of the project reveals that substantial progress has been made in the installation of Raman measurement capabilities which have turned out as the backbone of quantitative aerosol profiling. So far four additional stations have installed this important channel, two or three more may follow.

Fourteen stations presently have the possibility to determine true extinction profiles independently from backscatter profiles.

3.1.3 Plans for the next period

The work package is considered completed with very good success. As the last station Lisbon has started regular measurements, too. So far only few breakdowns of systems, mainly due to laser failure, occurred. Fortunately the institutions managed to organise a repair on their own expense in rather short time, so that the general status is still considered excellent. We are confident that this will be true for the future, too.

Station no.	ab	at	ba	gp	hh	ju	kb	la	lc	le	li	lk	mi	mi.2	mu	na	ne	pl	po	th
Detection channels																				
elastic backscatter																				
solar blind UV					u															x
UV	x	x		x	x	x	x	x	x	x		x	x	u	x	x	x		x	u
VIS		x	u	x	x	x	x			x	u		x	x	x		x	x	x	u
IR			x	x	x	x	x			x	x	u	x	x	x		x	x		
N_2 Raman scattering																				
solar blind UV					u															
UV	x	x			x	x	x	x	x	x		u		x	u	x	u		x	x
VIS			x			u	x			x					u			u		
water vapor channel	x				u	x	u	x	u	x										
temperature channel						u	x			x										
depolarisation channel					u	x	x			x							x	x		
scanning capability			x	x					u		x	x	x	x	x					x
system transportable			x	x	x						x	x			x		x			x
altitude limit low	0.5	0.5	.25	0.2	0.3	4.0	1.0	0.3	0.4	0.3	0.3	0.1	0.1	0.5	0.2	.25	1.0	0.5	1.2	0.7
altitude limit high	8.0	7.0	10.	10.	9.0	11.	35.	12.	7.0	12.	5.0	10.	30.	10.	5.0	3.0	10.	15.	8.0	8.0
range resolution (raw)	30	7.5	7.5	15	15	7.5	50	300	15	60	1.5	7.5	15	15	3.75	15	30	15	15	7.5
time resolution (raw)	330	360	1800	10	10	100	33	300	180	30	1	.1	10	200	0.1	60	200	10	60	240

Table 3.1: Overview over main system characteristics. x = existing, u = planned upgrade

ab	Aberystwyth	at	Athens	ba	Barcelona	gp	Garmisch-Partenkirchen	hh	Hamburg
ju	Jungfraujoch	kb	Kühlungsborn	la	L’Aquila	lc	Lecce	le	Leipzig
li	Lisboa	lk	Linköping	mi	Minsk	mu	München	na	Napoli
ne	Neuchâtel	pl	Palaiseau	po	Potenza	th	Thessaloniki		

3.2 WP2, Regular measurements

by Jens Bösenberg

3.2.1 Objective

The goal of this work package is the establishment of a comprehensive climatological database of the vertical distribution of aerosol over all stations of the network.

3.2.2 Scientific Achievements

The main achievement in the reporting period is that regularly scheduled measurements to establish the aerosol climatology have been performed at all stations, although with some differences in the resulting number of profiles. Mainly this is due to restrictions caused by weather (low clouds or precipitation), but some interruptions have been caused by other events, ranging from system breakdown over unavailability of personnel to blockage of premises by students on strike.

3.2.3 Plan for the next period

The regularly scheduled measurements will be continued as planned. It is expected that the performance of several stations will still improve with the personnel becoming better trained and the systems becoming better equipped for routine operation and evaluation.

3.3 WP3 Quality Assurance

This workpackage has been finished last year with a final report in September 2001. Here is a brief summary and some improvements which have been done since September.

3.3.1 Algorithm intercomparison

Backscatter algorithm intercomparison

Most of the lidar inversion algorithms are based on the methods given by [Klett, 1981, Klett, 1985, Fernald, 1984]. Because two unknowns, particle extinction and particle backscattering, determine the measured elastic backscatter signal, the algorithm considers a linear relationship between the extinction and the backscatter coefficient, the extinction-to-backscatter or lidar ratio. This input quantity is, in principle, unknown because it depends on the actual physical and chemical properties of the atmospheric particles. In addition, a reference value is needed for the inversion, which usually is set into a height region, where Rayleigh scattering dominates the measured signal. Rayleigh scattering is calculated from temperature and pressure values of a radiosonde ascent or a standard atmosphere. The synthetic data were generated with a sophisticated lidar simulation model. Three different data sets of elastic backscatter signals at wavelengths of 355, 532, and 1064 nm were simulated. A US standard atmosphere with a ground pressure of 1013 hPa and a ground temperature of 0 °C, a tropopause height of 12.0 km, and isothermal conditions above were assumed, see Fig. 3.1 (left). The signal profiles were simulated without signal noise. An incomplete overlap of laser beam and receiver field of view below 250 m was introduced.

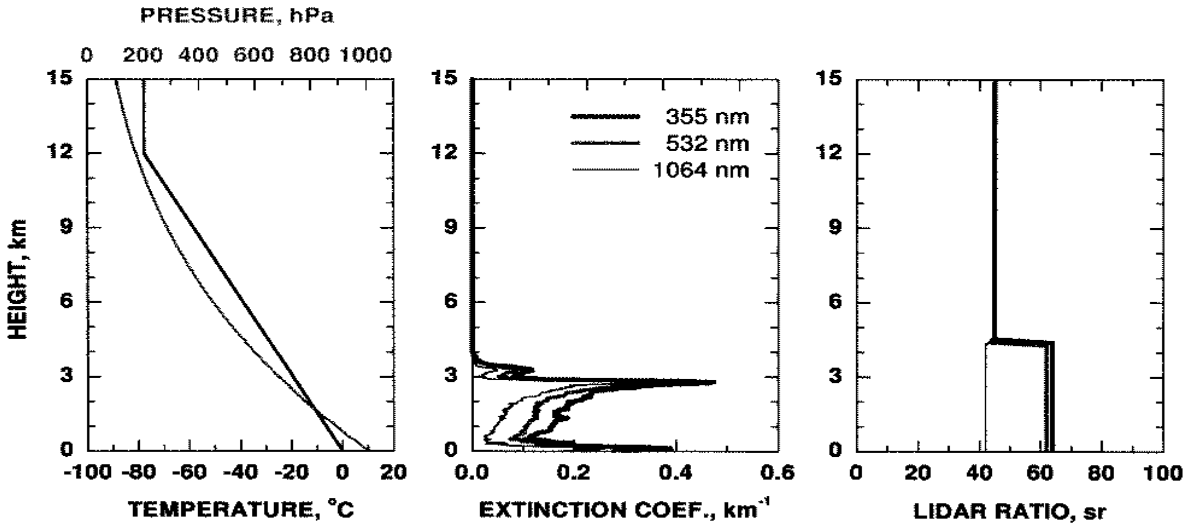

Figure 3.1: Input data for simulation example 2.

For the first example, the input profiles of extinction coefficient and lidar ratio were provided to the participants to allow an exercise with known solutions. In example 2, significant aerosol load up to 4000 m was simulated. A height-dependent extinction coefficient was assumed, see Fig. 3.1 (center). In addition, the extinction coefficient changed with wavelength, with highest values for the shortest wavelength and lowest values for the longest wavelength. The lidar ratio was height-independent in the aerosol layer, but took different values of 64 sr for 355 nm, 62 sr for 532 nm, and 42 sr for 1064 nm. Above 4500 m the lidar ratio was 45 sr for all wavelengths, see Fig. 3.1 (right).

	Lidar group	lidar ratio	integration direction	radio-sonde
A1	Lidar Group, École Polytechnique Fédérale de Lausanne, Switzerland	yes	yes	yes
A2	Observatory of Neuchâtel, Switzerland	yes	yes	yes
A3	Institut für Troposphärenforschung, Leipzig, Germany	yes	yes	yes
A4	Physics Department, National Technical University of Athens, Greece	yes	no	no
A5	Max-Planck-Institut für Meteorologie, Hamburg, Germany	yes	yes	yes
A6	Leibniz-Institut Kühlungsborn der Universität Rostok, Germany	yes	yes	yes
A7	Department of Physics, Università degli Studi, L'Aquila, Italy	yes	yes	yes
A8	Institute of Physics, National Academy of Sciences, Belarus	yes	yes	yes
A9	Laboratory of Atmospheric Physics, Aristotelian University of Thessaloniki, Greece	yes	yes	yes
A10	Meteorologisches Institut der Universität München, Germany	yes	yes	yes
A11	I.N.F.M. Napoli and Dipartimento di Scienze Fisiche Università di Napoli, Italy	yes	yes	yes
A12	Dipartimento di Fisica and I.N.F.M. Unità di Lecce, Italy	yes	yes	yes
A13	Fraunhofer-Institut für Atmosphärische Umweltforschung, Garmisch-Partenkirchen, Germany	yes	yes	no
A14	Universitat Politecnica de Catalunya, Barcelona, Spain	yes	no	no
A15	Institute Pierre Simone Laplace, Paris-Jussieu, France	yes	yes	yes
A16	Physics Department, University of Wales, Aberystwyth, United Kingdom	yes	yes	yes
A17	Istituto Nazionale per la Fisica della Materia, Potenza, Italy	yes	yes	yes
A18	Försvarets Forskninganstalt, Linköping, Sweden	yes	yes	yes

Table 3.2: Participating groups and their processing algorithms

In Example 3, significant aerosol load up to 3300 m was simulated. Realistic, height-dependent extinction coefficients and lidar ratios were introduced. The extinction coefficient varied quite differently with wavelength in different heights. The lidar ratio took values between 24 and 69 sr, but did not vary with wavelength. Above 3600 m the lidar ratio was again 45 sr. For all wavelengths see [Matthias et al., 2002].

The intercomparison was executed in three stages. The first stage was the most realistic and difficult one, because the input parameters were unknown. Therefore, not only the correctness and accuracy of the algorithm was tested, but also the experience in estimating the lidar ratio and choosing the reference value. In the second stage the lidar ratio was known, and in the third stage both input values were given to the participants. Thus, the final stage definitely tested the numerical correctness, i.e., the accuracy and stability of the algorithms. The results for example 2 for 532 nm are shown in detail in Fig. 3.2 as well as in the second and third column of Table 3.3 and 3.4. In the first stage the mean deviations from the correct solution are between 0% and 120%. Especially for the wavelength 355 nm the deviations are very large whereas with increasing wavelength the mean errors become smaller. The mean errors for all groups for the wavelengths of 355, 532, and 1064 nm are about 65%, 30%, see Fig. 3.2(a), and 15%, respectively. In the second stage with known lidar-ratio profil but still unknown reference value the mean deviations from the correct solution become visibly smaller and are approximately between 0% and 30% only. The mean errors for all groups for the wavelengths of

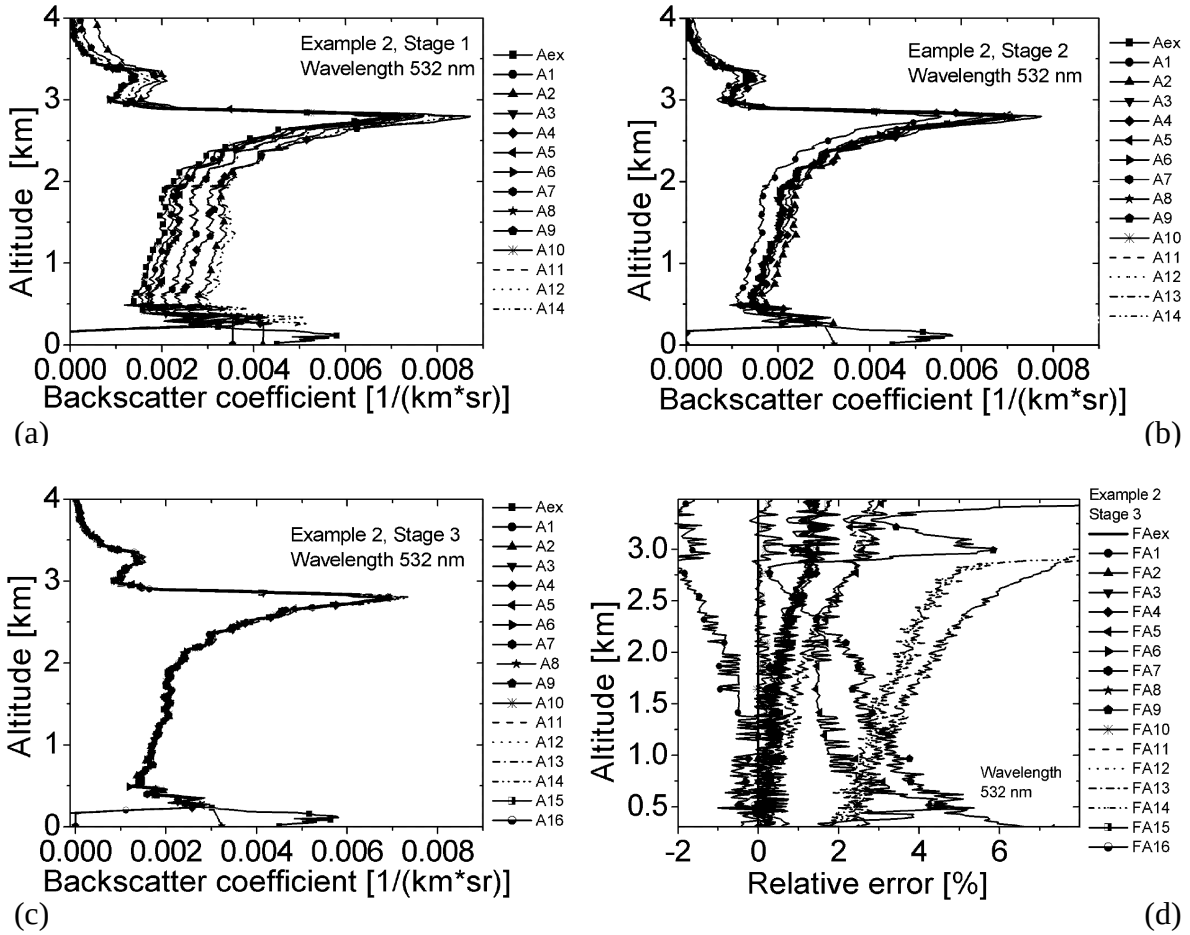

Figure 3.2: Retrieved particle backscatter-coefficient profiles at 532 nm in comparison to the simulation input profile of example 2 concerning the first (a), the second (b) and the third stage (c),(d).

355, 532, and 1064 nm are about 7%, 5%, see Fig. 3.2(b), and 8%, respectively.
The final stage is shown in Fig. 3.2(c),(d) in more detail including relative error profiles. First, with increasing knowledge on the input parameters (stages 2 and 3), the errors decrease well below 5% in almost all individual algorithms for all wavelengths in the range between 0.3075 and 3.4875 km. The mean error for all groups remains well below 2% for all wavelengths. Second, in the range from 3.5025 to 15.0675 km the mean absolute error for all groups is smaller than $1 \cdot 10^{-5}/(\mathrm{km} \cdot \mathrm{sr})$.
The results for example 3, which is a more realistic one with a height-dependent lidar ratio but still without statistical noise and without clouds, are shown in the fourth and fifth column of Table 3.3 and 3.4. For the stages 1 and 2 the mean errors are more or less in the same ranges as for example 2. In detail, the mean errors of all groups for the first stage for the wavelengths of 355, 532, and 1064 nm are approximately 40%, 20% and 17%, respectively. Moreover, for stage 2 the respective errors are about 10%, 8% and 7%. For the third stage the errors are somewhat larger than for example 2, which is mainly caused by the height-dependent lidar ratio. In the range between 0.3075 and 3.0075 km, see Table 3.3 and 3.4, the mean error for all groups remains well below 3% for all wavelengths. Second, in the range from 3.0225 to 15.0675 km the mean absolute error for all groups is smaller than $1 \cdot 10^{-5}/(\mathrm{km} \cdot \mathrm{sr})$.
The algorithm intercomparison showed that in general the data evaluation schemes of the different groups work well. Differences in the solutions can mainly be attributed to differences in the estimate

Stage 3: 532 nm				
	Example 2		Example 3	
Group	mean relative error [%] 0.3075-3.4875km	mean absolute error [1/(km · sr)] 3.5025-15.0675km	mean relative error [%] 0.3075-3.0075km	mean absolute error [1/(km · sr)] 3.0225-15.0675km
A1	0.91±0.72	9.68e-7±1.00e-6	1.36±0.39	1.24e-6±1.80e-6
A2	0.71±0.46	1.16e-7±6.13e-7	0.97±0.23	2.12e-7±1.33e-6
A3	0.62±0.47	2.24e-7±4.92e-7	0.88±0.28	3.32e-7±1.14e-6
A4	0.71±0.48	1.80e-7±5.69e-7	1.17±3.35	2.97e-7±1.28e-6
A5	2.34±1.07	9.97e-7±1.39e-6	2.24±0.66	1.29e-6±2.96e-6
A6	0.72±0.46	1.75e-7±6.20e-7	0.98±0.24	2.74e-7±1.36e-6
A7	0.71±0.46	1.13e-7±6.12e-7	0.97±0.23	2.11e-7±1.34e-6
A8	0.68±0.43	1.23e-7±5.92e-7	0.94±0.23	2.16e-7±1.28e-6
A9	2.90±1.59	5.54e-6±1.22e-5	2.88±3.41	7.31e-6±5.30e-6
A10	0.16±0.14	4.90e-7±4.61e-7	0.19±0.08	5.34e-7±5.04e-7
A11/A17	1.36±0.82	3.98e-7±1.24e-6	1.84±0.44	5.95e-7±2.57e-6
A12	0.70±0.44	1.27e-7±6.04e-7	0.95±0.23	2.14e-7±1.31e-6
A13	5.22±2.73	1.92e-5±1.15e-5	6.39±1.73	1.45e-5±1.65e-5
A14	4.54±2.78	3.44e-5±1.53e-5	5.45±1.78	3.49e-5±1.67e-5
A15	0.81±0.52	2.28e-6±1.91e-6	8.18±2.88	4.36e-6±7.19e-6
A16	0.63±0.46	1.98e-7±7.77e-7	0.90±0.25	3.57e-7±1.70e-6
A18	-	-	-	-
mean values	1.48	4.10e-6	2.27	4.18e-6

Table 3.3: Mean errors of both examples for the wavelength 532 nm in stage 3. The groups A1 to A18 can be identified as given in table 3.2.

of the input parameters. If the input parameters are known, remaining errors are of the order of a few percent. The unknown lidar ratio had the largest influence on the solutions. To overcome this problem, independent measurements of the particle extinction coefficient with the Raman method are or will be performed at most of the network stations.
Improvements have been made since the dissemination of the Quality Assurance report in September 2001. The Swedish group A18 finished the development of a suitable algorithm and delivered results for the wavelength 355 nm, see Table 3.4. Newly included in this table are also some improvements of the algorithms from groups A4 and A9 for 355 nm.

Stage 3: 355 nm				
	Example 2		Example 3	
Group	mean relative error [%] 0.3075-3.4875km	mean absolute error [1/(km · sr)] 3.5025-15.0675km	mean relative error [%] 0.3075-3.0075km	mean absolute error [1/(km · sr)] 3.0225-15.0675km
A1	1.54±0.91	1.72e-5±1.28e-5	1.01±0.85	1.85e-5±1.41e-5
A2	0.46±0.40	1.43e-7±5.42e-7	0.63±0.29	2.38e-7±1.24e-6
A3	0.45±0.38	3.94e-7±5.42e-7	0.60±0.30	4.94e-7±1.14e-6
A4	3.73±5.65	8.76e-7±2.56e-6	1.39±1.45	1.92e-6±4.73e-6
A5	1.84±2.14	3.91e-6±2.59e-6	1.51±0.79	4.14e-6±3.15e-6
A6	0.46±0.40	2.59e-7±5.20e-7	0.63±0.28	3.43e-7±1.22e-6
A7	0.46±0.40	1.41e-7±5.36e-7	0.63±0.28	2.34e-7±1.22e-6
A8	0.45±0.41	4.27e-7±6.52e-7	0.68±0.47	5.41e-7±1.34e-6
A9	5.57±3.25	2.18e-5±4.62e-5	5.34±3.86	2.89e-5±5.67e-5
A10	2.45±1.56	2.79e-5±2.08e-5	1.58±1.32	2.99e-5±2.26e-5
A11	2.25±1.21	2.28e-5±1.71e-5	1.86±1.21	2.44e-5±1.86e-5
A12	0.45±0.40	2.95e-7±5.76e-7	0.63±0.28	9.31e-7±2.17e-6
A13	4.82±1.85	4.41e-5±1.71e-5	3.76±2.14	3.15e-5±2.58e-5
A14	0.90±0.80	6.73e-5±3.76e-5	0.96±0.72	6.53e-5±3.81e-5
A15	0.48±0.42	2.32e-6±1.42e-6	12.88±8.27	7.44e-6±1.40e-5
A16	1.76±1.05	5.01e-6±4.27e-6	0.72±0.47	5.07e-6±3.81e-6
A18	3.66±0.62	6.65e-6±4.85e-6	3.11±0.72	6.46e-6±5.64e-6
mean values	1.87	1.30e-5	2.23	1.33e-5

Table 3.4: Mean errors of both examples for the wavelength 355 nm in stage 3

Raman algorithm intercomparison

The main goal of the Raman algorithm intercomparison is to test the correctness and accuracy of the algorithms used by each group for the retrieval of the aerosol extinction profile starting from nitrogen Raman lidar signals. For this purpose, synthetic lidar signals were calculated with the IfT lidar simulation model and two different signals, one with a shot noise for 10000 and the other with a shot noise for 1000 laser pulses, were simulated. The results of this intercomparison are reported in the final quality assurance report. In order to draw attention to special problems in the analysis of Raman lidar data, such as appropriate averaging and error determination two further cases with different degree of difficulty have been prepared:

Case 2: The second case represents the same simple step-wise changing extinction profile as for case1, but in this case a series of 15 profiles, with 3600 laser shots each, were simulated.

Case 3: Case 3: In the third case, a series of 20 profiles corresponding to 3600 laser shots each, with an abrupt change of aerosol properties after the first 10 profiles, were simulated.

A1	JUNGFRAUJOCH	Sliding average
A2	NEUCHATEL	Sliding average
A3	LEIPZIG	Sliding linear least-squares fit
A4	ATHENS	Sliding average filter and polynomial fit
A5	HAMBURG	Sliding average
A6	KUEHLUNGSBORN	Binning
A7	L'AQUILA	2^{nd} order digital filter Savitzky-Golay
A9	THESSALONIKI	Least-square fit
A11	NAPOLI	Sliding linear fit
A12	LECCE	Sliding linear least-squares fit
A16	ABERYSTWYTH	Linear and quadratic fit
A17	POTENZA	Sliding linear least-squares fit
A20	POTSDAM	Kaiser filter for data smoothing

Table 3.5: Participating groups and the used averaging procedure in Raman algorithm intercomparison

In table 3.5, the groups which participated in the intercomparison for the extinction retrieval are listed with the indication of the used algorithm. For case 2, each group has been asked to provide solutions and error values for three different temporal averages of 10, 20, and 30 minutes with a maximum statistical error of 10% in the 500-2000 m height range. Hence, all participating groups had the opportunity to test their own algorithm in terms of different averaging in time and space and of error evaluation. Results obtained for case 2 (30 minutes) are reported in figure 3.3. Figure 3.3a shows the results obtained by each group, while in figure 3.3b relative statistical errors are reported. All groups derived the extinction coefficient profile with statistical errors below 10% up to 2000 m of height as requested for case 2. Deviations between the results and the solution are always within 10% up to 2 km which is consistent with the statistical errors.
In case 3 no solution was provided and the intercomparison was really blind. The given record corresponds to a period of 40 minutes average and a jump in aerosol properties is present in the second 20 minutes. Each group has been asked to provide the mean aerosol extinction profile for the

entire time period with an error lower than 10% in the 500-2500 m height range. Because of this quite large and fast jump in the aerosol properties it is necessary to calculate the extinction profile for the two separate periods (first 20 minutes and second 20 minutes) and then calculate the mean extinction profiles for the 40 minutes period. This procedure takes the atmospheric variability into account and avoids a systematic deviation of about 10-15% due to the change in the extinction properties. Figure 3.4 shows the results of case 3. Each group has correctly considered the atmospheric variability and good agreement can be found between the solution and each profile. Almost all statistical errors are less than 10% up to 2500 m and just few points are above this limit. In this case deviations from the solution in the region up to 2.5 km are within 10% for most groups. The height region around 1 km where a large stepwise change in the extinction profile is present has been excluded for the calculation.

Summarizing it can be said that the extinction determination can be done with good accuracy, in most cases the mean deviations were not larger than the statistical error. Additional simulations for the determination of aerosol backscatter from Raman and elastic measurements as well as for a different wavelength (355 nm) are planned in the next future.

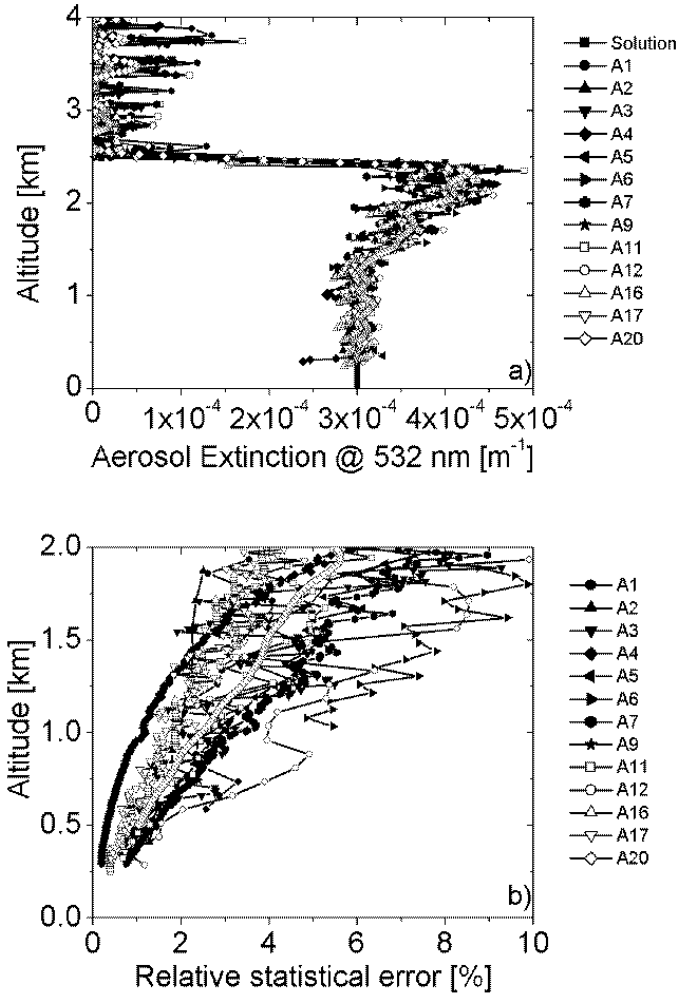

Figure 3.3: Results of case 2 for each lidar station, corresponding to 30 minutes average (54000 laser shots): comparison with the given solution (a), relative statistical error (b).

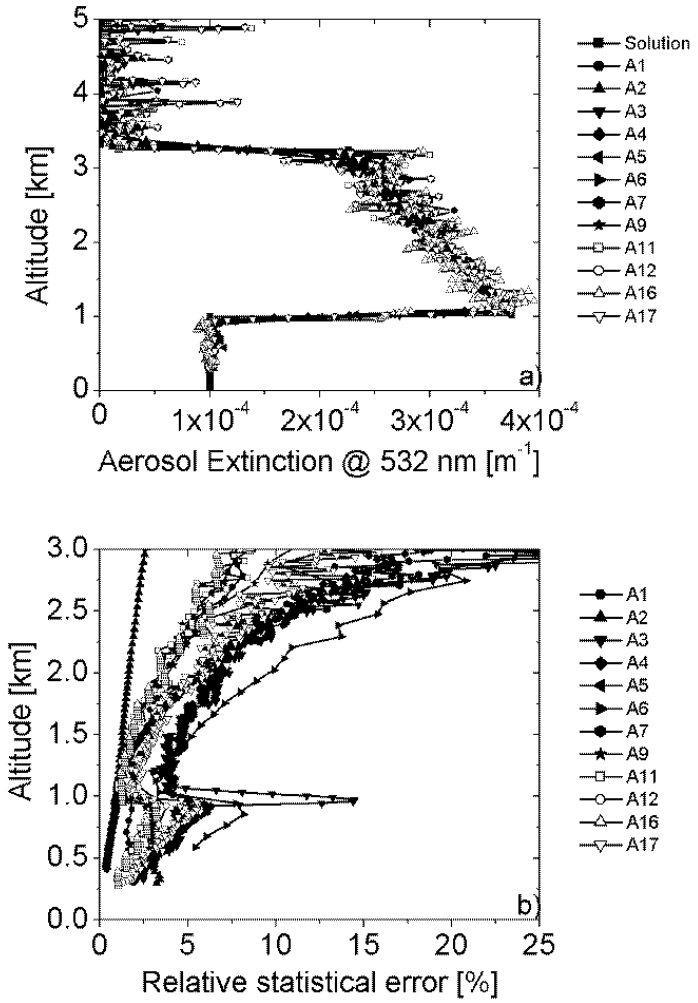

Figure 3.4: Results of case 3 for each lidar station, corresponding to 40 minutes average (72000 laser shots): comparison with the given solution (a), relative statistical error (b).

3.3.2 System intercomparisons

The system intercomparisons have been completed in August 2001 and all details can be found in the QA document. The whole set of intercomparison experiments turned out to be a good and hard test for all systems. In several cases improvements of the systems could be done after the measurements. Many of the existing problems would have certainly not been detected without the intercomparison measurements. Besides that in almost all cases a high quality of the measurements could be stated and the predefined goals could be reached. Figure 3.5 gives the deviations and standard deviations in the PBL for all aerosol backscatter intercomparisons reported here. Almost all values are well within the given 20 % limits, most of them even within $\pm 10\%$. Only two cases have significantly higher deviations in the atmospheric dust layer. However those cases are connected with low aerosol load and the absolute deviations stay well below the allowed value of $5 \cdot 10^{-7} (\mathrm{m} \cdot \mathrm{sr})^{-1}$.

The standard deviations exceed in some cases the predefined 25 % margin. Again these cases are

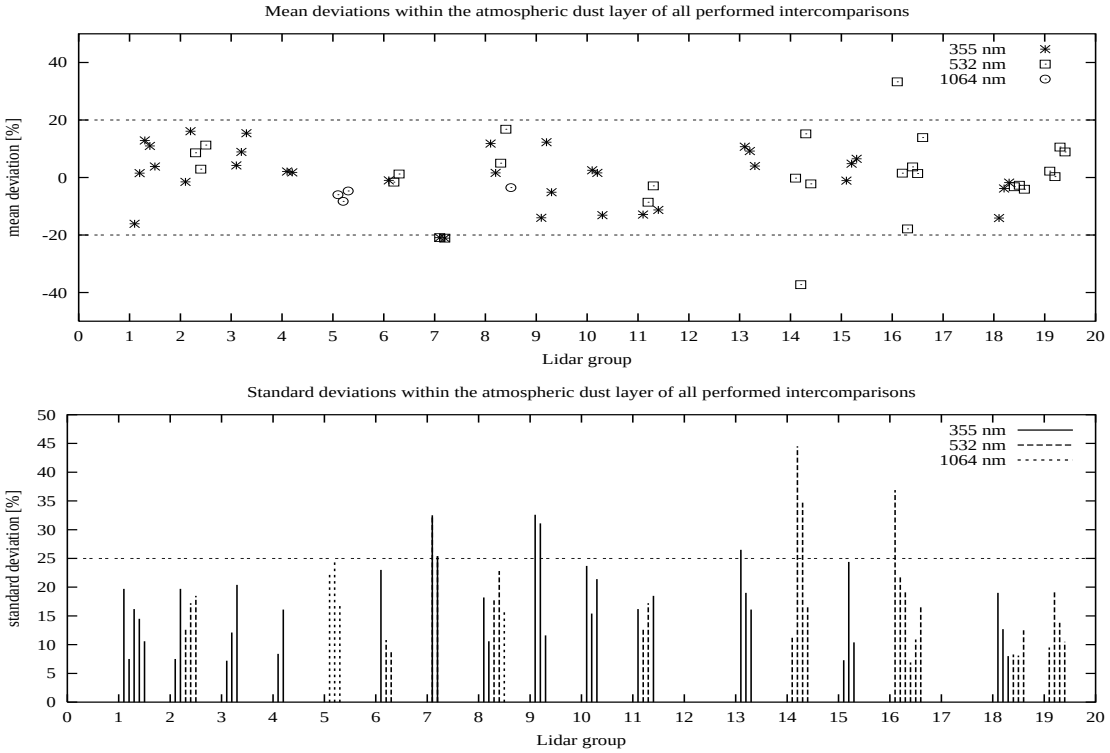

Figure 3.5: Mean deviations and standard deviations of all aerosol backscatter intercomparisons in the dust layer. 1: MPI, 2: MIM, 3: UABER, 4: NTUA, 5: UPC, 6: IFU, 7: EPFL, 8: IAP, 9: ULAQ, 10: INFM(L), 11: IFT, 12: IST, 13: FOA, 14: IPNANB, 15: INFM(N), 16: OCN, 17: LMD, 18: INFM(P), 19: AUTH.

generally connected with low aerosol load and the absolute deviations are still acceptable. Overestimation of the errors sometimes occurs if small differences in height have been detected. The used point to point calculation of the differences can lead to quite high differences if strong gradients occur in the aerosol profile.

The absolute deviations between all compared profiles in regions with low aerosol are displayed in figure 3.6. Here mean deviations stay in almost all cases below $2 \cdot 10^{-7} (\mathrm{m} \cdot \mathrm{sr})^{-1}$ and this value holds also for the standard deviation. In those cases where higher standard deviations have been detected, higher averaging, especially in height, would lead to lower fluctuations. Since usually no aerosol structures have to be resolved in the free troposphere, this is an appropriate procedure to increase the

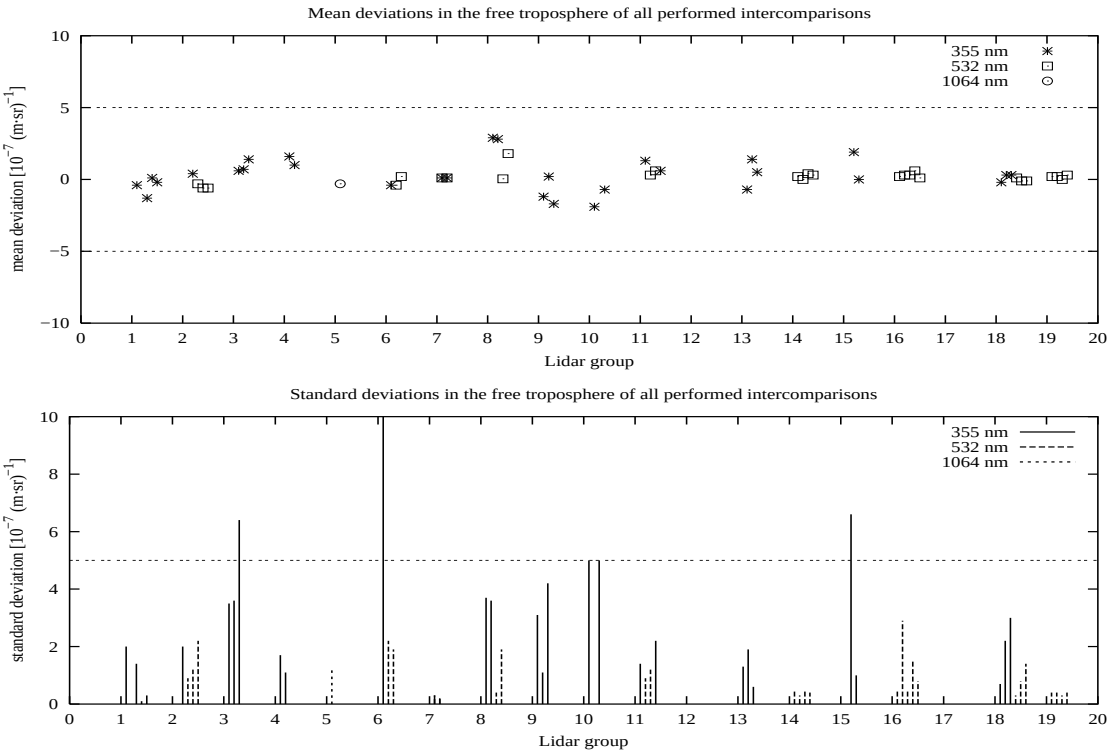

Figure 3.6: Mean deviations and standard deviations of all aerosol backscatter intercomparisons in the free troposphere. 1: MPI, 2: MIM, 3: UABER, 4: NTUA, 5: UPC, 6: IFU, 7: EPFL, 8: IAP, 9: ULAQ, 10: INFM(L), 11: IFT, 12: IST, 13: FOA, 14: IPNANB, 15: INFM(N), 16: OCN, 17: LMD, 18: INFM(P), 19: AUTH.

data quality in higher altitudes.
Intercomparisons of aerosol extinction profiles could only be done in one case because only the MPI lidar is transportable *and* equipped with Raman channels. The second transportable Raman lidar, from Leipzig, was not available for intercomparison experiments. The effort to move the MPI system is much higher than for the one from Munich, therefore the Munich system was chosen to travel to Italy where all systems have Raman channels but none of them is transportable. The extinction profiles measured by MPI and UABER in May 2001 showed good agreement although the calculated standard deviation is 35 % in one case. The allowed absolute limits were nevertheless not exceeded. Two groups, LMD Palaiseau and IST Lisbon, had to repeat the system intercomparisons due to hardware problems during the measurements carried out in September 2000 in Palaiseau. The LMD system has been modified and first intercomparison measurements with the LMD microlidar show promising results. It is planned to perform further measurements in spring 2002 and compare the microlidar afterwards to the Neuchâtel lidar.
The group from IST Lisbon has upgraded their system by emitting an additional wavelength (now 532 nm and 1064 nm) and made a complete new installation into a van. They will repeat their intercomparison measurements by travelling to Barcelona and comparing to the system from UPC also in spring 2002.

3.4 WP4, Compilation of trajectory data

by Ina Mattis

3.4.1 Objectives

Atmospheric trajectories provide information on the origin of observed aerosols. Thus they are a very useful tool for the interpretation of measured profiles of aerosol optical properties.
In the framework of EARLINET trajectories are used for the identification, interpretation, and prediction of long-range aerosol transport events (WP7), for studying air-mass modification processes over the European continent (WP9), for the analysis of source regions (WP16), and for investigations concerning the differences between urban and rural aerosols (WP12). In addition analytical trajectories can be used not only for the interpretation of special events, but also to perform climatological studies on the relationship between aerosol profiles and the origin of the observed air masses.

3.4.2 Methodology

The atmospheric trajectories, which are used for the EARLINET project, are calculated by the German Weather Service (DWD) for all EARLINET lidar sites for six arrival pressure levels and for two arrival times per day. The latter correspond approximately to the times of the routine lidar observations at noon and at sunset. The analytical as well as the prognostic trajectories are 4-day backward trajectories and are available since May 2000 for all EARLINET participants. The trajectories are stored in a data base at IfT Leipzig. All EARLINET partners have access to the trajectory archive via an interactive web page (http://earlinet.tropos.de:8084).
There is a cooperation between EARLINET and the group of Andreas Stohl (Technical University of Munich, Germany), whose trajectory model FLEXTRA provides a better and variable height and time resolution compared to the DWD model. Such detailed FLEXTRA trajectories are more appropriate for a comprehensive discussion of special events like Saharan dust outbreaks than the standard DWD trajectories.

3.4.3 Scientific achievements

For the Saharan dust outbreak of August 2-3, 2001, (see WP7) detailed FLEXTRA trajectories were calculated with an arrival-height resolution of 250 m and an arrival-time resolution of 3 hours for all 20 EARLINET lidar stations. During this very important event the dust layers covered almost the whole European continent for a period of several days. The trajectories are used for all lidar stations to identify the origin of the observed aerosol layers in the free troposphere and to distinguish Saharan dust layers from those of other sources, e.g., from aerosol layers due to the Etna eruption in the same time period.
As an example Figure 3.7 shows a time series of the backscatter coefficient at 532 nm observed at Leipzig. Two Saharan dust layers, each with an optical depth of 0.13 at 532 nm, could be observed. The first layer stretched from 6 to 10-km height. Later a second layer appeared between 3 and 6-km height. The colored symbols indicate the arrival heights and times of selected FLEXTRA-trajectories shown in Figure 3.8. The trajectories show that the aerosols within the layers were advected from arid regions of the African continent. In contrast, the trajectory arriving at 18 UTC in 3-km height

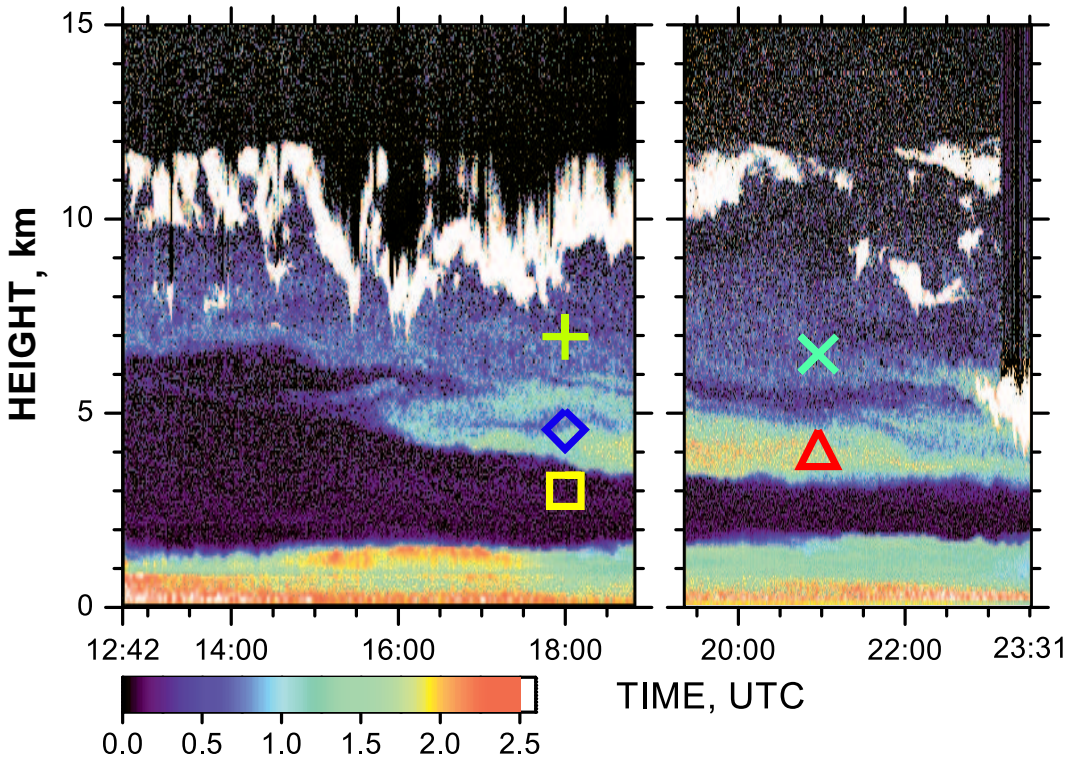

Figure 3.7: Time series of the particle backscatter coefficient at 532 nm in $Mm^{-1}sr^{-1}$ observed at Leipzig on August, 2–3, 2001. White colors indicate clouds. The symbols show the arrival heights and times of selected FLEXTRA-trajectories.

illustrates that the relatively clean region between the boundary layer and the Saharan dust layer originated from the Atlantic Ocean.

3.4.4 Plan and objectives for the next period

In the final year of the project the use of the trajectory data base by other workpackages is expected to increase. As an example, the spatial distribution of Saharan dust layers will be studied on the basis of all EARLINET data observed between 2–4 August, 2001, and between 11–16 October, 2001, which represents another huge outbreak of Saharan dust. In addition to the statistical analysis of the complete data set of the obtained aerosol profiles in a climatological sense (WP14), a combined statistical analysis of trajectories and lidar profiles will be performed.

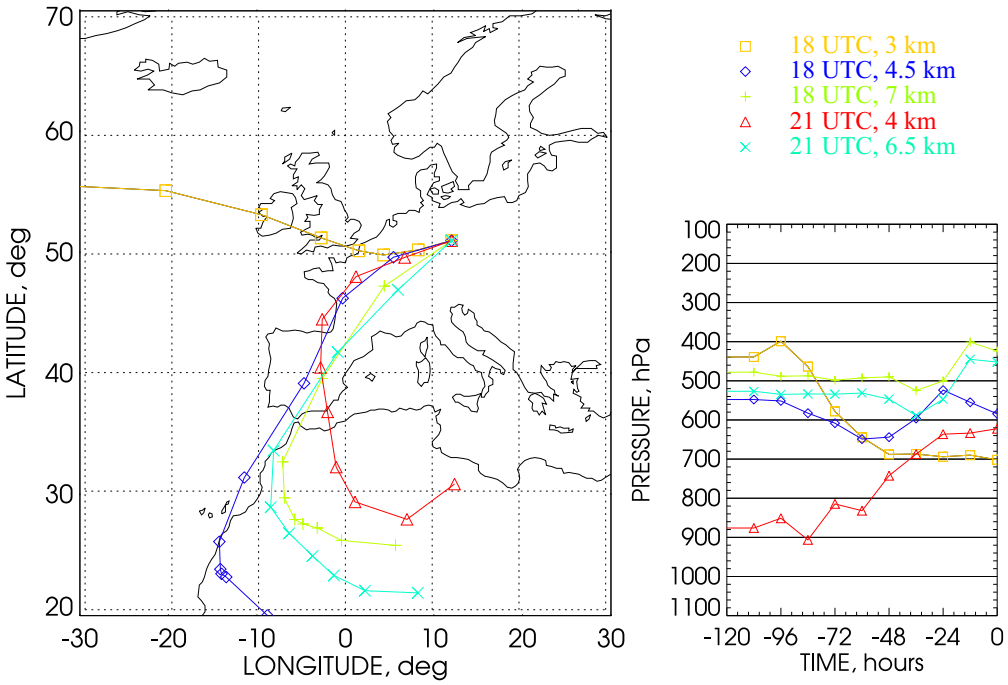

Figure 3.8: FLEXTRA trajectories, arriving at Leipzig, on 2 August 2001. Arrival times and heights are given in the legend.

3.5 WP5, Compilation of aerosol profile data

by Holger Linné

3.5.1 Objectives

The goal of this work package is the establishment of a large data base on aerosol profiles in a way that allows for easy access and automated processing of the results from all different stations. Selection for special conditions should be possible, e.g. for climatology, Saharan dust events, forest fires, photochemical smog events, studies of the diurnal cycle, special stratospheric meeasurements, studies of the differences rural/urban aerosols, ”studies of the eruption of mount Etna, or files containing cirrus cloud observations.

3.5.2 Methodology

A statistical analysis of a large data set requires automated processing of files originating from many different stations. Therefore it is a crucial requirement that a common format is used by all parties. Netcdf was chosen as a platform-independent, self-describing format that offers sufficient flexibility for later additions as they become necessary. For ease of access all data files are collected in a single data base at MPI Hamburg, which is automatically updated every night from the data stored at the participating institutions. Selection for special conditions is made possible through special category files, in which al files from all sites belonging to one of the abovementioned categories are listed. These files are also updated automatically, so that at any time a complete list of measurements for selected conditions is available.

3.5.3 Scientific achievements

Until the end of this reporting period, February 2002, a total of 8811 files was collected in the data base. Substantially more files are already existing, but some minor problems with the formatting prevented them from being included by automated processing. This problem will soon be overcome. The number of climatology files, based only on the regularly scheduled measurements, is roughly 3500 presently. The number of files for studies of Saharan dust events is 1034. For both areas the EARLINET data base is by far the largest existing collection.

By automated check procedures it is verified that the data base is internally consistent. E.g. it is checked that measurement times and dates are meaningful, duration is not excessive, mandatory parameters can be retrieved, climatology files have been labeled correctly, etc. As can be expected for a large data base constructed from many individual contributions there are still some inconsistencies within the files. Through automated checking and notification of the data producers these inconstiencies are presently being removed or at least substantially reduced. It is considered a major achievement that two years after the start of the project a fairly homogeneous data base could be established from a large number of initially quite heterogeneous contributions. The data base is already very useful now, and it is expected that the usability will increase substantially in the near future. The tools that are necessary for the studies planned within the project are now existing, the content of the data base is continuously growing.

3.5.4 Plans for the next period

The collection of data will continue as scheduled. No major changes in the data format are forseen. Acces to the data for all partners and authorised external users will be maintained.

3.6 WP6, Temporal cycles

by Jacques Pelon

3.6.1 Objectives

In this work package the task performed is related to the analysis of observations of the aerosol properties in the lower troposphere and more particularly in the planetary boundary layer at different time scales. This encompasses the diurnal and seasonal cycle of aerosols in the boundary layer as it is controlled by solar and synoptic forcing.
It is reminded that temporal variations due to special events are not included in this work package. The analysis of the boundary layer height and extinction statistics is also part of WP14.

3.6.2 Methodology and scientific achievements

All groups but one are involved in this work package. The main focus of this WP is put on the aerosol in the planetary boundary layer (PBL). The terminology ”boundary layer” means the atmospheric layer directly coupled with the surface in a dynamical way over a diurnal cycle.
In our analysis we differentiate the residual layer and the active boundary layer formed during the day. The residual layer is a result of growth cycles over the previous days leading to an increased number of particles and pollutants in the upper atmosphere. As a result from the local scale dynamics, moistening and larger scale transport, aerosol properties are different in both layers helping characterising the difference between the various layers.
The strategy for the measurements needed within these WP has been discussed in detail during the Leipzig workshop in autumn 2001.
In this second year of the EARLINET programme, the focus has been set on the acquisition of new data sets and the consolidation of the methods of analysing lidar data from all stations. Several alerts have been set to include more cases of diurnal cycle observations. Observations made are summarised in Table 3.6.

Time series special IOPs	Simultaneous Diurnal Variation at European Scale for different seasons
IOP1 : 02 April 2001	Spring 1
IOP2 : 28 - 29 May 2001	Spring 2
IOP3 : 14 - 15 August 2001	Summer
IOP4 : 16 November 2001	Autumn
IOP5 : 3 & 4 January 2002	Winter
standard observations	statistical seasonal analysis
2000 - given time	

Table 3.6: Measurement types used in WP6

Let us first consider the daily cycle. The accumulation of the aerosol load during the day in the planetary boundary layer (PBL) is depending on the aerosol source itself (natural or man-made), surface wind speed (dynamic forcing), and solar flux (thermal forcing) leading to turbulence development. The vertical stability (linked to the potential temperature gradient) and synoptic forcing are critical to the development of the boundary layer, and may lead to an increase of aerosol particles

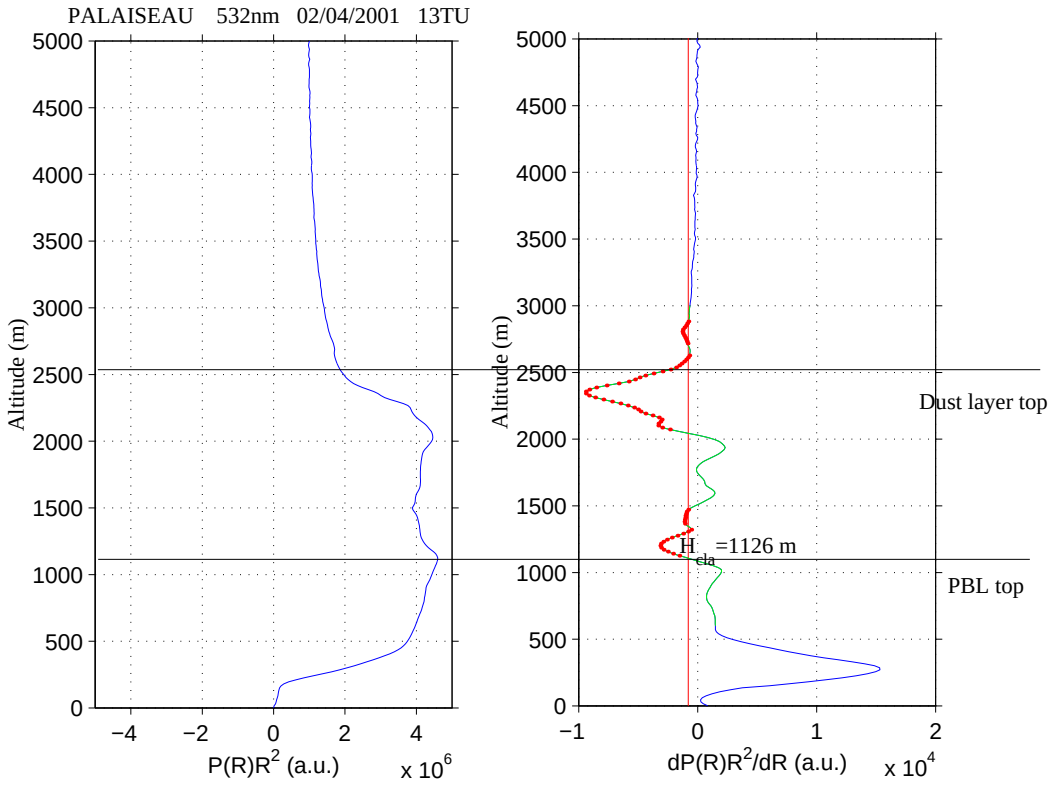

Figure 3.9: Left : Range corrected signal proportional to attenuated backscatter showing the increase in signal in the developed boundary layer observed during IOP 2 at Palaiseau. Right : First order derivative and determination of PBL and dust layers top heights from the analysis.

and pollutants when the growth of the boundary layer is blocked. The variation of the optical properties of the aerosols which is observed by lidar is further depending on moisture. The development of the boundary layer could thus be identical at different places or for several days, but the optical properties may differ. Periods of observations are related to unperturbed weather conditions, ideally in a high pressure system. This allows to favour simultaneous observations at different stations and quantify the behaviour of aerosol at the regional scale.

As the aerosol particles are accumulated in the lower layers, the PBL height can be deduced from the measurements using the first derivative filtered signal. This analysis also accounts for the retrieval of the residual layer (called dust layer) evidenced using the same method. An example is reported in Fig. 3.9 for IOP 2 observations at Palaiseau. The increase in signal in the lower altitude range is due to the overlap factor which may introduce a bias in the analysis One should be careful in the analysis not to ”miss” the true PBL height.

The PBL height is about 1000m and the dust layer at 2500 m. The bottom of the derivative and the top respectively correspond to these altitudes.

During the morning, the growing boundary layer is eroding the stable and residual layers of the previous night and day, respectively. This is illustrated by results reported in Figure 3.10. It is seen from Figures 3.9 and 3.10 that the development of the PBL requires to be detected to perfom measurements in the first hundreds of meters. This is a problem for lidar as the overlap factor may introduce a bias in wintertime analysis. This may be partly accounted for using a correction of the overlap function before taking the derivative.

First results have been presented at the Barcelona workshop last February on structural parameters

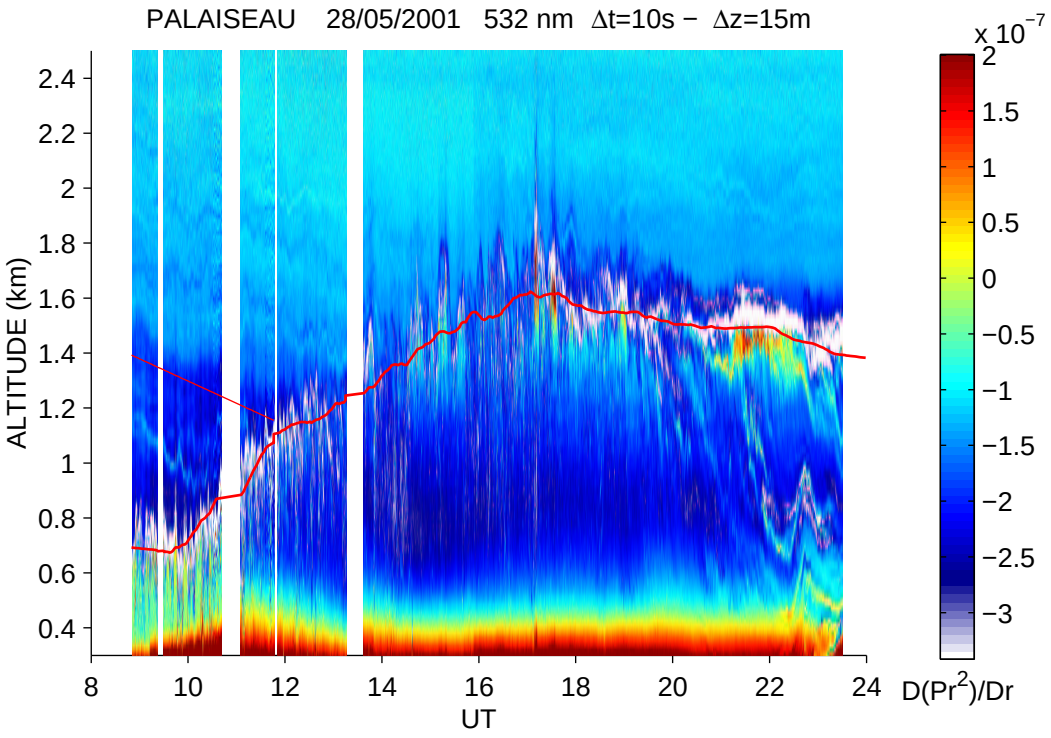

Figure 3.10: First order derivative signal and smoothed PBL height derived for IOP 2 observations made at Palaiseau. The straight line is indicating the observed decrease of the residual layer.

and optical properties of the boundary layer during time series and statistical analysis (in relation with WP14). The time series are complemented by the analysis of standard measurements performed at regular observation times. The same procedure is applied to the analysis of data in time series and standard observations.

An example of statistical results is reported in Fig. 3.11a. Data have been obtained at Hamburg from regular post sunset measurements. The boundary layer height obtained here is the one of the residual layer of the day which is well developed at the end of the day. It is seen that a seasonal increase in summer due to a larger heating of the surface can clearly be observed on the averaged data. Further analysis is to be made using the standard backscatter measurements performed at the different stations.

The strength of Earlinet is that backscatter measurements during daytime have been reinforced by Raman measurements before and/or after sunset. This avoids hypothesis to retrieve the extinction in the boundary layer and allows a survey of the evolution of extinction by particles in the PBL at several locations. An example is reported in Fig. 3.11b from observations made at Hamburg. Again a large dispersion is observed but an average distribution showing two peaks in spring and autumn can be observed. As observations are made after sunset, the reformation of the stable layer in the mixed PBL and the sedimentation of large particles may induce some additional effects to analyse in more details. This type of analysis is being done by the different groups involved in WP14 (statistical analysis) and WP6.

3.6.3 Socio-Economic relevance and policy implication

The daytime evolution of the boundary layer is of importance as it may lead to reinforced pollution events when dynamical forcing prevents its development. The accumulation of aerosols and pollu-

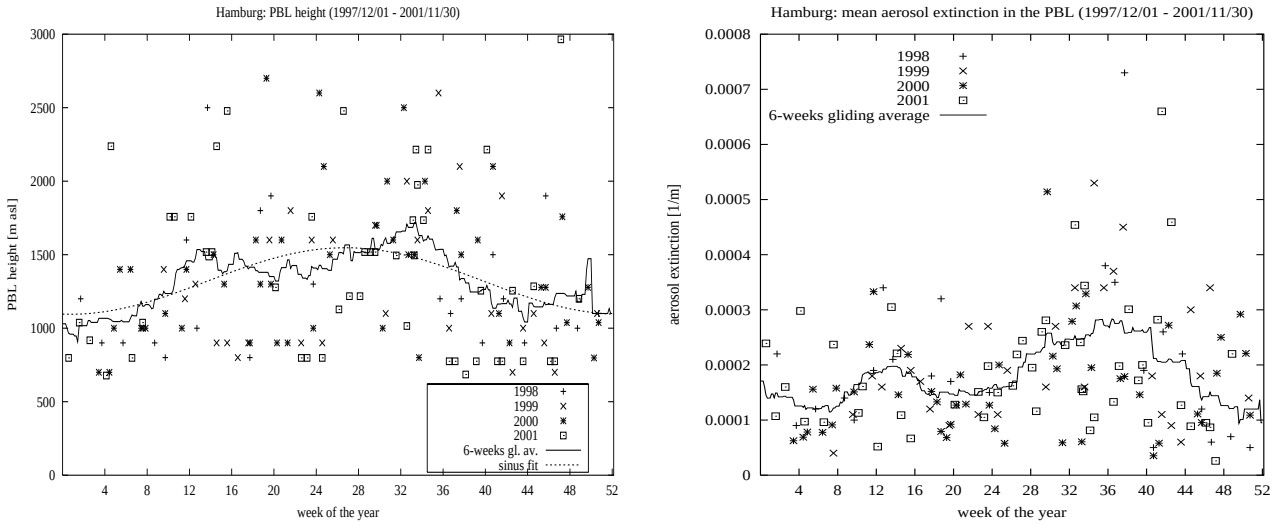

Figure 3.11: a) Evolution of the PBL top height as a function of the month of the year as analysed at Hamburg from the routine operation measurements using the first derivative analysis. b) Extinction coefficient measured after sunset in the PBL at Hamburg with Raman technique as a function of the week of the year.

tants is thus increased, and specific actions may be necessary, such as limiting car traffic or industrial activity to avoid health damage on population. It is not only affecting local areas but also has an impact at the regional scale. It is very important to forecast these events due to their impact. This can be derived from diurnal cycle analysis. The a posteriori control of large accumulation of particles can be made on a statistical basis from regular observations.

3.6.4 Discussion and conclusion

New data sets have been obtained in the frame of WP6 at several stations during the passed year. Several cases are being studied. In this phase, observations are analysed both in the groups and at IPSL using a standard approach to check data quality and procedures.

3.6.5 Plan and Objectives for the next period

Results have been presented after this second year at the Barcelona workshop. Coordinated observations at the european scale during favourable meteorological situations have been performed. This will be continued. The objective is to make three measurement series (a series is a diurnal cycle observed during a day) per season (as for example during the summer season June-July-August) at all stations involved. Quasi-continuous measurements are aimed at for the retrieval of the structural parameters. The time interval between profiles should be shorter than during the regular measurements (typically five minutes). However standard sequences of thirty minutes can be used. Specific addition of boundary and residual layer heights to the files archived in the ftp site will be made.

3.7 WP7, Observation of special events

by Alexandros Papayannis

3.7.1 Objectives

The main objectives of WP7 are focused on the implementation of a routine monitoring scheme, mainly in the South-European region for the observation of specifically high aerosol loads in the lower troposphere, resulting from extreme dust events (transport of Saharan dust, break of forest/industrial fires, intense photochemical smog episodes, volcano eruption etc.).

3.7.2 Methodology

To achieve the objectives of this WP, eight of the EARLINET lidar stations located in the Southern Europe (Portugal, Spain, France, Italy and Greece) have been selected to perform extra lidar soundings, under conditions of particularly high aerosol loads. The measurement frequency was initially set to 6-8 events/year, with 4-6 h measurements per event. Additional lidar stations were also selected in Central and Northern European sites (Switzerland, Germany, Poland, Belarus), to investigate on the long-range transport of Saharan dust aerosols across the European continent.
The coordination of the special lidar measurements was performed by the NTUA group, using forecasted Saharan dust events data available on the World Wide Web (http://forecast.uoa.gr), validation data from satellite measurements:
aerosol optical thickness data from NOAA/AVHRR at
http://psbsgi1.nesdis.noaa.gov:8080/PSB/EPS/Aerosol/data/aerday.html,
aerosol index data from the TOMS instrument at http://jwocky.gsfc.nasa.gov/ ,
visible images of Saharan dust storms from the SeaWIFS instrument at
http://seawifs.gsfc.nasa.gov/SEAWIFS/IMAGES/IMAGES.html ,
meteorological observations from METEOSAT satellite at http://www.wetterzentrale.de/ ,
meteorological forecast data from ECMWF/UK at http://grads.iges.org/pix/euro.fcst.html ,
and historic meteorological analysis data from Infomet Spain at http://www.infomet.fcr.es/arxiu/.
Ancillary measurements included routine observations of the aerosol optical depth at several UV/VIS/IR wavelengths using automated sun-tracking photometers and spectral UV radiance measurements, at selected EARLINET sites (IPSL/France, INFM/Italy, AUTH/Greece).

3.7.3 Scientific achievements

Saharan dust events during 2001

As in the previous year (2002) the NTUA group was in charge of the emission of special warnings, forecasting (12-24 hours before) the time the Saharan dust events would overpass the respective EARLINET lidar sites. Table 3.7, presents a summary of the Saharan dust events occurred during the 2nd reporting period. In total, more than 29 (42 since May 1, 2000) Saharan dust episodes (each ranging from 1 to 5 days) were successfully forecasted by NTUA, and were subsequently identified and monitored by the EARLINET stations, as will be detailed in the next paragraph.

	Station Dates	at	ba	be	gp	hh	ju	ku	la	lc	le	li	mi	mu	na	ne	pl	po	th
1	**30.01-06.02.01**	X			X		X			X			X			X	X	X	
2	08-16.02.01				X					X				X	X	X		X	
3	17-19.02.01															X		X	
4	21-28.02.01									X					X	X			
5	01-03.03.01									X						X	X	X	
6	08-10.03.01									X									X
7	13-18.03.01	X	X							X					X	X	X	X	
8	**19-26.03.01**	X								X					X		X		
9	29-31.03.01		X							X									
10	01.04.01	X																	
11	05.04.01			X						X			X						
12	**19-22.04.01**	X	X																
13	**24-26.04.01**		X							X						X		X	
14	**02-05.05.01**	X								X						X		X	
15	**15-22.05.01**	X	X		X					X					X	X	X	X	X
16	**05-10.07.01**	X				X		X		X			X	X		X		X	
17	**16-18.07.01**	X	X							X					X			X	
18	19-23.07.01	X	X							X		X	X	X	X			X	
19	**23-26.07.01**	X								X			X		X	X	X		
20	**28.07-06.08.01**	X	X		X	X	X	X		X	X	X	X		X	X	X	X	
21	21.08.01									X									
22	06.09.01	X													X		X		
23	20-22.09.01	X																	
24	24-27.09.01	X													X	X	X	X	
25	**04-05.10.01**																	X	
26	**11-16.10.01**		X	X							X			X	X	X	X		
27	25.10.01																X		
28	29.10-01.11.01				X	X					X						X		
29	15.11.01	X																	

Table 3.7: List of Saharan dust episodes occured in the Mediterranean Region and over Europe, in the period 01.01.01 - 31.12.01.

Bold dates (5 cases) correspond to major Saharan dust events (Aerosol Index $>$ 1.8 in the 0.3-2.3 scale of the TOMS instrument). Special attention should be paid to the case of **28/07/01-06/08/01**. This was a major dust event case which lasted as long as ten days and was successfully followed by 14 lidar stations across Europe (see Table 3.7). In this successful case distinct Saharan dust layers were generally observed in the height region from 2.5 km up to 5 km ASL (over the Mediterranean area), while they reached heights between 3-7 km ASL (and locally up to 8-10 km) when they overpassed Central Europe. Figure WP7-2 presents some selected altitude-resolved lidar profiles, where distinct layers of Saharan dust are clearly seen.
In support to the lidar observations, backward air-mass trajectory analysis was performed (see WP4) by the German Weather Service (DWD), valid for each lidar station every day at 13:00 UT and 19:00 UT. In the case of the detected Saharan dust layers, all backward trajectory data (2-4 days earlier) had as origin the Saharan region (Fig. WP7-2). Additionally, the day-to-day analysis of the available meteorological and satellite observations (i.e. TOMS aerosol index, NOAA aerosol optical thickness, SeaWifs images) verified the lidar observations and confirmed the horizontal extent of Saharan dust events over Europe (Fig. WP7-2).

Forest fires

In addition, during the same reporting period, plumes from one forest fire were observed by the lidar system located over the city of Athens on 02.08.01. In this case the largest aerosol concentrations were observed over the top of the Atmospheric Boundary Layer (ABL) between 2-3 km ASL.
Localisation of Industrial air pollution sources.

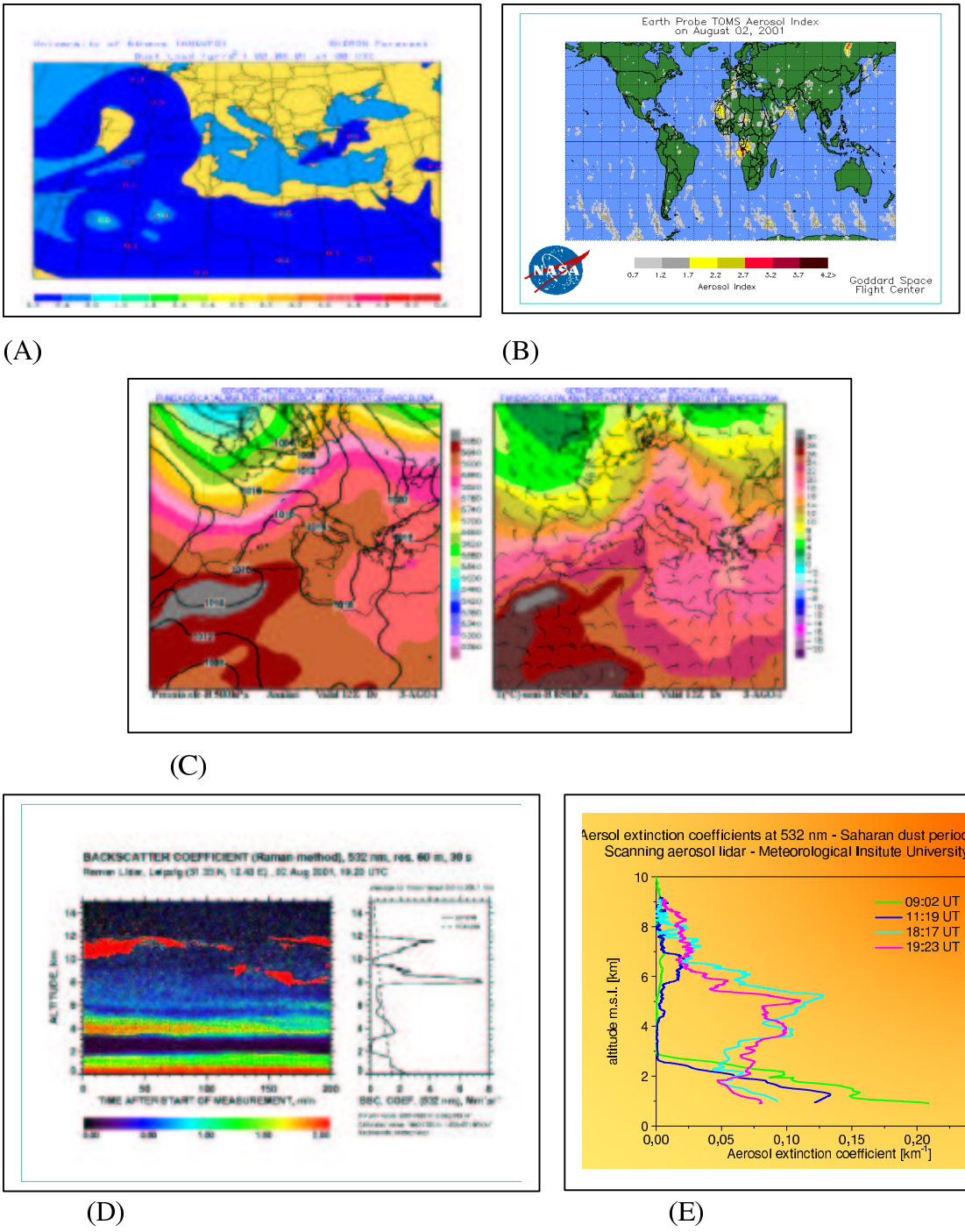

Figure WP7-2: Saharan dust episode observed over central Europe: A: Dust event forecasted by the University of Athens (00:00UT), B: TOMS Aerosol Index data, C: Meteorological analysis from University of Barcelona (12:00UT). Aerosol backscatter (D) and extinction (E) lidar data obtained over Leipzig and Munich, respectively, at 532 nm.

In conjunction with the European ”Minos Experiment” which took place over Greece, during August 2001, the lidar measurements over Athens revealed the presence of an important aerosol layer located between 3-5 km height. This dust plume originated from the Black Sea three days earlier and was

attributed to a major local industrial air pollution source.

Photochemical Smog episodes

Regarding photochemical smog episodes, at least five important cases were monitored by the NTUA's lidar group in Athens, Greece, during the summer and autumn period of the year 2001 and two cases during January 2002. In all cases the aerosol backscatter coefficients observed at 532 nm, exceeded the mean values (0.005-0.01 km-1sr-1) valid for the city of Athens, by a factor at least 1.5 to 3. In all cases, the highest aerosol concentrations were observed between 1.5-2.0 km ASL, around 13:00-14:00 UT, while the ABL height reached maximum values of 2.5-3 km ASL (spring/summer seasons) and 2-2.5 km ASL (autumn season) around 13:00 UT.

3.7.4 Socio-economic relevance and policy implication

The main direct product of WP7 during its second year of operation is the very large data set on the vertical, horizontal and temporal distribution of aerosols, occured during special events (Saharan dust outbreaks, forest/industrial fires, photochemical smog episodes) over Europe. This is the first data set on a continental scale, therefore there will be a significant interest in the science community to use these data, for the improvement of global/regional atmospheric or of climate prediction models, as well for the correction of satellite images. Scientific publications and conference presentations, resulting from WP7, already gave (and will give) the opportunity to the science community to address the mechanisms of local aerosol formation, to study the trans-boundary transport processes of air pollution over Europe and to study the impact of aerosol loads in the earth's radiation budget and their link to Global Change. Finally, the necessary measures could be proposed for an air pollution abatement strategy in Europe, in compliance with the EU air pollution abatement/Climate Change policy.

3.7.5 Discussion and conclusion

Important activities, in full accordance with the contract, were implemented right from the start of the project. The strong activity of this WP has been amplified during 2001, with contributions from nearly all stations. Since February 1, 2001 more than 29 Saharan dust episodes have been identified by several stations of the network, thus giving a total of 42 cases observed since May 1, 2000. This has established the largest data set on the vertical and horizontal distribution of Saharan dust aerosols ever observed over the European continent. Contrary to the last winter, this winter was characterized by the total absent of Saharan dust episodes over Europe. The most important cases have been already analyzed using lidar and ancillary data (sun photometric and satellite observations) leading to major results concerning the horizontal and vertical evolution of the Saharan dust aerosols over Europe. In addition one forest fire event was observed over Athens during summer 2001, as well as five severe photochemical smog episodes at the same site. The eruption of the Etna volcano in June 2001 was associated with important aerosol load injection into the atmosphere, which was monitored by several lidar stations, basically in Italy, Greece, Germany, and probably other countries. Meteorological conditions were not very favorable for the observation of the main volcano cloud because wind direction was mainly northerly, blowing the cloud over the sea to the African coast. The effects of emissions at different altitudes and consequently different flow directions will be studied using the lidar data. In addition, and in conjunction with the Minos Experiment which took place over Greece during August 2001, the lidar measurements over Athens revealed the presence of an

important aerosol layer located between 3-5 km height. This dust plume originated from the Black Sea 3 days earlier and was attributed to a major local industrial air pollution source.The material collected so far forms a very solid basis for detailed analysis of Saharan dust episodes occuring over Europe.

3.7.6 Plan and objectives for the next period

The detailed plan and objectives for the year 2002, include the same forecasting and monitoring scheme, in view to maximize, not only the number of events observed, but also the monitoring period, to get a more detailed follow-up of the diurnal variation of the horizontal and vertical extent of the aerosols distribution over Europe, during the occurence of important Saharan dust events. Data analysis from routine observations of the aerosol optical depth at several UV/VIS/IR wavelengths, using automated sun-tracking photometers and spectral UV radiance measurements, at selected EARLINET sites (IPSL/France, INFM/Italy, AUTH/Greece) will be performed also during 2002. The scientific material collected so far, for all three subsets (Saharan dust events, photochemical smog episodes, forest/industrial fires), forms already a very solid basis for relevant detailed studies of the associated meteorological and photochemical processes over Europe. The output of WP7 could be directly used for the quantification of the Saharan dust transported from Africa to the European continent.

3.8 WP8, Impact on satellite retrievals

by Matthias Wiegner

Aerosols play an important role in our climate system by influencing the radiation budget, atmospheric chemistry and the hydrological cycle. To observe aerosols on a global scale, satellite remote sensing is the only means. However, with respect to aerosols, the potential of radiometers is limited: while the monitoring of the aerosol optical depth over oceans shows some encouraging results and is almost operational (though with a limited accuracy), the retrieval of aerosol properties over land is in principle difficult and still in the stage of testing. The main reasons are the relative high (and inhomogeneous) surface albedo and complex influences of the orography. As a consequence, sophisticated inversion algorithms are required which need independent high-quality data for validation.
The knowledge of the vertical aerosol distribution is even more limited. Typical profiles as well as their variability are needed to run realistic numerical models, which in turn enable studies of processes and the development of improved parameterization schemes. In this context, aerosol data serve as input to model realistic scenarios, but also to study the sensitivity of radiances at the top of the atmosphere on aerosol height distribution, extinction coefficient profile, aerosol type and single scattering albedo.
So, in summary, EARLINET lidar data will support the satellite community in two ways: with respect to validation of aerosol retrievals and with respect to model calculations. Workpackage No. 8 provides this link between active remote sensing from ground and passive remote sensing from space.
It is clear, that due to the limited resources potential applications of lidar data can only be done in form of demonstrations, not on a regular basis. In spite of their limited spatial and temporal coverage of EARLINET data, three classes of joint efforts have been identified, two of them dealing with validation and calibration, and one with numerical modelling.

3.8.1 Measurements

Measurements include two possible contributions: one includes the provision of special lidar measurements to validate co-incident and co-located satellite measurements. This could be done if the spatial resolution of the satellite radiometer is high, i.e. in the range of 1 km or even better. Otherwise, it can not be guaranteed that the lidar measurement is representative for the satellite information. Furthermore, additional measurements at the surface must be included to fully characterize the states of the atmosphere and the surface. It is obvious that such validation campaigns have to be coordinated in advance for pre-selected satellite overpasses, hoping that cloudfree conditions occur.
The benefit of lidar data to contribute to the validation of high resolved satellite data will be demonstrated in case of the CHRIS-radiometer onboard of PROBA, which was launched on October 22, 2001. This radiometer provides a very high spatial resolution of 25 m and delivers multi-spectral and multi-angle data. It is agreed with partners of the 'Ground Truth Center Oberbayern' (GTCO, Germering, Germany) to run four such experiments during overpasses in May, June, July and August 2002 in Gilching near Munich.
Another contribution of EARLINET measurements to satellite remote sensing is the provision of local aerosol data that can be compared to respective quantities derived from satellites. Several attempts of direct negotiations with different institutes suffered from limited resources of time and personnel allocatable for 'new' tasks. To allow the satellite community longer planning periods it

was decided to publish a survey of our aerosol extinction coefficient data base on a website where interested groups can select data that fit to their own data sets with respect to time, place and wavelength. This opportunity might be interesting to test pre-operational algorithms based on e.g. SeaWIFS data. When ENVISAT, confirmed for launch on March 1, 2002, is fully operational quickly, several instruments (e.g., MIPAS, GOMOS, MERIS and SCIAMACHY) might benefit from ground based lidar measurements, too.
Within the ENVISAT CAL/VAL project (http://nadir.nilu.no/calval), preliminary activities have already been directly carried out by several EARLINET lidar stations. In particular, the lidar of Dipartimento di Fisica - Università Degli Studi - L'Aquila will provide aerosol extinction and backscattering profiles as well as the water vapor mixing ratio profiles. It is planned to participate on a couple of campaigns to test the single ground station efficiency in responding to the satellite overpass alerts and the following data submission, in the correct HDF format (Hierarchical Data Format) to the common database (NADIR at NILU). The relative success of such campaigns allows to solve, among others, the problem of what should be the right form of the scientific products to be exchanged between lidar and satellite comunities.

3.8.2 Modelling

The second topic of this workpackage includes the modelling of the aerosol influence on radiances as measured by satellites. Such model calculations – with realistic aerosol profiles gained from the EARLINET measurements – can help to assess the radiative forcing of aerosols, to develop corrections for atmospheric masking, to determine the required sensitivity and accuracy for deriving aerosol products from satellite-data, and to investigate typical spatial and temporal scales adequate for averaging. In particular the last point is of interest because the spatial resolution from space is often quite poor.
The modelling of the aerosol influence requires sophisticated radiative transport codes: they must consider arbitrary aerosol distributions (vertical profile, optical properties) and determine radiances with a high angular resolution to cover all realistic observation geometries. Here, RSTAR (curtosy F. Wagner, GTCO) has been used which is based on the adding and doubling method. Calculations have shown that the aerosol type and the optical depth are most important to correctly describe the aerosol influence on the radiance field at satellite level. The vertical layering is important if layers of different aerosol types (e.g. absorbing and non-absorbing particles)are present at the same time. The lower the surface albedo the stronger is the aerosol effect. A typical distribution of the radiances is shown for illustration in Fig. 3.12.

3.8.3 Summary

This workpackage is very ambitious, in particular in view of the very limited resources allocated to it. Therefore, it is necessary to restrict ourselves to the investigation of the most urgent problems. According to this, all activities are within the milestone plan and were successful. We are going to demonstrate that ground based lidar networks like EARLINET can contribute significantly to several aspects of satellite remote sensing. More results can be expected at the end of this project when the CHRIS validation has been completed; the delay of the PROBA launch was outside the contractor's responsibility. The full benefit can be expected on a long term perspective when partners from the satellite community can reliably count on a continuous flow of high quality lidar data and consider this fact in future proposals.

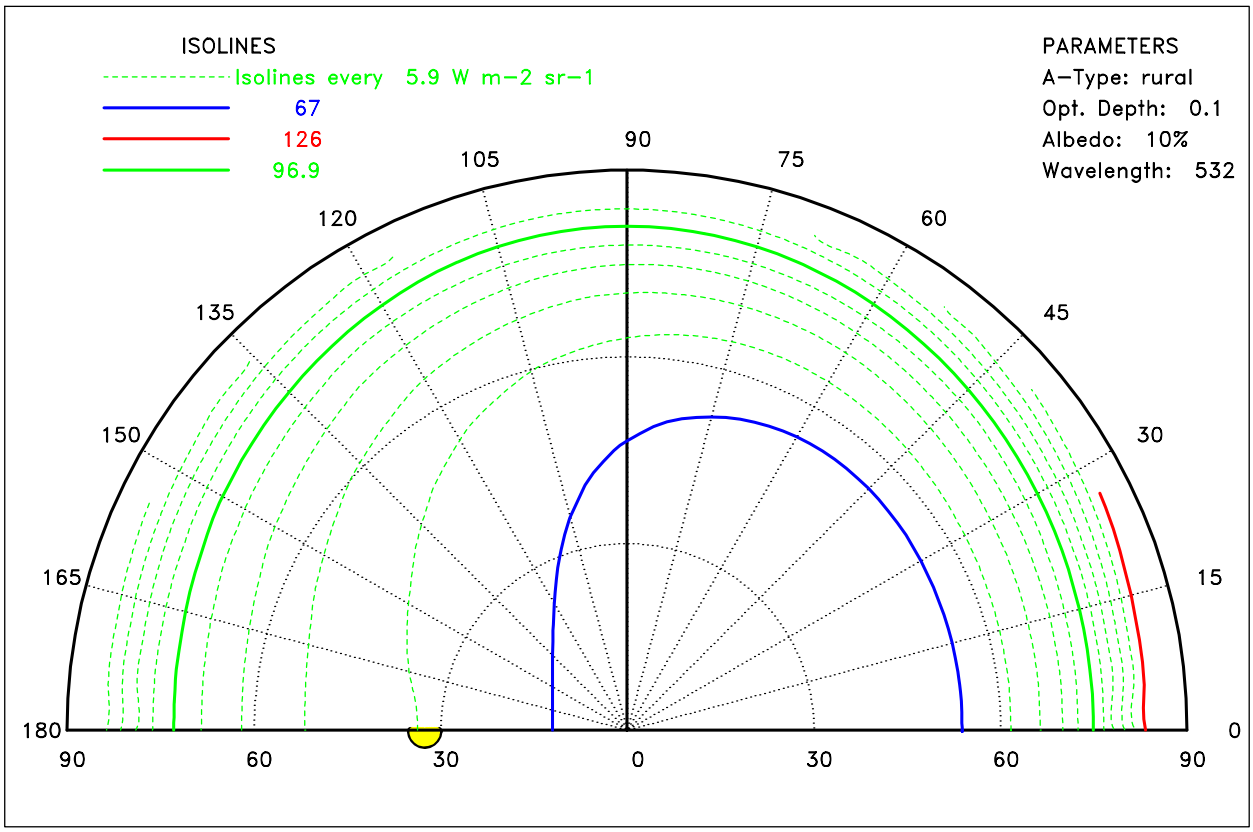

Figure 3.12: *Radiance at the top of the atmosphere for 532 nm (example for rural aerosol distribution), solar zenith angle is 32.5°.*

3.9 WP9, Air mass modification processes

by Ulla Wandinger

3.9.1 Objectives

The distribution of the lidar-network stations in Europe gives the opportunity to study the anthropogenic influence on the aerosol. Clean (pristine) air arriving from maritime and polar regions is detected by the most northerly and westerly stations (Linköping, Aberystwyth, Kühlungsborn, Hamburg). Traveling across Europe, these air masses are modified through anthropogenic activities, by which precursor gases and particles are emitted into the atmosphere. Depending on travel distance and residence time over the source regions, particle number concentrations, the physical and chemical state, and thus the optical properties of the aerosol change. The comparison of particle backscatter and extinction profiles measured at the stations in central and eastern Europe (Paris, Leipzig, Munich, Belsk, Minsk) with those at the boundaries of the network will permit us to quantify the anthropogenic impact. The investigations will be limited to the northern part of the network, where orographic effects on aerosol modification processes are of minor importance.

3.9.2 Methodology

It was decided to concentrate the activities of this workpackage on a statistical approach. On the basis of the routine, long-term measurements at the different stations (data from WP2 and WP5) and an appropriate analysis of analytical backward trajectories (data from WP4), the increase of the aerosol load in air masses that cross Europe from (north)west to (south)east can be quantified. For the remote stations, so-called reference profiles for air masses reaching Europe from the Atlantic can be determined, e.g., in dependence on the season. These profiles are compared with those taken in central and eastern Europe under conditions, for which the air masses traveled from the Atlantic across well-defined European source regions to the measurement sites. Trajectory analysis helps to classify the measurements. Emission maps for aerosol precusor gases such as SO_2 can be used to identify the most important source regions.

3.9.3 Scientific achievements

Figure 3.13 shows measurements of the particle backscatter coefficient at 355 nm performed under clean conditions at Aberystwyth during summer 2001. The trajectories in Fig. 3.13 represent typical westerly and northerly flows under which these measurements were made. Aberystwyth is located directly at the west coast of Wales. The arriving air masses very often did not have any land contact for several days before detection. Taking the average of these profiles (red curve in Fig. 3.13), one can define a reference profile for clean marine conditions. This profile describes the typical air mass reaching Europe from the North Atlantic. Integrating the mean backscatter profile up to the (mean) top of the dust layer (about 1600 m) and multiplying that value with a typical lidar ratio for marine aerosols of 25 sr, one obtains an aerosol optical depth of 0.05.
Figure 3.14 shows measurements of the particle backscatter coefficient at 355 nm performed under northerly and northwesterly flows (see trajectories in Fig. 3.14) at Hamburg during summer 2001. It is expected that relatively clean air masses can be observed under such conditions in Hamburg

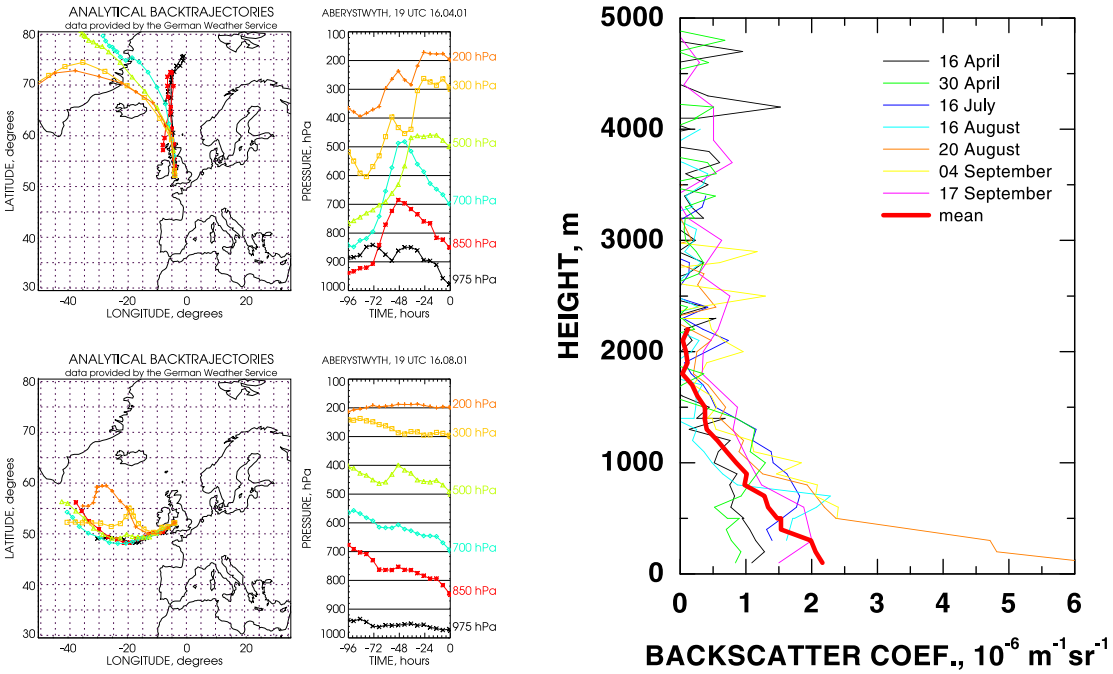

Figure 3.13: Typical 4-day backward trajectories for the arrival of marine air masses at Aberystwyth (left) and corresponding backscatter-coefficient profiles at 355 nm for such advection patterns measured in Aberystwyth during the summer of 2001 (right).

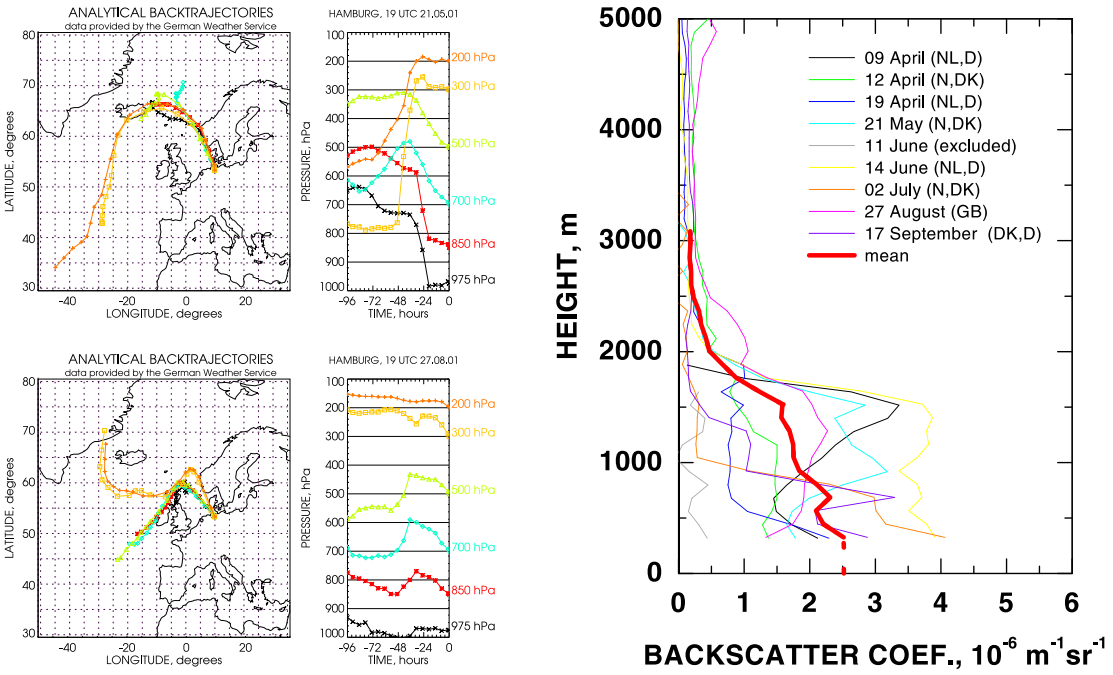

Figure 3.14: Typical 4-day backward trajectories for the arrival of marine air masses at Hamburg from the northwest(left) and corresponding backscatter-coefficient profiles at 355 nm for such advection patterns measured in Hamburg during the summer of 2001 (right). Influence from non-marine regions as indicated by the trajectectories is given in the legend (right, D=Germany, DK=Denmark, GB=Great Britain, N=Norway, NL=The Netherlands).

as well. In a few cases (19 April, 12 April, 27 August), backscatter profiles similar to those at Aberystwyth were observed indeed. However, the comparison of the mean backscatter profile (red curve in Fig. 3.14) with the mean profile for clean conditions in Aberystwyth (red curve in Fig. 3.13) indicates a significant higher aerosol load at the Hamburg site. Industrialized regions adjacent to the North Sea, the immense ship traffic in the North Sea, and local sources are obviously responsible for the increased aerosol load. With a lidar ratio of 35 sr for slightly polluted aerosols one can estimate the aerosol optical depth to 0.13 in this case. The mean dust-layer height is about 1800 m, and a significant particle load up to 3000-m height is found in most cases, which is probably caused by convection over land before the air masses reach Hamburg.

Even higher aerosol loads are observed when the air is advected from the west to Hamburg as shown in Fig. 3.15. The trajectories indicate that the air masses, which originated in the North Atlantic, have passed highly industrialized regions in northwestern Europe, namely Belgium and The Netherlands and/or England. The longer residence time over land leads to an increase of both aerosol load and dust-layer height. The optical depth is estimated to 0.30 with a lidar ratio of 50 sr for polluted aerosols. The dust layer reaches to 3100-m height which causes a dilution of the aerosol, so that the maximum values of the backscatter coefficient are not much higher than those observed under northwesterly flows with smaller dust-layer heights.

Finally, Fig. 3.16 shows measurements made under northwesterly flows in Leipzig. Compared to the results for northwesterly flows in Hamburg (see Fig. 3.14) both the dust-layer height and the aerosol load are increased. While the optical depth, which is estimated to 0.32 with a lidar ratio of 50 sr for polluted aerosols, is similar to the optical depth observed under polluted conditions (westerly flows) in Hamburg, the mean dust layer reaches to about 2500-m height only. Consequently, maximum backscatter values are somewhat higher in Leipzig than in Hamburg.

In summary, the observations of aerosol backscatter profiles at a common wavelength of 355 nm at three different stations of the network have clearly shown the uptake of aerosol particles between the North Atlantic, the North Sea, and central Europe. Figure 3.17 summarizes the findings in terms of the mean backscatter-coefficient profiles presented in Fig. 3.13–3.16 . Column backscatter coefficients of the aerosol dust layer of $2.1e{-}3\ sr^{-1}$ at Aberystwyth for westerly and northerly flows, $3.8e{-}3\ sr^{-1}$ at Hamburg for northwesterly flows, $6.0e{-}3\ sr^{-1}$ at Hamburg for westerly flows, and $6.5e{-}3\ sr^{-1}$ at Leipzig for northwesterly flows were observed during the summer of 2001. These values were converted to optical depths of 0.05, 0.13, 0.30, and 0.32, respectively, by the use of typical lidar ratios for marine (25 sr), slightly polluted (35 sr), and heavily polluted aerosols (50 sr). Such lidar ratios are typically obtained from Raman measurements at the corresponding sites (see also WP15).

3.9.4 Socio-economic relevance and policy implication

WP9 will deliver for the first time a coherent data set on the modification of air masses in terms of aerosol optical parameters on a continental and vertically resolved scale. The data set is of major scientific interest. It can be used to improve air-pollution and climate-prediction models, to address aerosol formation and transport mechanisms, and to calculate the impact of aerosols on the radiation budget. The data set can help to develop strategies for the reduction of air pollution in Europe.

3.9.5 Discussion and conclusion

The objectives of WP9 are tackled on the basis of the regular measurements (WP2 and WP5) and of analytical backward trajectories (WP4). In this way, statistically significant results will be obtained.

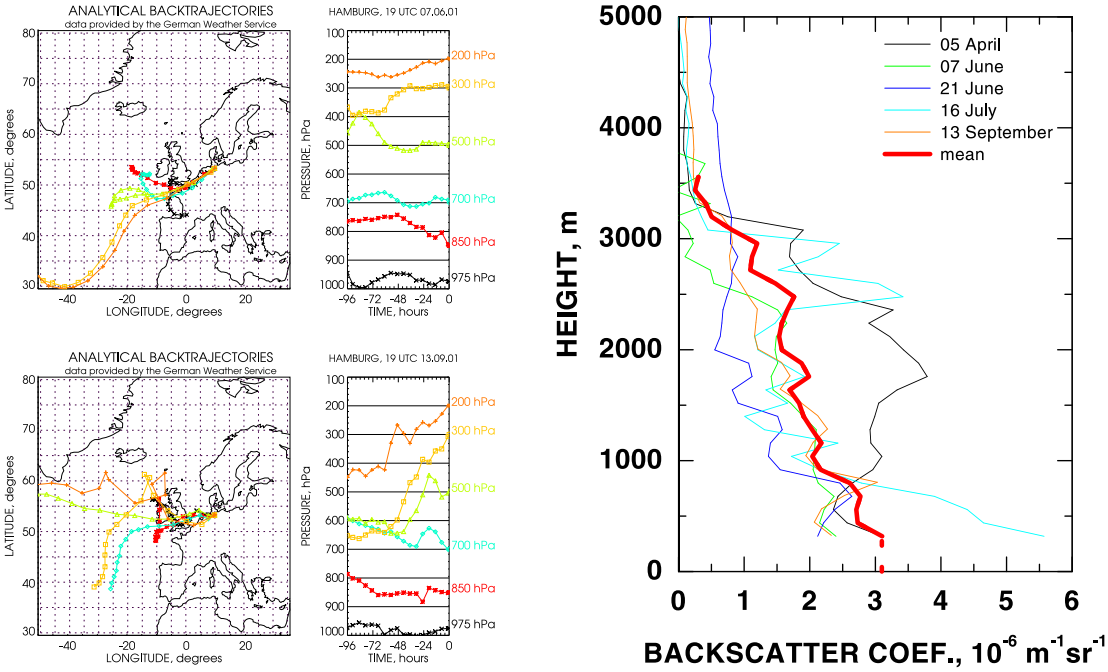

Figure 3.15: Typical 4-day backward trajectories for the arrival of air masses at Hamburg from the west (left) and corresponding backscatter-coefficient profiles at 355 nm for such advection patterns measured in Hamburg during the summer of 2001 (right).

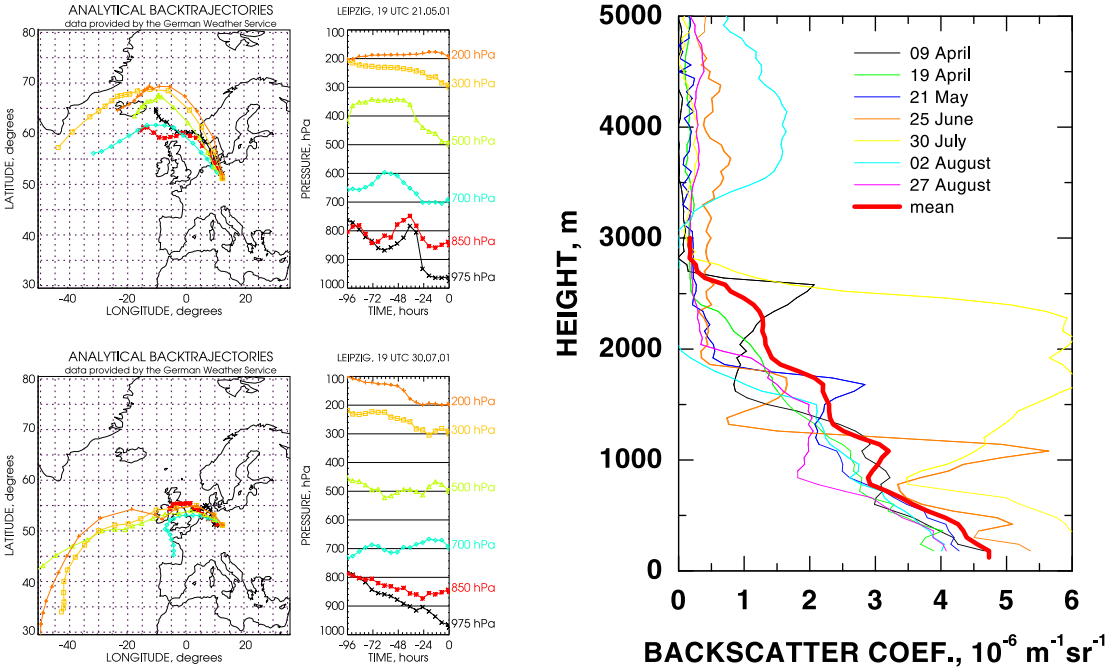

Figure 3.16: Typical 4-day backward trajectories for the arrival of air masses at Leipzig from the northwest (left) and corresponding backscatter-coefficient profiles at 355 nm for such advection patterns measured in Leipzig during the summer of 2001 (right).

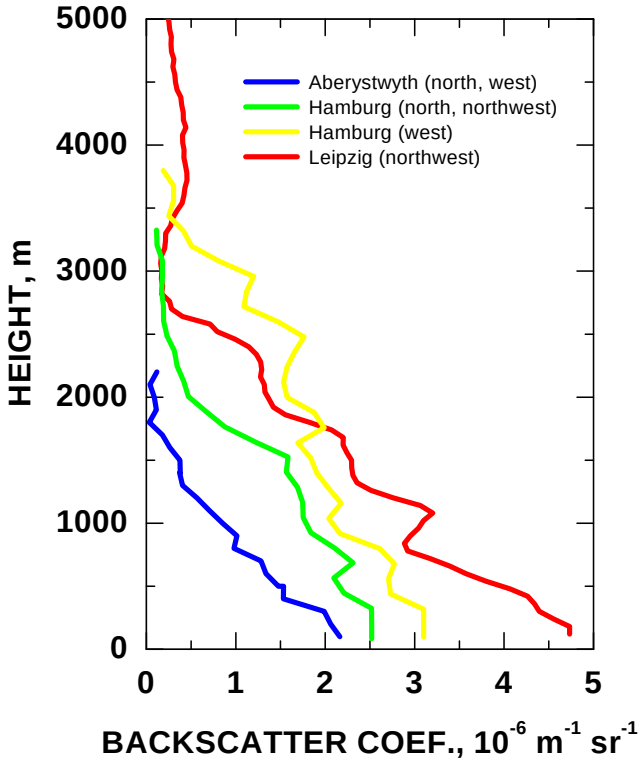

Figure 3.17: Mean backscatter-coefficient profiles at 355 nm for different air flows measured in Aberystwyth, Hamburg, and Leipzig during summer 2001.

First studies, based on a single season and three network stations only, already resulted in very impressive findings with respect to air mass modification over Europe. An increase of the mean aerosol optical depth by a factor of 6 was found in air masses traveling from the North Atlantic to central Europe. It is expected that WP9 will lead to an important improve of our knowledge of air mass modification processes.

3.9.6 Plan and objectives for the next period

In the final year of the project the investigation of air mass modification processes will be intensified. The increasing number of regular measurements will help to improve the statistical significance of the findings. Measurements at a variety of stations, i.e., Linköping, Kühlungsborn, Lisbon, Paris, Munich, Belsk, and Minsk in addition to Aberystwyth, Hamburg, and Leipzig, will be used to extend the study to an almost continental scale, which will allow us to evaluate different aerosol source regions in Europe. Different seasons and different optical quantities (extinction and backscattering at different wavelengths) will be investigated. The software for the combined analysis of trajectories and lidar data (WP4) can be used as well. A final quantification of the modification processes will also require the consideration of cloud modification and washout effects as well as of the humidity effect. It is expected that, because of a drying of the air mass during travel over the continent, the size of the particles and thus their scattering efficiency is reduced. This effect would lead to an apparent decrease of aerosol load over the continent.

3.10 WP10, Orography and vertical transport

by Thomas Trickl

3.10.1 Objectives

The main objective is to study air pollution export from the boundary layer promoted by mountains under the rather different conditions of the individual partner stations. It is desirable to obtain material on the interaction with the synoptic wind and on how the boundary-layer air is eventually injected to the free troposphere. For all stations involved in this topic the characterization of the diurnal cycle caused by the local wind system is crucial for the understanding of the boundary-layer development and the aerosol climatology derived for the respective station.

3.10.2 Methods

The aerosol backscatter coefficient, under conditions of low to moderate humidity, is an excellent tracer for air-mass exchange. The transport processes are followed by diurnal series of lidar soundings. Information on the wind field is crucial for an interpretation of the data. This information may be provided by radio-sonde ascents, meteorological station data or aircraft flights with wind sensors.

3.10.3 Scientific achievements

In 2001, three stations (Athens (AT), Garmisch-Partenkirchen (GP) and Neuchatel (NE) have been active for WP10. In addition, Barcelona (BA) may decide to contribute to this topic on a volunteer basis due to the interest derived from earlier, published work. Most activities of this work package will take place during the third year of the project when all data will be accumulated and a meaningful analysis will be possible covering a reasonable number of cases.
Some preliminary conclusions could be made by IFU for the Alpine wind system in the vicinity of Garmisch-Partenkirchen. This conclusion has been made possible by the existence of a few more years of sounding data, a few cases even from the 1991 series of measurements with the ozone lidar. Three types of profiles are found during the warm season:
1. Bimodal distributions of the aerosol backscatter coefficient with upper boundary between typically 3.5 and 4.0 km a.s.l., i.e., 1 to 1.5 km above the height of the highest mountain ranges next to the station,
2. Vertical distributions with less pronounced structure and with an upper boundary between typically 3.5 and 4.0 km,
3. Vertical distributions with less pronounced structure and with significantly lower upper boundary.
Bimodal distributions are not that frequently found, a total of 7 days have been encountered within four to five years. This, of course, is likely to be far from a complete coverage- However, the bimodal distributions yield the easiest explanation of the Alpine thermal wind system. They are explained by an upvalley flow at lower elevations (valley wind) sucking polluted air from outside the mountains into the Alps and a reverse (compensating) wind (anti-valley wind) aloft which forms with a delay of a few hours because this air is lifted from the bottom of the valley to high altitudes in the upper part of the valley. In contrast to the situation at IFU, the results obtained in the deep Mesolcina Valley (300 m to 3000 m) in the Swiss Alps during the 1996 VOTALP field campaign have yielded a rather reproducible bimodal distribution during the entire week of that field campaign. This difference is ascribed to the rather open structure of the Loisach valley near Garmisch-Partenkirchen with

mountains peaking near 2000 m on both sides of the valley and a high barrier in the south between 2500 and 3000 m. The valley base is near 700 m. Due to the lower average height of the mountains the flow in the upper part of the Alpine boundary layer (up to 4000 m) is not channeled as in the case of the Mesolcina valley thus allowing the synoptic wind to interact stronger with the orographic wind system. The effiency of the upward transport is high, the reduction in backscatter coefficient being caused by the enhancement in valley cross section at higher altitudes. In the Mesocina Valley a transport efficiency of about 80 similar estimation in the Loisach valley is more comlicated and will require detailes information on the wind field and perhaps some modelling.

Type 1 was analysed by using data from the Munich radio sonde ascents which should be rather representative for the free troposphere also above Garmisch-Partenkirchen. It was found that in all cases the wind speed was below 5 m/s and the wind direction between east and south. The second type differs from type 1 by more pronounced exchange between the different layers. We assume that the wind conditions are less calm than in the case of the bimodal distributions. For the third case we examined a few examples which all corresponded to strong northerly winds. This indicates that the formation of an anti-valley wind was impeded by the interference of the synoptic wind in these cases.

It had been planned to measure the wind field in the Garmisch-Partenkirchen area simultaneously to the lidar measurements. For this purpose the IFU ultra-light aircraft had been planned to become equipped with a suitable wind sensor, based on a high-resolution GPS and a five-holes sonde. Due to the numerous field campaigns of the aeroplane in summer 2001 the development of the wind sensor system could not be started before autumn 2001. Meanwhile, the testing of the sensor system is almost completed. In spring and summer 2002 concentrated measurement campaigns with the lidar and the aeroplane will take place in particular as a joint effort of EARLINET and the German VERTIKATOR project.

For the case of Athens there are 2 cases to be examined concerning the influence of the vertical transport of aerosols over the Greater Athens Area (GAA). Meteorological and radiosonde data analysis will provide the necessary input to evaluate the role of the sea breeze circulation on the vertical profiling of aerosols and especially on their vertical transport. This work is in progress.

In Neuchatel, most activities will take place during the final year of EARLINET. In 2001, the backscatter profiles have been examined for features indicating the influence of the local orography.

3.10.4 Socio-economic relevance and policy implications

The air-pollution export from the boundary layer to the free troposphere is crucial for the hemispherical distribution of pollutants. Significant amounts of trace gases such as ozone, but also some aerosol are transported from continent to continent. This should have severe implications for the most productive source regions for air pollution such as South-East Asia, North America and Europe.

3.10.5 Discussion and conclusion

A full discussion is not yet possible at this stage of the project. First conclusions for the Loisach valley are given above. A strong influence of the synoptic wind conditions afe obvious.

3.10.6 Plan and objectives for the next period

Intensified efforts will be made at IFU. At least two field campaigns including aircraft measurements are planned. In addition, the difference of the boundary-layer height between the network stations Munich and Garmisch-Partenkirchen will be determined. In the Athens area a second lidar will be added and six to seven cases will be studied. The influence of the wind direction on the local circulation will be evaluated. The analysis will be based on sonde data and modelling. The investigations at Neuchatel have just been started, after defining the measurement requirements. The lidar measurements will be accompanied by meteorological measurements next to the lidar and above the mountain behind Neuchatel belonging to the Jura range and radio sounding at Payerne.

3.11 WP11, Stratospheric aerosol

by Bertrand Calpini

The primary goal of WP11 is coordination of stratospheric aerosol observations within the EARLINET project and detection of smaller scale features of stratospheric aerosol distribution and its interdependence with dynamics and heterogeneous chemistry.
At present, seven stations situated in Aberystwyth, Jungfraujoch, Kühlungsborn, L'Aquila, Leipzig, Minsk and Napoli are taking part in these observations. EPFL is in charge of the coordination of the measurements and has the responsibility to warn for special events, such as volcanic eruptions.
Stratospheric aerosols are of natural and anthropogenic origin. Primary natural factors include, first of all, powerful volcanic eruptions, usually accompanied by massive emissions of sulfur gases into the stratosphere, which subsequently leads to the formation of sulfate aerosols. Atmospheric circulation plays a major role by influencing the thermodynamic conditions for aerosol formation and its transportation. The main anthropogenic sources include stratospheric aircraft flights and the transport to the stratosphere of long living carbonyl sulfide gas (the product of fuel combustion) where it is oxidized to sulfuric acid vapor. The last powerful volcanic eruption happened in June 1991 (Mount Pinatubo) and according to different lidar, satellite and sun photometer data [McCormick et al., 1995, Rosen et al., 1994, Jäger et al., 1995, Ansmann et al., 1997] lead to a maximum stratospheric aerosol optical depth of approx.0.2 at green wavelengths for the Northern hemisphere in the winter-spring of 1992. No other major volcanic eruptions affecting the stratosphere have occurred during the decay phase and in 1997 the stratospheric aerosol levels fell close to those of the pre-Pinatubo period or even lower - to the values of 1979. For example the total optical depth in December 1997 between 15 and 30 km at 532nm that is attributed to the combination effects of the molecular atmosphere, ozone and aerosol, was 0.057. Of these only approximately 0.003 was due to aerosol [Kent and Hansen, 1998]. Nowadays the aerosol content is considered to be close to the equilibrium background level observed in 1979 and during the pre-Pinatubo period 1989-1991 since no significant eruptions able to perturb the stratosphere occurred after 1997. This is confirmed by the long-term observations of stratospheric aerosol performed in Minsk [Zuev. et al., 2001] for altitudes of up to 30km that show a total backscatter coefficient between 13 and 30km in the order of 1.10^{-4} sr^{-1}. This data is in good agreement with the measurements performed in Siberia by a team of the Institute for Atmospheric Optics in Tomsk for 15-30km integration path as seen from Fig. 3.18 [Zuev. et al., 2001].
The sun photometer measurements of the stratospheric aerosol depth performed at Jungfraujoch (3560m) also show low values of the aerosol optical depth below 0.04 for the period after 1997 [Ingold et al., 2001]. The low values of the lidar scattering ratio (Fig. 3.19) taken in Aberystwyth and in Minsk during the last months also illustrates the very low aerosol load in the atmosphere. The maximum of this ratio observed at Aberistwith at altitude of 20km is around 1.07, while it reaches 1.135 over Minsk at about 23km. All this data shows that the aerosol load at present is at its background level. For its correct measurement more sophisticated lidar methods and more precise data of the stratospheric air density and ozone distribution are needed .We have to note here that anomalous aerosol layers can episodically be observed even in periods of background state of the stratospheric aerosol. This may be attributed to clouds such as the polar stratospheric (PSC) that form between 15 and 25 km at high and middle latitudes after rapid temperature decreases. Changes of the thermodynamic conditions in the stratosphere may also trigger the processes of aerosol nucleation at altitudes of 25 -35km [D.Hofman et al., 1985]. These layers can be measured and even though

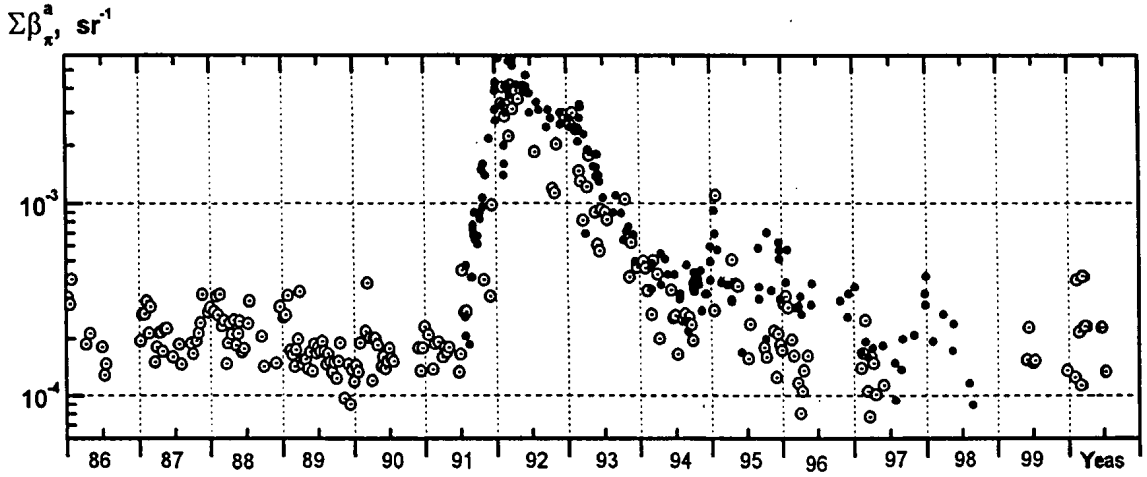

Fig. 1. Temporal behavior of the total aerosol backscattering coefficient $\sum \beta_\pi^a$ at $\lambda = 532$ nm over Tomsk (56.5°N, 85.0°E) between 15 and 30 km (open circles with dot) and over Minsk (53.9°N, 27.5°E) between 13 and 30 km (solid circles).

Figure 3.18:

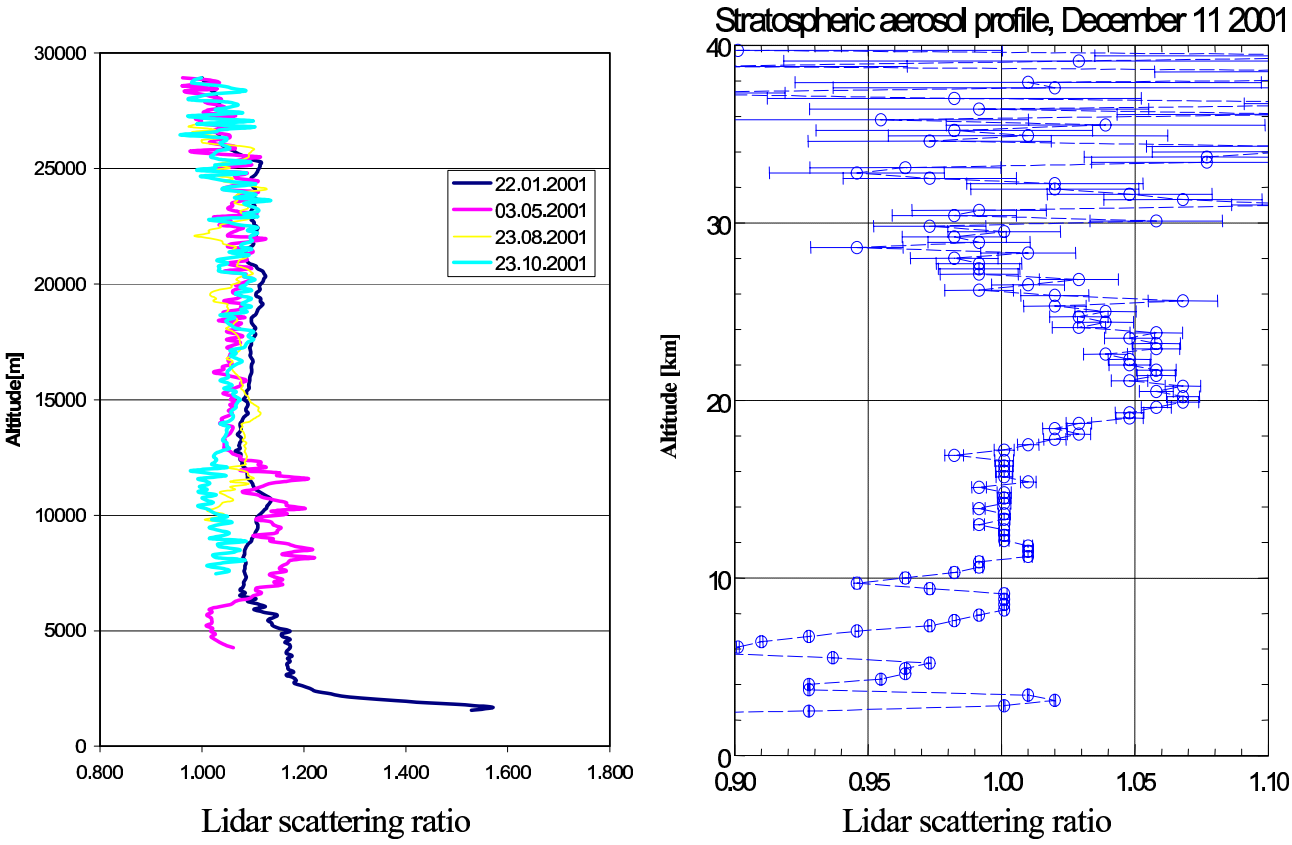

Figure 3.19: Lidar Scattering ratio profile taken in Minsk (left) and in Aberystwyth (right)

they appear seldom they are of scientific interest. What is more, statistical data from the last century shows that power volcanic eruptions occur at period of 10 to 15 years. This shows the necessity of

maintaining the ability to perform stratospheric measurements within the present EARLINET lidar network.

3.12 WP12, Differences rural-urban aerosols

by Jacques Pelon

3.12.1 Objectives

The objective of the work to be performed in this WP is close to the one of WP6, as focusing on the difference between urban and rural aerosols which can be observed during temporal cycles. The diurnal and seasonal cycle of the aerosols in the boundary layer is different over urbanised and agricultural surfaces as solar forcing and dynamical production will be different at the surface. A heat island is formed in urban areas, which modifies circulation, and transport of aerosols at the meso-scale. Furthermore, important sources of pollution are present in or near cities as traffic is more important as well as industrial activity. This impacts the optical parameters of the aerosol layers, which are different in urban and rural areas.

3.12.2 Methodology and scientific achievements

Five pairs of groups were initially involved in this work. Due to the large difference in distance between the two eastern european sites (Minsk and Belsk), it has been decided to focus on sites providing close by measurements (Athens, Hamburg, Napoli, Paris). Methodology is similar to WP6 and implies to observe the optical properties of the stable nighttime and the more convective daytime boundary layer, and analyse the wind direction to infer which station is influenced by the other to perform differential analysis. This should help to evidence the differences between and rural urban boundary layers, due to both an increase in roughness at the surface due buildings elevation, to the anthropogenic heat flux caused by heat accumulation during daytime and manmade production of particles in urban areas. In both morning and evening transition phases the profile of the extinction coefficient is not constant with altitude. Morning transitions are important as particles and pollutants formed during daytime on the previous day can be stored in the upper part of the residual boundary layer and further possibly transported in the middle or upper troposphere. During the formation of the stable nocturnal layer, this layer may include less particles and pollutants as no photochemical production will occur. The erosion of the residual layer above it during the following cycle may lead to a pollution increase near the surface, as the residual layer is mixed with the new growing active boundary layer. The structural and optical properties of these aerosol layers are thus important to be measured especially in the transition phases. This is made easier by the fact that this can be achieved in night-time periods, where Raman lidar can be operated.

The same remarks made for WP6 apply to WP12 for data acquisition and analysis. It is necessary to make measurements in the first hundreds of meters which is not simple. First cases have been analysed. A new system has been implemented in the south of Hamburg to make combined measurements in this area. First results have been reported by the Hamburg group at the Barcelona meeting this year involving a new station at Bergerdorf (south of Hamburg). Time series obtained on a first case confirms that the boundary layer layer height is higher at Hamburg before the morning transition. Napoli, Potenza and Lecce have been operated on several days. An illustration of first results obtained is reported in Figure 3.20.

Optical depth in Potenza is seen to be larger than the one observed in the westerly located town of Napoli. This is probably due to pollution as a high polluting industrial plant has been located very near to the lidar station. Furthermore Potenza is not located at the same altitude as Napoli which also introduces additional complexity in the analysis. A new system is being developed in Potenza

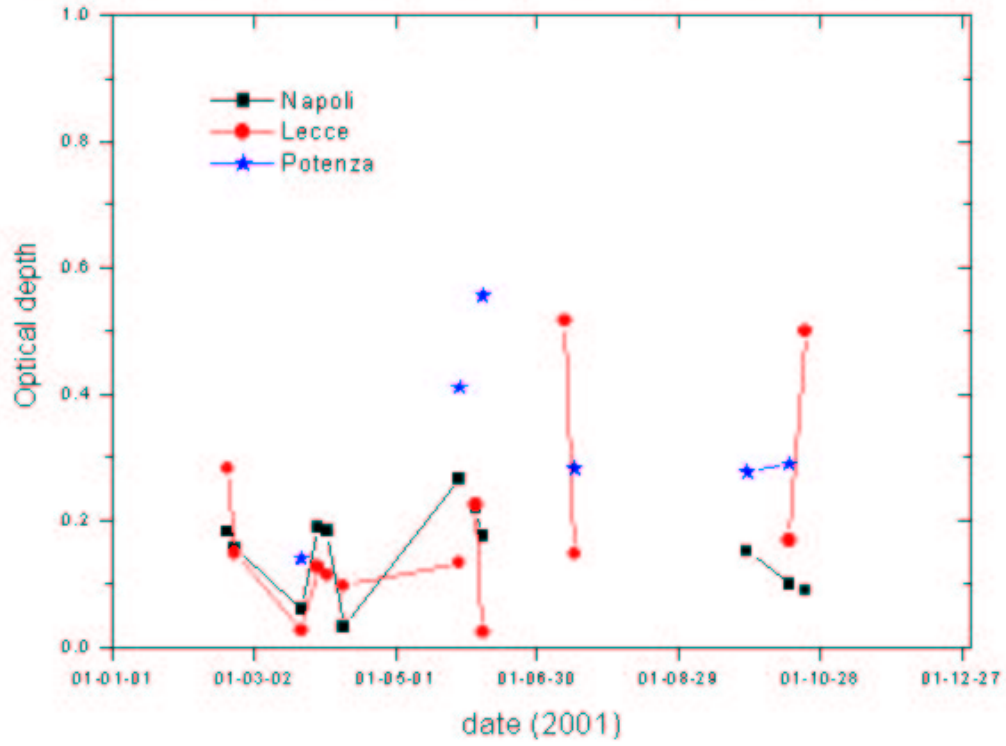

Figure 3.20: Optical depth simultaneously measured at the three stations Napoli, Potenza and Lecce.

which could be displaced for specific observations. Other systems are being developed at Athens and Paris to more directly combine observations with the existing stations.

Socio-Economic relevance and policy implication

The daytime evolution of the boundary layer is of importance as it may lead to reinforced pollution events when dynamical forcing prevents its development. Transport of particles and primary pollutant from cities may lead to secondary pollutants formation (such as ozone) over rural areas, far from the pollution areas. The accumulation of small particles and pollutants is thus increased, and specific actions may be necessary, such as limiting car traffic or industrial activity to avoid health problems on population even outside urban areas. It is very important to forecast these events due to their impact.

Discussion and conclusion

A few cases have been obtained at different stations (Athens, Hamburg, Napoli) during 2001, but the analysis is complicated by the distribution of the stations. New measurements have been recently made south of Hamburg in and first data have been taken simultaneously by the two German stations. New systems are still in development at Athens, Paris and Potenza and will be involved in 2002.

Plan and Objectives for the next period

New systems will be involved to analyse aerosol characteristics in the boundary layer (boundary layer height, backscatter coefficient in the boundary layer, extinction coefficient at sunset). Method-

ology is comparable to the one defined for WP6 (analysis of PBL structure and of optical parameters), and the analysis implies to account for wind direction so to know which station is influenced by the other in each ensemble of two stations.

3.13 WP13, UV-B and optical properties

by Dimitris Balis

3.13.1 Objectives

The main objectives of WP13 were:

- To perform UV-B radiation measurements simultaneously with the lidar measurements
- To validate the radiative transfer models against UV-B measurements, using additional the lidar as input to the model calculations.
- To estimate the impact of different aerosol conditions on the UV-B radiation field, using both measurements and model calculations

3.13.2 Methodology and scientific achievements

At the Thessaloniki station two UV spectrophotometers (one single and one double monochromator) operate continuously and monitor, with a 0.5 nm spectral resolution, the whole UV solar spectrum. In addition measurements of global total, UV-A and UV-B radiation, direct and diffuse erythemal irradiance are being performed. In addition a program for monitoring the O_3 and SO_2 total columns is in operation, which has been used as input to the model calculations. At Athens measurements of the global UV erythemal irradiance are available. During the first year of EARLINET, the Tropospheric Ultraviolet and Visible (TUV) Version 4 model was tested against spectral UV-B measurements and its accuracy was found to be better than 10% when the input parameters were well defined [Balis et al., 2002, Kazantzidis et al., 2001]. For the determination of the aerosol optical properties that are relevant to the transmission of the UV-B radiation through the atmosphere the following parameters were measured or estimated. Profiles of the aerosol extinction coefficient at 355 nm and corresponding profiles of the lidar ratio were used from the Raman lidars of LAP and NTUA. For certain cases aerosol optical depth measurements at 416nm from a filter radiometer were also available at Thessaloniki. Backward trajectories at certain levels in the troposphere were provided in the frame of EARLINET by DWD and were used to determine the origin of the aerosols observed. For days with clear sky conditions, when both UV, ozone and lidar measurements were available an effective single scattering albedo was determined with the methodology described in the next paragraph [Bais et al., 2002].

3.13.3 Discussion and conclusion

From the available spectral UV measurements we selected to examine 4 cases which according to the aerosol measurements and to the trajectory analysis corresponded to distinct aerosol conditions. These cases include:

a) High tropospheric SO_2 values as indicated by satellite measurements with extreme high aerosol optical depth measured both by the lidar and the filter radiometer versus a clean case (9-Aug-2001 vs 16-Aug-2001).

b) Two days with same total ozone and same aerosol optical depth but with different lidar ratio and UV irradiance (13-Sep-2001 vs 29-Oct-2001).

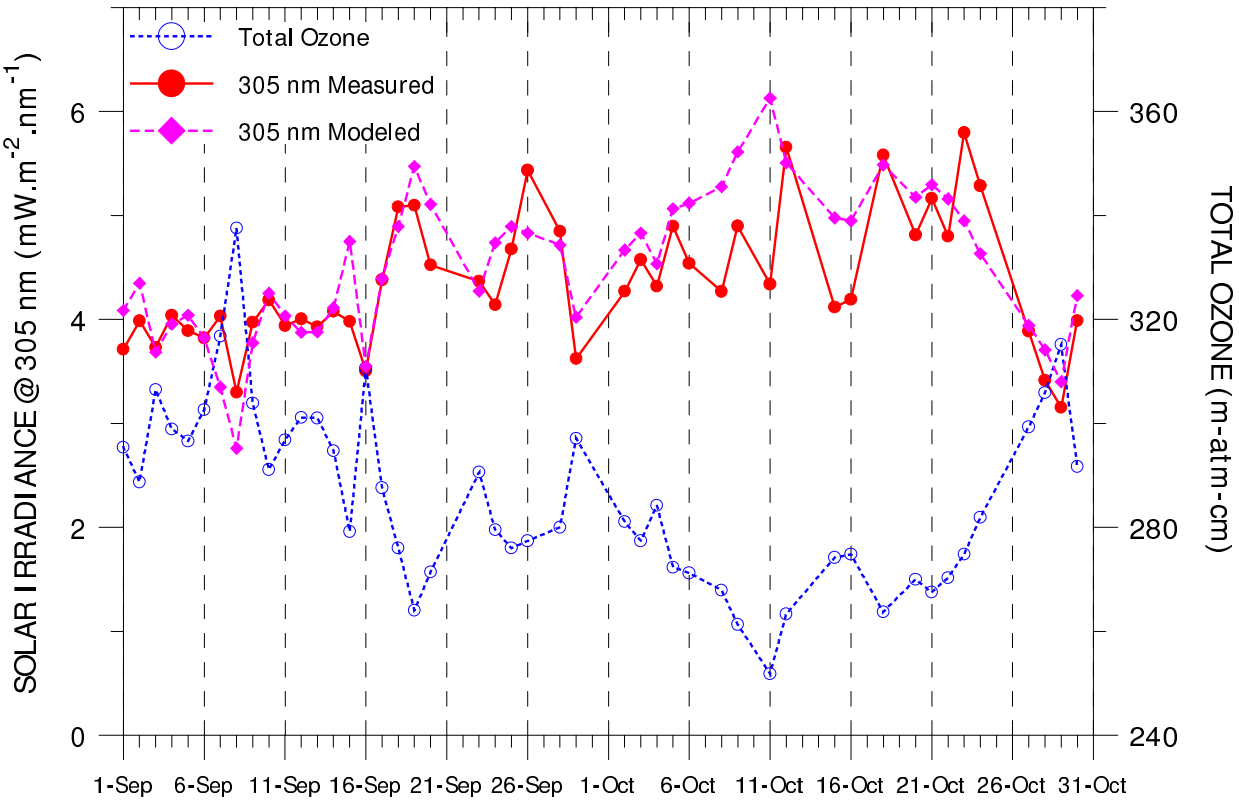

Figure 3.21: Total ozone and global UV irradiance measurements at Thessaloniki, Greece for the period Sep-Oct 2001.

c) A Sahara dust event versus a clean case (25-Sep-2001 vs 17-9-2001)

d) A pollution episode, where the total ozone decline is accompanied by a decrease in UV irradiance, compared with a clean case (11-Oct-2002 vs 4-Oct-2002).

The above mentioned cases are presented in Figure 3.21. This figure shows the total ozone measurements and the measurements of the global irradiance at 305 nm, a wavelength where absorption by ozone is very strong and the accuracy of the measurements better than 5%, for the period of two months. The circles show the measured values of the UV irradiance, while the diamonds show the modeled values assuming only the effect of ozone absorption in the calculations. The differences between the two curves show the effect of the aerosols on the attenuation of the UV irradiance at the surface.

Measurements of global and diffuse irradiance and of direct-to-diffuse irradiances ratio were compared with model calculations, which were based on the actually measured total ozone column and aerosol optical depth. From these comparisons we determined the values of SSA for which the model and the measurements were in agreement of better than 1%. Depending on the sensitivity of each quantity to changes in SSA, more than one values of SSA may satisfy the above condition. The mean of these values was considered the effective single-scattering albedo of the layer above the measuring site. For the same cases we calculated the mean lidar ratio as determined by the nearest in time measurement with the Raman lidar of LAP. For all these cases we also calculated the ratio of the spectra that correspond to high aerosol load over the ones that correspond to clear aerosol conditions. The results are listed in table 3.8. These results show the attenuation of the UV irradiance at

DATE	Remarks	Effective SSA	Mean LR	UV attenuation
9-8-2001 vs	High SO_2	0.91	70	20%
16-8-2001	Clean	0.88	-	
13-9-2001 vs	Same TOZ	0.77	10	10%
29-10-2001	Same AOD	0.87	80	
25-9-2001 vs	Sahara dust	0.83	30	5-10%
17-9-2001	Clean	0.89	10	
11-10-2001 vs	Polluted (hazy)	0.85	60	20%
4-10-2001	Clean	0.88	75	

Table 3.8: Effective SSA and mean lidar ratio for cases selected from the EARLINET database

the Earth's surface due to different aerosol types and also show independent determination of SSA and LR, which depend on the microphysical properties of the aerosol. However the number of cases is limited and does not allow for the moment any conclusions. As it is demonstrated in the table same AOD and same TOZ show differences up to 10% in the UV irradiance attributed to differences in the aerosol type (see LR and SSA). SO2 plumes are accompanied with extreme high AODs and cause an attenuation of 20% in the UV.

3.13.4 Plan and objectives for the next period

During the next period the above methodology will be applied to all quasi-simultaneous spectral UV and lidar measurements available at LAP and NTUA in order to be able to have a statistical presentation of the results. In addition UV and AOD data are expected from MPI-Hamburg (LACE experiment), IFU and the University of Munich. These data are expected to significantly increase the number of cases where the determination of UV attenuation, effective SSA and mean LR are possible and thus will allow to meet the objectives of WP13. One paper based on the activities within the WP13 of EARLINET will be submitted to ILRC21, while a journal paper is in preparation.

3.14 WP14, Statistical analysis

by Volker Matthias

This workpackage is based on the routine measurements performed since more than one year and a half at each EARLINET station. The collected data now allows first steps in the statistical analysis. Because at some German stations (e.g. at Hamburg) the routine observations began already in the end of 1997 in the frame of the German lidar network, these timeseries cover already more than four years of measurements. Therefore some of the methods that are planned be applied to all stations have first been demonstrated for Hamburg.

3.14.1 Methods

For the first analysis, only the quantitative Raman measurements giving aerosol extinction profiles have been used. They are performed each week on Monday and Thursday evening directly after sunset if no low clouds, fog or rain prevent them. For the statistical evaluation only one profile for each of those days is used to avoid a bias for "fair weather" situations. For the same reason also days with low clouds are included in the statistics, if some data points could be taken below the cloud layer. The number of collected profiles at the individual stations mainly depends on the mean local cloud coverage, leading to more measurements in southern Europe than at the northern stations. This especially holds for the winter months. However also some lidar system parameters like typical necessary averaging time for an extinction profile and the lowest altitude for a full overlap between laser beam and telescope field of view determine the number of usable profiles. Up to now it varies between 26 and 114 extinction profiles collected in 19 months and stored in the data base.
Because most of the aerosol particles can be found in the planetary boundary layer (PBL), the statistical evaluation has first been restricted to this layer. Typical PBL heights are between only few hundred meters (especially in winter) and 3 to 4 km on some days in summer. Because the lowest data point of the lidar profiles is typically between 500 and 700 m above ground, mean values of the aerosol extinction in the PBL have been derived by extrapolating this lowest data point down to ground and then integrating over the whole layer. This assumption can in most cases be made without large errors because the boundary layer is usually still well mixed at sunset when the measurements are taken. In those few winter cases when the lowest measurement height is above the boundary layer, representative extinction values can not be determined for the lowest layer and the cases are excluded for the statistics. The determination of the boundary layer height out of the lidar data is done looking at the most significant gradient in the range corrected lidar signal, which is due to a high decrease in aerosol backscatter caused by lower particle concentration and humidity above the PBL.

3.14.2 Results

From more than 140 extinction profiles measured at Hamburg in the UV at 351 nm (up to 30 November 2000) or 355 nm (since then) a mean annual cycle of the aerosol optical depth and the mean aerosol extinction in the PBL has been plotted (figure 3.22). The values show large scattering with highest values in late summer and early fall. A second less pronounced maximum is found in spring. Lowest values occur in winter which is especially true for the optical depth. This is connected with

	aerosol extinction				optical depth			
category	μ $[10^{-4}\mathrm{m}^{-1}]$	σ $[10^{-4}\mathrm{m}^{-1}]$	γ	median $[10^{-4}\mathrm{m}^{-1}]$	μ	σ	γ	median
1998 - 2001	1.88	1.17	1.65	1.60	0.25	0.19	1.76	0.20
1998	2.05	1.50	1.87	1.70	0.26	0.21	1.30	0.19
1999	2.09	1.18	0.91	1.82	0.30	0.25	1.58	0.20
2000	1.63	0.96	1.26	1.48	0.23	0.17	1.86	0.18
2001	1.91	1.17	1.71	1.60	0.24	0.15	1.03	0.20

Table 3.9: Characteristic quantities of the frequency distribution of the aerosol extinction and optical depth in the boundary layer in Hamburg, distinguished between the 4 years of measurements. μ: average, σ: standard deviation, γ: skewness.

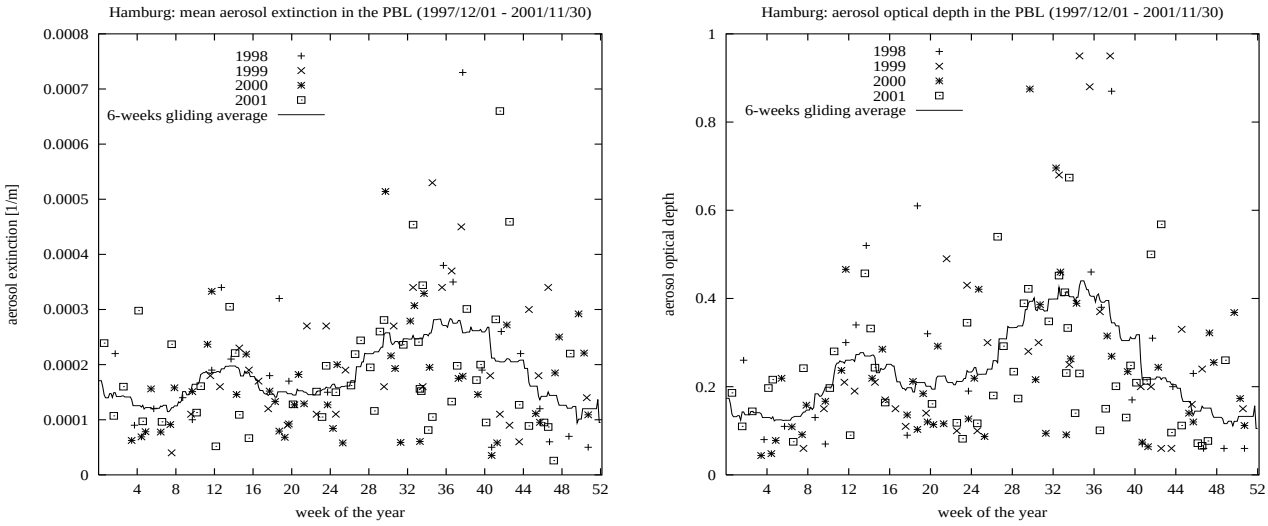

Figure 3.22: Annual cycle of the mean aerosol extinction and the aerosol optical depth in the planetary boundary layer in Hamburg 1 December 1997 - 30 November 2001.

lowest boundary layer heights between November and January.
An annual cycle of the planetary boundary layer height is shown in figure 3.23. Obviously PBL heights have their largest values in summer (ca. 1500 m in average) and their lowest values in winter (ca. 1000 m). Assuming a sinusoidal shape of the mean PBL heights with a one year period, one gets highest values around July 14 which is a phase shift against the maximum of the incoming solar radiation of 24 days. However, there is a wide spread of the individual values (mean value is 1347 m, standard deviation is 510 m) and relatively low PBL heights of ca. 800 m can appear in summer as well as in winter. On the other hand the largest values (PBL height $>$ 2000 m) appear mainly between March and October.
A statistical evaluation of the mean aerosol extinction and the optical depth in the PBL for the 4 years of measurements gives a mean aerosol extinction of $1.88 \cdot 10^{-4}\mathrm{m}^{-1}$ and a mean optical depth of 0.25 at 355 nm. The standard deviation of more than 60 % for extinction and more than 75 % for optical depth shows the large variability of the individual values. The interannual variability is much smaller and stays below 20 % for the 4 years of observations. The probability distributions of extinction and optical depth show high skewness with γ-values between 0.91 and 1.87 (see table

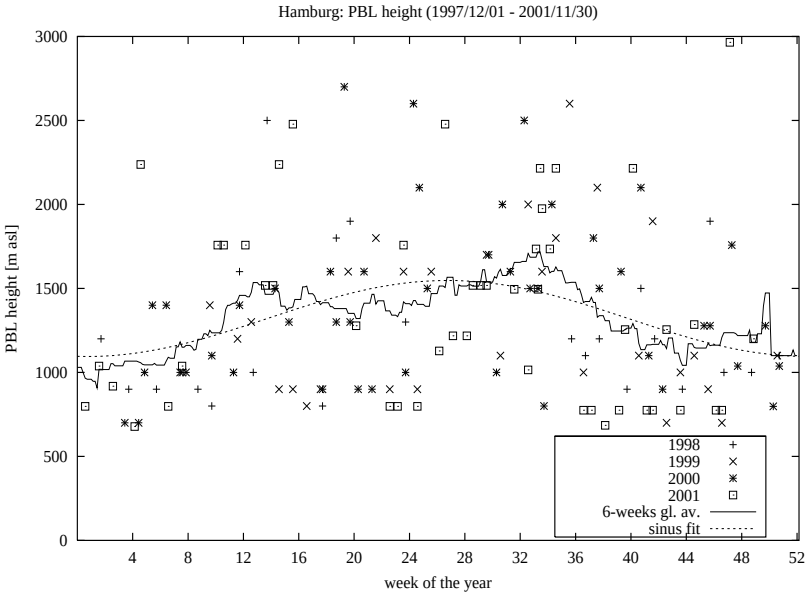

Figure 3.23: Annual cycle of the planetary boundary layer height in Hamburg December 1 1997 - November 30 2001. Data points and six weeks gliding average are plotted together with a sinus fit.

3.9) as typical for many meteorological quantities with only positive values. Therefore the median is much more representative for most likely values than the mean. A fit to the cumulative probability distribution has been made showing that the measured distribution is very close to a lognormal distribution (figure 3.24). Goodness of fit tests confirm this result.
The aerosol extinction profiles from 8 additional EARLINET stations have been taken and a statistical evaluation has been done as shown for Hamburg although the time series which is available up to now is much shorter than for Hamburg and includes only 19 months of measurements (between 26 and 114 profiles). First results from Aberystwyth (Wales), Napoli, Lecce and Potenza (all Italy) show similar mean values in the lowest 2000 m in Aberystwyth and higher values in Lecce, Napoli and Potenza compared to the same height interval in Hamburg.

3.14.3 Summary and outlook

Statistical parameters of the aerosol distribution at one EARLINET station (Hamburg) have been calculated and some of the methods that will we applied to the whole data set have been demonstrated. During the automatic data processing of the aerosol profiles from all EARLINET stations, problems with some small differences in the file format and with the existence of a few questionable profiles occurred. Therefore all files stored up to now will be checked again by the individual groups and they will calculate statistical numbers for their station for five different layers: 0-1 km, 1-2 km, 2-5 km, 5-12 km and the dust layer. Those results will be based on both aerosol extinction and backscatter profiles. Afterwards comparative studies using data from all EARLINET stations will be made.

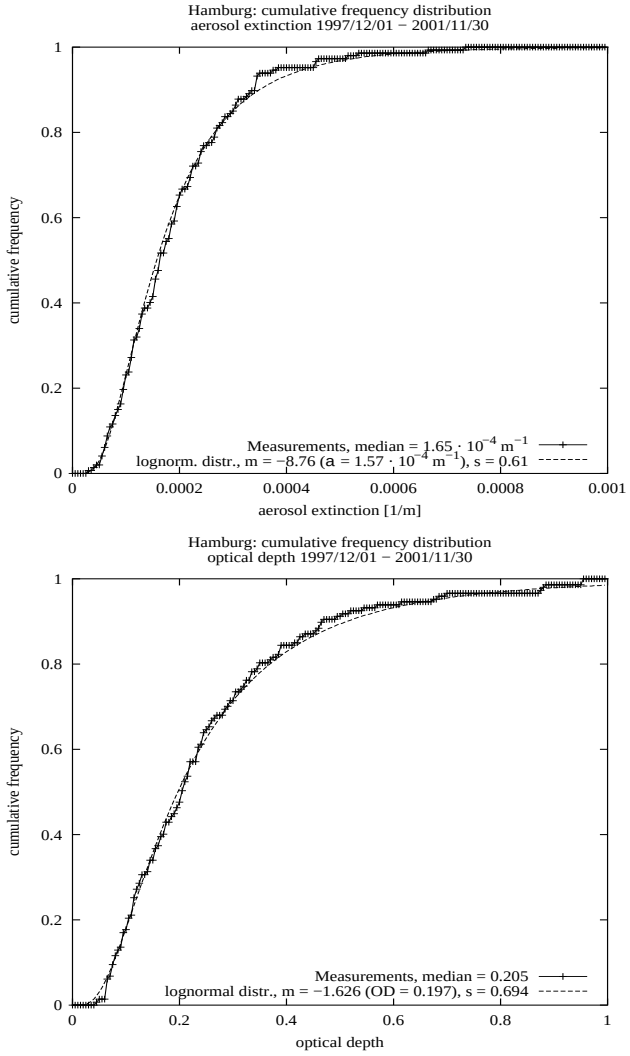

Figure 3.24: Cumulative distribution functions for the measured aerosol extinction and optical depth in the boundary layer at Hamburg. m denotes the mean of the logarithmic values and s their standard deviation. Lognormal distributions have been fitted to both measured distribution.

3.15 WP15, Lidar ratio data base

by Gelsomina Pappalardo

3.15.1 Objectives

The main objective of WP15 is the compilation of a statistically significant data set concerning the ratio of aerosol extinction to backscatter (lidar ratio) starting from both regular and special measurements. Lidar ratio data are retrieved from simultaneous and independent lidar measurements of aerosol extinction and backscatter. These measurements, in conjunction with information on the air masses characteristics, will provide information on microphysical properties of the aerosol over a wide range of meteorological conditions on continental scale. Moreover, this data set will be very useful to investigate the climate impact of aerosols.

3.15.2 Methodology

To achieve the objectives of WP15, all the EARLINET lidar stations providing simultaneous aerosol extinction and backscatter measurements have been selected. Eleven lidar stations have the capability of measuring Nitrogen Raman scattering in the UV simultaneously to the elastic backscatter; among these lidar stations, two have the capability to measure Nitrogen Raman scattering also in the visible domain (Kühlungsborn and Leipzig). One lidar station has a scanning capability (München) and hence these data can be used to retrieve the aerosol extinction profile. Within the EARLINET community, a big effort has been devoted to upgrade the Raman capability and an increasing number of stations is going to be equipped with Raman channels. In order to assure high quality for the aerosol extinction data, an intercomparison of the algorithms used by each group for Raman technique has been performed. Algorithms used for the Raman extinction retrieval have been tested using synthetic lidar data covering different experimental conditions, such as different level of noise and timing variable aerosol properties. The intercomparison showed that the aerosol extinction evaluation can be accomplished with good accuracy for all participating groups.
Lidar ratio data are retrieved from simultaneous and independent measurements of aerosol extinction and backscatter. For the lidar ratio evaluation, extinction and backscatter are obtained with the Raman method and are processed with the same averaging in height and time. These aerosol extinction and backscatter data have been delivered to the data base, for all involved stations, in a common format for Raman files.

3.15.3 Scientific achievements

In table 3.10 all the stations providing independent aerosol extinction measurements are listed with the corresponding used technique and wavelength. All lidar ratio data that have been delivered in the correct “Raman format to the EARLINET data base have been collected and a statistical analysis has already started. Data have been divided into regular and special measurements. Regular measurements can provide a significant data set of lidar ratio values obtained over a broad range of meteorological conditions on a continental scale. Special measurements can provide a data set of values of the lidar ratio during special events (Saharan dust outbreaks, forest/industrial fires, photochemical smog episodes, volcanic eruptions, etc.) over Europe. Both these data set are important for investigating the aerosols impact on climate. In particular, lidar ratio data have been divided in different typologies concerning different categories of measurements defined in the common database:

station		technique	wavelength
Aberystwyth	ab	Raman	355 nm
Athens	at	Raman	355 nm
Hamburg	hh	Raman	351 nm
Jungfraujoch	ju	Raman	355 nm
Kühlungsborn	kb	Raman	355 nm and 532 nm
L'Aquila	la	Raman	351 nm
Lecce	lc	Raman	351 nm
Leipzig	le	Raman	355 nm and 532 nm
München	mu	Scanning	355 nm and 532 nm
Napoli	na	Raman	351 nm
Potenza	po	Raman	355 nm
Thessaloniki	th	Raman	355 nm

Table 3.10: Lidar stations (providing simultaneous aerosol extinction and backscatter measurements), used techniques and wavelenghts.

- Routine measurements establishing the climatology
- Saharan dust events
- Forest fires events
- Photochemical smog events
- Special stratospheric measurements
- Differences rural/urban aerosols
- Mount Etna eruption
- Cirrus clouds observations

Of course, the largest data set regards routine measurements. Figure 3.25 shows the calculated mean values of the lidar ratio vertical profiles in the first 1.5 km of height above lidar station for each group. The number of measurements is not the same for each station reflecting quite different weather conditions. Because of technical problems, there are not extinction measurements in L'Aquila during the first year of measurements, while Napoli has to deliver Raman files in the right format for the period May 2000 - November 2000 and Thessaloniki started Raman measurements in March 2001. Results from Athens, Jungfraujoch and Kühlungsborn are not reported in the figures because these groups have to reprocess all data in the right Raman format.
Mean values of the lidar ratio for the whole period of measurements have been calculated in the first 1.5 km of height above each lidar station starting from the routine measurements establishing the climatology. These values are reported in table 3.11 together with the mean values obtained for autumn-winter and spring-summer periods. All the mean lidar ratio values calculated in the period May 2000 - November 2001 are in the range 44 - 65 sr, while the winter mean values range from 43 sr up to 71 sr and the summertime mean values range from 38 sr up to 59 sr. For each station, the seasonal variation and the frequency distribution of the mean value of the lidar ratio in

station	wavelength (nm)	mean value (sr)	winter mean value (sr)	summer mean value (sr)
Aberystwyth	355	54	51	55
Hamburg	351	55	54	56
Jungfraujoch	355	45	45	45
L'Aquila	351	58	55	59
Lecce	351	44	52	38
Leipzig	355	61	71	57
	532	70	83	60
Napoli	351	59	64	53
Potenza	355	52	46	55
Thessaloniki	355	49	43	58

Table 3.11: Mean values of the lidar ratio calculated in the first 1.5 km of height above lidar station.

the first 1.5 km of height have been studied. This is the first time that mean values of lidar ratio have been measured on continental scale starting from a large data set covering 20 months of systematic observations. Therefore there will be significant interest in the scientific community to use these data for the improvement of both global/regional atmospheric and climate prediction models. Moreover, these data will be important for aerosols studies performed by future space based lidar.

3.15.4 Plan and objectives for the next period

The statistical analysis on the lidar ratio data set obtained during the first almost two years of measurements in the framework of the project will continue. Mean values of lidar ratio will be calculated for different ranges of height starting from the routine measurements. Further analysis on the lidar ratio data set will regard special measurements. In particular, there are already many cases of lidar ratio measurements during Saharan dust events. Moreover, lidar ratio data will be studied in more details for the case of the Etna eruption. In this case, lidar ratio evaluation can help to distinguish between aerosol of volcanic origin and dust from Sahara. Particular care will be devoted to study lidar ratio data in cirrus clouds. When possible, the wavelength dependence will be studied both for regular and special measurements. Results will be combined with information on the air-mass characteristics. Data provided by the groups performing simultaneous aerosol extinction and backscatter measurements will be collected continuously in order to increase the data set concerning the lidar ratio. To this purpose, it is important to note that an increasing number of stations is going to be equipped with Raman channels, so that more data will become available in the next future. Moreover, extinction measurements performed by using the multiple zenith angle technique will be delivered to the data base together with the backscatter, with the same averaging in height and time and these measurements will also improve the lidar ratio data set in the next future.

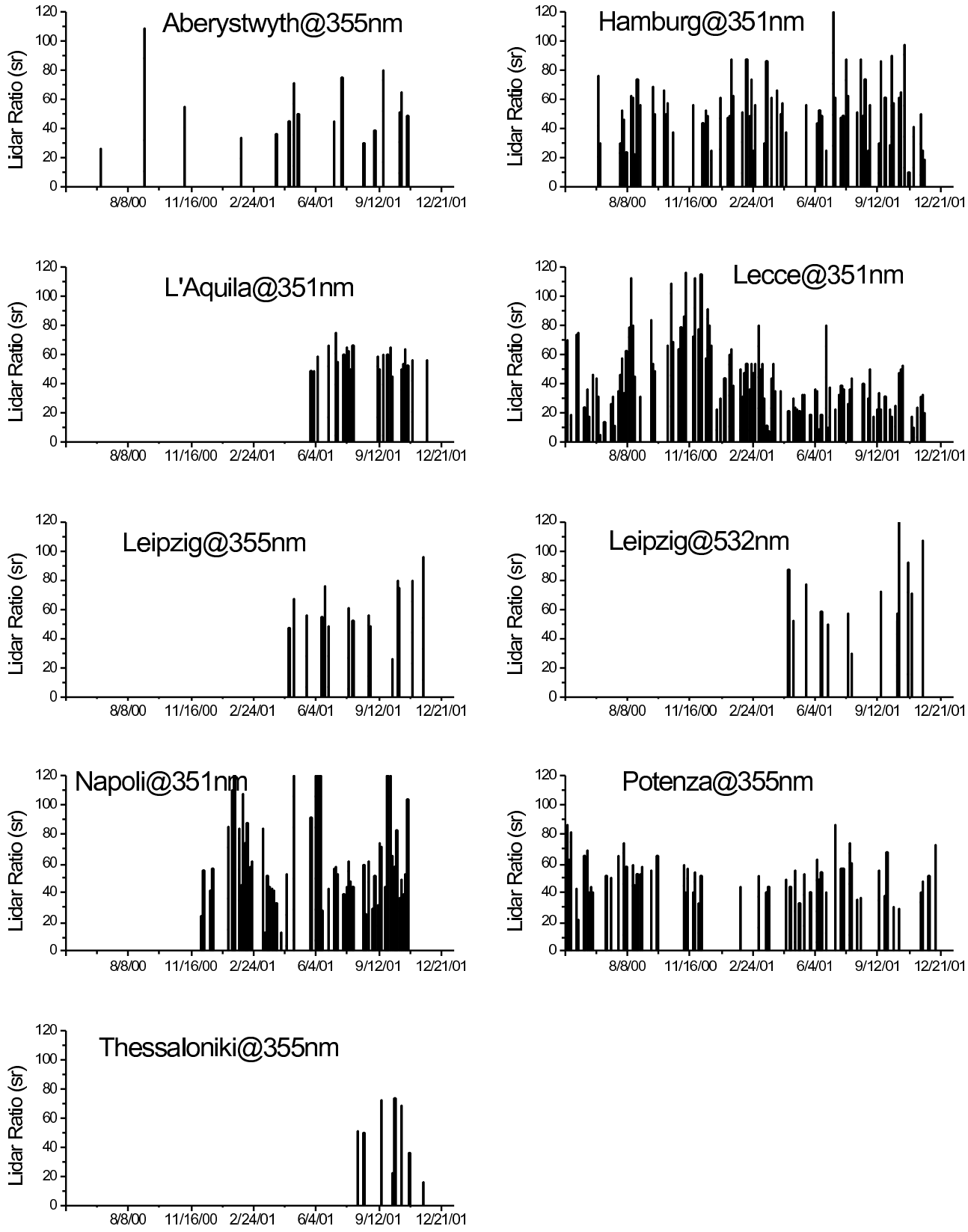

Figure 3.25: Mean values of the lidar ratio data in the first 1.5 km of height above each lidar station starting from all the climatological data.

3.16 WP16, Analysis of source regions

by Thomas Trickl

3.16.1 Objectives

Based on the aerosol soundings within the lidar network the importance of different medium and long-range transport pathways will be determined contributing to the aerosol distribution over Europe on a more or less regular basis. Although also some effort to determine European contributions to the aerosol budget was promised the focus is on extra-European aerosol sources such as the Sahara desert, the U.S.A. and wild fires in North America, in particular in the boreal regions of Canada. As to the European contributions it is anticipated that it will be extremely difficult to go beyond the achievements of Work Package 7 (Aerosol Modification Processes) due to the absence of modelling and lidar measurements in some of the principal European source areas. In 2002, also the Meltemi winds over the Agean Sea were identified as an important source of air pollution over Greece, originating in the heavily industrialized zones around the Black Sea.

3.16.2 Methods

Aerosol signatures in the free troposphere are an excellent tracer for boundary-layer air. The importance of long-range transport from different source regions may be estimated from relating the cases with aerosol in the free troposphere to the total number of routine measurements. A more refined analysis will be based on distinguishing various classes of backward trajectories. The determination of relative fluxes can be attempted, but may be strongly biased due to elimination by processes such as washout in fronts.

3.16.3 Scientific achievements

Partners for WP16 are the institutes in Hamburg, Athens (NTUA), Thessaloniki, Barcelona, Minsk, Portugal, Munich and Garmisch-Partenkirchen (IFU). Although most of the analyses will be made during the final year of EARLINET first results have already been obtained.
Most progress has been achieved for the investigation of Saharan dust event, which is a joint effort with Work Package 7 (Observation of special events), co-ordinated by NTUA. These results have been summarized in a manuscript recently submitted to the Journal of Geophysical Research. Observations have been made at EARLINET stations in the Mediterranean area, Central Europe and in the north east. It was verified that the air masses from the desert are most commonly lifted to the free troposphere by prefrontal upward transport. Typical upper boundaries over Italy and Greece are 2.5 to 5 km, over the Northern Alps 5 km. The observation at more remote stations (even as far as Belarus) is a remarkable achievement of EARLINET. It was found that the upper boundary above the stations in northern Central Europe and Belarus may be high as 7 to 11 km.
In addition, the potential input from a few North American wild fires was examined. The trajectory analyses and the inspection of satellite images has not been sufficiently conclusive. Thus, the analysis is not yet completed.
A concept for a statistical analysis of the aerosol import to the free troposphere over Central Europe was prepared by IFU. The analysis of a few years of the data from the big aerosol lidar of IFU (minimum height 3 km) has shown that there is an interesting annual seasonal cycle of the aerosol with a pronounced spring peak. The main contribution to this spring peak will be examined by a

trajectory analysis. In order to improve the statistical relevance the analysis must be extended over a longer period of time. The IFU series focussing on stratospheric aerosol starts in 1978, an extension of the profiles down free tropospheric should be available at least for the period after 1990. We have started to put a new key question: Is there a good correlation with the well-known spring maximum of ozone and is there a common origin of these observations? The analysis will be complemented by including data from relevant network stations, even of stations not officially contributing to this work package, e.g., Aberystwyth as the first station to monitor air masses entering Europe.
As a new source area relevant for the aerosol distribution over Greece the heavily polluted region around the Black Sea was identified. Mostly in July and August the northwesterly Meltemi winds advect pollution from that area to the Aegean Sea and Greece. The examples obtained in 2001 show an upper boundary of these contributions of up to 4 km. Due their occurrence in the free troposphere, they are clearly lower than the local pollution over Athens, but still quite remarkable.

3.16.4 Socio-economic relevance and policy implications

The importance of intercontinental transport has long been overlooked. Signicant amounts of trace gases such as ozone, but also some aerosol are transported from continent to continent. This should have severe implications for the most productive source regions for air pollution such as South-East Asia, North America and Europe.

3.16.5 Discussion and conclusion

A full discussion is not yet possible at this stage of the project.

3.16.6 Plan and objectives for the next period

The work will proceed as indicated in Sec. 3.16.3. The focus continues to be on extra-European source areas. The analysis of the North-American contribution the free tropospheric aerosol distribution will be intensified with some emphasis on the impact of the huge wild fires frequently occurring during the dry season.

3.17 WP17, Microphysical retrieval algorithms

by Christine Böckmann

3.17.1 Objectives

Several instruments of the EARLINET lidar network deliver information on particle extinction and backscatter coefficients at multiple wavelengths. This information can be used to invert physical particle properties such as particle size, number, surface-area, and volume concentration, as well as complex refractive index. However, the inversion problem in a mathematical sense is non-linear and ill-posed and its solution requires the application of appropriate mathematical regularization methods. Therefore, one part of the project is to develop, to improve and to investigate inversion algorithms for optical data sets, which are obtained with different lidar systems of the network.
The set of backscatter coefficients at 355, 532, and 1064 nm and of extinction coefficients at 355 and 532 nm (case 3+2) is the standard output of an advanced aerosol Raman lidar based on a single Nd:YAG laser. The stationary systems at IAP Kühlungsborn and IfT Leipzig make use of this configuration in EARLINET and some other groups plan an upgrade of their instruments to this standard output (Jungfraujoch-Station, Lausanne; Station of Potenza). The IfT Leipzig system has the possibility to deliver three backscatter coefficients at 400, 710 and 800 nm (case 6+2) , additionally. The IBNANB Minsk is able to get between two- and four-frequency sounding results.
The main objectives of WP17 are focused on the development of suitable retrieval algorithms for various systems and on theoretical mathematical investigations concerning the complex refractive index, the shape of the aerosol particles and new regularization techniques.

3.17.2 Methodology

The mathematical model, which relates the optical and the physical particle parameters, consists of a Fredholm system of two integral equations of the first kind for the backscatter and extinction coefficients β^{Aer} and α^{Aer}:

$$\beta^{Aer}(\lambda, z) = \int_{r_0}^{r_1} K_\pi(r, \lambda, m, s)\; n(r, z)\; dr = \int_{r_0}^{r_1} \pi\; r^2\; Q_\pi(r, \lambda, m)\; n(r, z)\; dr, \tag{3.1}$$

$$\alpha^{Aer}(\lambda, z) = \int_{r_0}^{r_1} K_{ext}(r, \lambda, m, s)\; n(r, z)\; dr = \int_{r_0}^{r_1} \pi\; r^2\; Q_{ext}(r, \lambda, m)\; n(r, z)\; dr, \tag{3.2}$$

where r denotes the particle radius, m is the complex refractive index, s is the shape of the particles, r_0 and r_1 represent suitable lower and upper limits, respectively, of realistic radii, λ is the wavelength, z is the height, n is the particle size distribution we are looking for, K_π is the backscatter and K_{ext} is the extinction kernel. The kernel functions reflect shape, size, and material composition of the particles.
The following formulas hold for extinction and backscatter efficiencies of homogeneous spheres:

$$Q_\pi = \frac{1}{k^2 r^2} \Big| \sum_{n=1}^{\infty} (2n+1)(-1)^n (a_n - b_n) \Big|^2,\; Q_{ext} = \frac{2}{k^2 r^2} \sum_{n=1}^{\infty} (2n+1) \mathrm{Re}(a_n + b_n), \tag{3.3}$$

where k is the wave number defined by $k = 2\pi/\lambda$ and a_n and b_n are the coefficients which one can get from the boundary conditions for the tangential components of the waves. Now Eqs. (3.1) and (3.2) are formulated into a more specific and more solid form:

$$\Gamma^{Aer}(\lambda, z) = \int_{r_0}^{r_1} K^{v}_{\pi/ext}(r, \lambda, m)\; v(r, z)\; dr = \int_{r_0}^{r_1} \frac{3}{4r}\, Q_{\pi/ext}(r, \lambda, m)\; v(r, z)\; dr, \tag{3.4}$$

where the $v(r, z)$ term is the volume concentration distribution we are finally looking for. Γ^{Aer} stands for β^{Aer} and/or α^{Aer}, respectively, depending on the measurement data. The determination of the particle volume distribution v from a small number of backscatter and extinction measurements is an inverse ill-posed problem and because the refractive index m in the kernels $K^{v}_{\pi/ext}$ is an unknown, too, the problem is a highly nonlinear one, i.e., solutions are non-unique and highly oscillating without the introduction of appropriate mathematical tools such as discretization and regularization.

3.17.3 Scientific achievements

Algorithm I (UPIM): Based on mathematical knowledge, a special hybrid regularization technique was developed. This hybrid regularization technique is designed to work with different kind and number of optical data, i.e., experimental data obtained with different systems at various wavelengths can be evaluated. The algorithm does neither require any *a priori* information on the analytical shape of the investigated distribution function nor an initial guess of it. Even bimodal and multimodal distributions can be retrieved without any knowledge of the number of modes in advance.

Software implementation
Based on the development of the hybrid regularization technique in the retrieval of aerosol size distribution a user friendly software implementation was developed. This paragraph deals with the description of the implementation *version 0.9 beta* for Windows-PC's. The software is able to evaluate measurements or to examine simulations, see Fig. 3.26.

Firstly, for the initialization of simulations a lot of different possibilities are allowed. One can deal with homogeneous spheres, spheroids with some different aspect ratios and with inhomogeneous layered spheres. Concerning the used size distributions on the one hand mono-modal as well as multi-modal distributions and on the other hand various kinds, e.g. log-normal and gamma distributions with different parameters, are possible to use, see Fig. 3.26.
Secondly, one can deal with correct and noisy simulated extinction and backscatter coefficients of different noise level and can make with one noise level a lot of randomly different data sets.
Thirdly, the used wavelengths can be written directly into the input window and can be saved or can be loaded from a suitable file. The format of the wavelength input file is an ASCII-file with two columns. The first column indicates with the value "1" that the following wavelength belongs to an extinction coefficient and with the value "2" that the following wavelength belongs to a backscatter coefficient. The second column comprise the wavelengths, see Fig. 3.26.
Finally, one has to write the desired complex refractive index which can depends on the wavelength into a second input window.

After the initialization one is mainly interested in the retrieval of the volume distribution. Therefore, it is necessary to choose suitable regularization parameter ranges for using the hybrid regularization

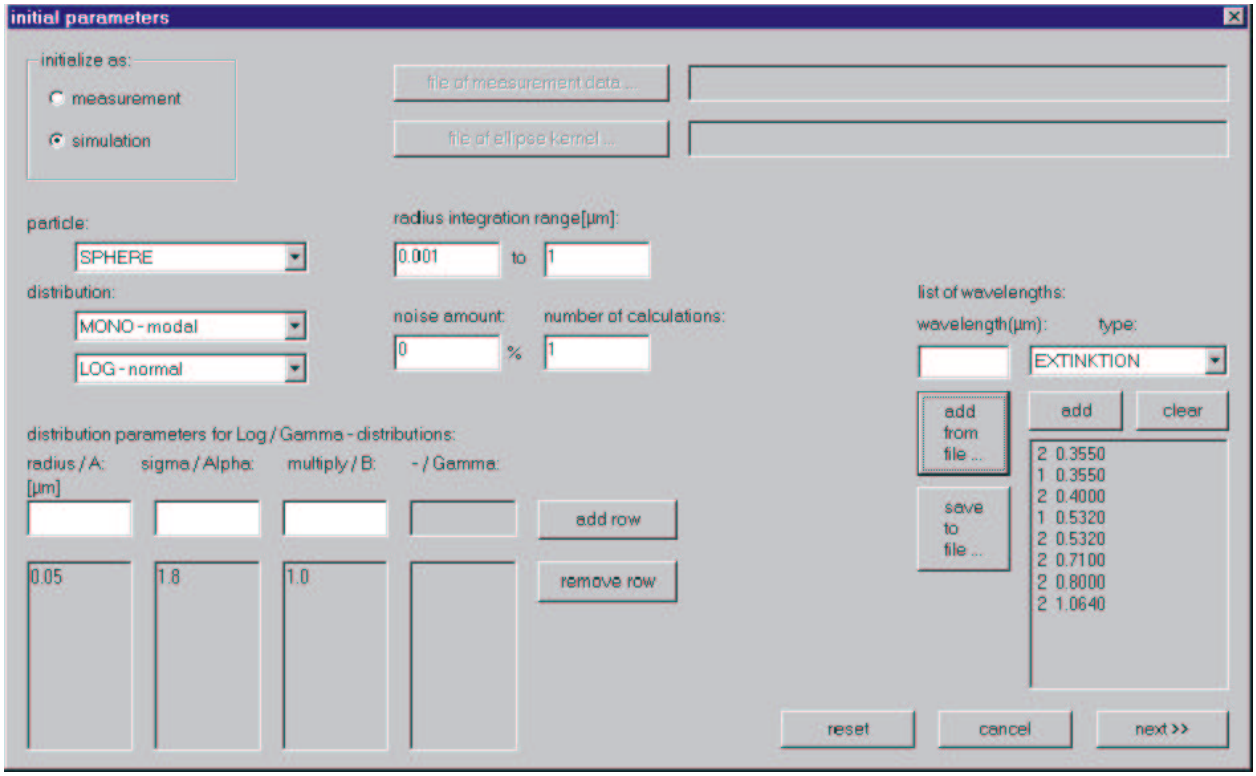

Figure 3.26: Input window for measurements and for initialization of simulation, respectively.

technique. Fig. 3.27 contains all the necessary information.

Firstly, one has to choose a suitable norm. Our experiences show that in all most all cases the Tschebyscheff-norm is the best one. The same is true for the choice of the distribution of the used B-spline functions where the distribution with respect to the left sided roots of the Tschebyscheff-polynomials is the best one.
Secondly, one can deal during the retrieval process with homogeneous spheres, spheroids with some different aspect ratios and with inhomogeneous layered spheres.
Thirdly, the dimension range of the projection, the order range of the B-splines and the integration ranges have to be given into the retrieval input window, see Fig. 3.27.
Finally, it is possible to start the inversion with known or unknown refractive index. In the last case one has to choose a suitable refractive index grid.

If the retrieval process is finished it is allowed -in the case of unknown refractive index retrieval- to select the solution domain of the refractive index by marking the desired domain, see Fig. 3.28.

The last retrieval step consists in recalculating the marked refractive index range and in creating tables with the determined microphysical parameters, see the next paragraph.

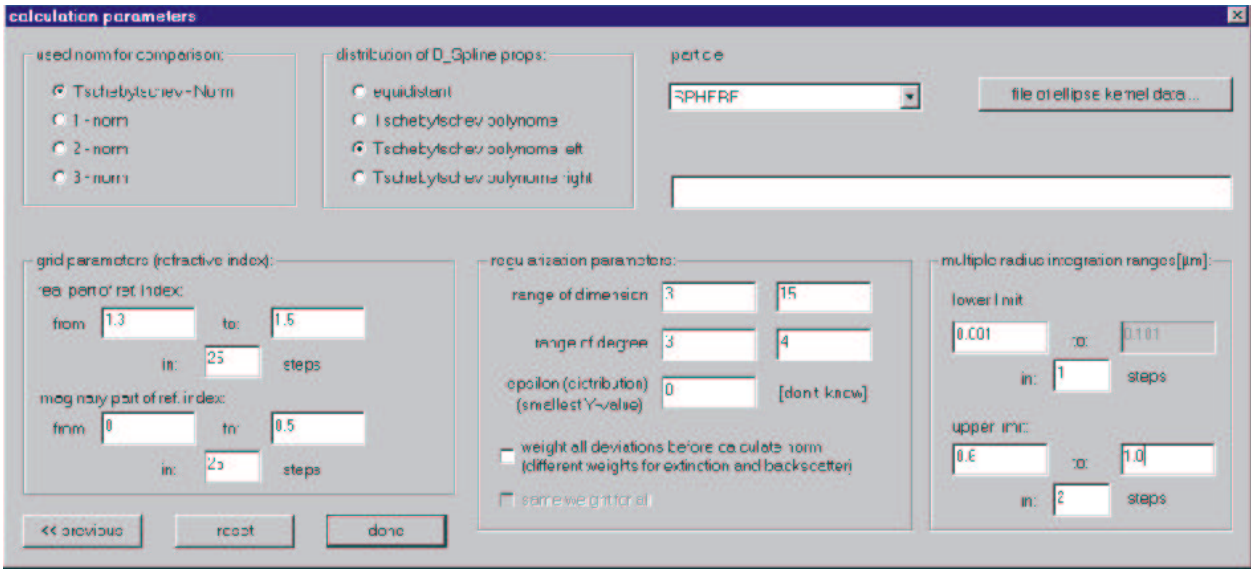

Figure 3.27: Input window for various parameters concerning the inversion and the regularization.

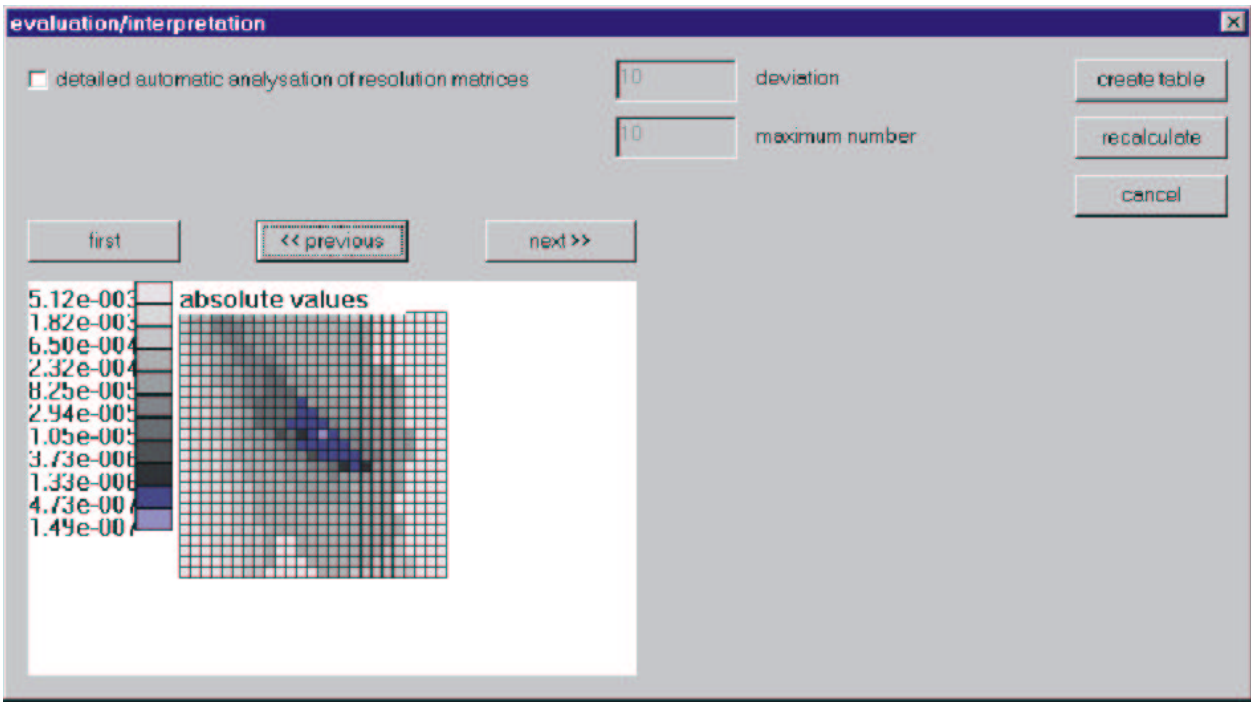

Figure 3.28: Output window of the retrieved refractive index range with respect to the absolute deviations to the input backscatter and extinction coefficients.

Simulation studies

After retrieving the volume or size distribution one can determine the microphysical parameters as ,e.g., the effective radius, i.e., the surface-area weighted mean radius, the total surface-area, volume and number concentrations:

$$r_{\text{eff}} = \frac{\int n(r)\, r^3 \, \mathrm{d}r}{\int n(r)\, r^2 \, \mathrm{d}r}, \;\; a_{\text{t}} = 4\pi \int n(r)\, r^2 \, \mathrm{d}r, \;\; v_{\text{t}} = \frac{4\pi}{3} \int n(r)\, r^3 \, \mathrm{d}r, \;\; n_{\text{t}} = \int n(r) \, \mathrm{d}r \qquad (3.5)$$

and the SSA.

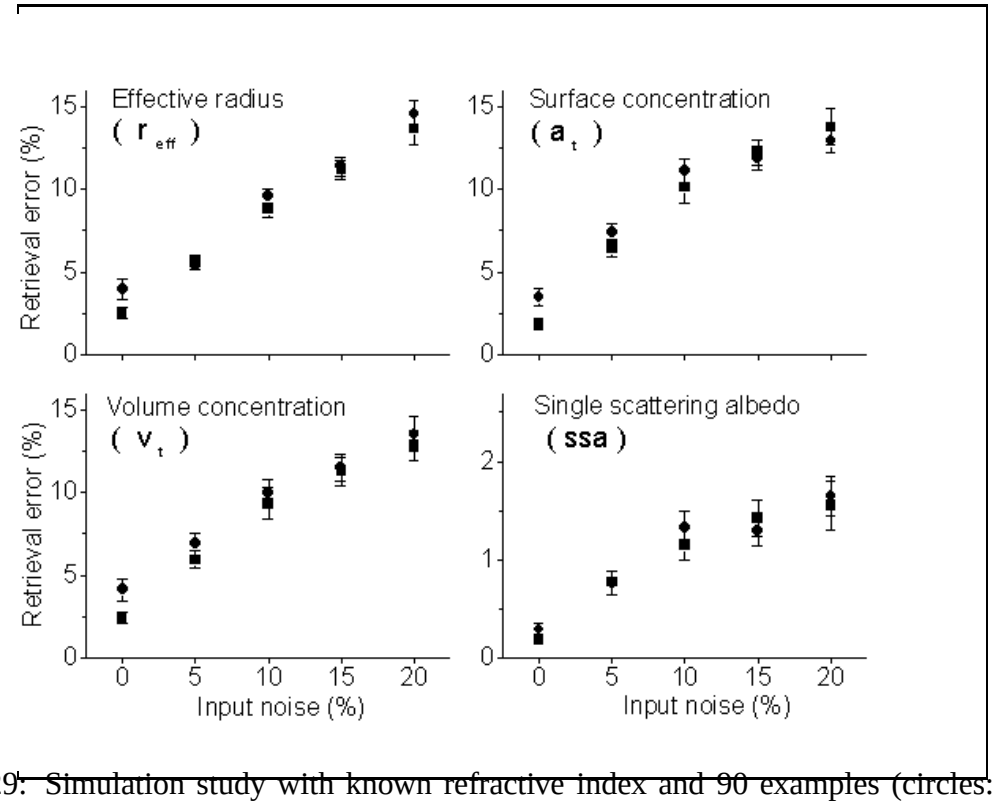

Figure 3.29: Simulation study with known refractive index and 90 examples (circles: case 3+2, squares: case 6+2).

Firstly, we investigate in an extensive simulation study with known complex refractive index by computing 90 examples with lognormal size distributions by using different mode radii (0.05, 0.1, 0.3 μm), mode widths (1.4, 1.6, 1.8), real parts (1.4, 1.55, 1.7), imaginary parts of refractive indices (0.0, 0.005, 0.01, 0.05, 0.1, 0.5) and normally distributed noise levels (0, 5, 10, 15, 20%) with 10 runs per noise level. Therefore, we compare the relative errors of the retrieved microphysical particle properties between the 3+2 case and a more extensive case 6+2 with three additional backscatter coefficients at 400, 710 and 800 nm, see Fig. 3.29 . In the noiseless case for 6+2 coefficients the errors stay well below 2.5% for the effective radius, the surface and volume concentration and about 0.2% for the SSA which is mainly influenced by the imaginary part of the refractive index which is known here. For 3+2 coefficients the errors increase to well below 5% and 0.4%, respectively. However, with increasing noise level on the input parameters α and β the retrieval errors grows up to 15% and to 2%, respectively, in the 20%-noise level in both cases (3+2, 6+2). In general, one observes that in all noisy data levels it is not important to make use of three additional backscatter coefficients. Therefore, by knowing the refractive index from, e.g., *in situ* chemical examinations

or almucantar measurements a 3-wavelength Raman lidar is suitable for retrieving microphysical particle properties from the optical ones.

Secondly, we investigate in the unknown complex refractive index case. Since in the previous case

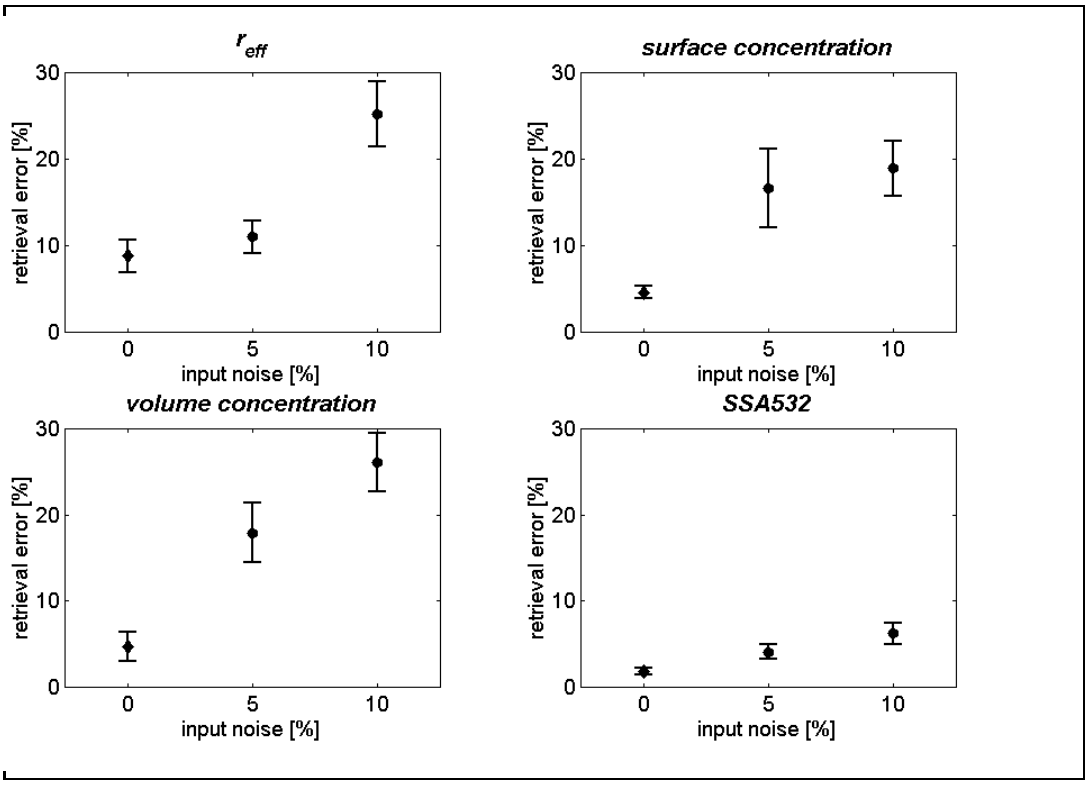

Figure 3.30: Simulation study with unknown refractive index for 3+2 coefficients (circles: 26, diamond: 6 examples).

we observed that different real parts of the refractive index influence only slightly the retrieval errors this simulation study is justified with 26 examples for 5 and 10% input noise. In the noiseless case the retrieval errors are situated between 5 and 10% for the first three microphysical parameters and for the SSA the error is again very small about 2%, see Fig. 3.30. That result is remarkable if one has in mind that from a mathematical point of view in that case the operators (3.1),(3.2), i.e., the kernel functions $\pi r^2 Q_{\pi/ext}(r, l; m)$ are not exactly known. The complex refractive index m is a second unknown with two parts in Eqs. (3.1),(3.2). For 10% input noise the retrieval errors are situated between 20 and 30% and about 8%, respectively. First results in comparison with the 6+2 case show the same behavior as in the previous case especially for the SSA. In contrast Fig. 3.31 shows that the retrieval of the refractive index is influenced by the number of used coefficients with increasing noise level. In the unknown refractive index case a 3-wavelength Raman lidar could also be suitable for retrieving microphysical properties from the optical ones but only if special care is taken concerning the measurement errors and conditions. Otherwise this hybrid regularization method could fail because of a few noisy input data only and ill-posedness.

Measurement results

As a measurement example we chose the six-wavelength lidar observation of the Institute for Tropospheric Research in Leipzig from 9. August 1998 of Lindenberg Aerosol Characterization Experiment (LACE 98), see [Wandinger et al., 2002]. The physical particle properties retrieved with our hybrid method could be validated by particle *in situ* measurements performed aboard the aircraft Falcon (German Aerospace Center) in the vicinity of the field site during the time of the lidar obser-

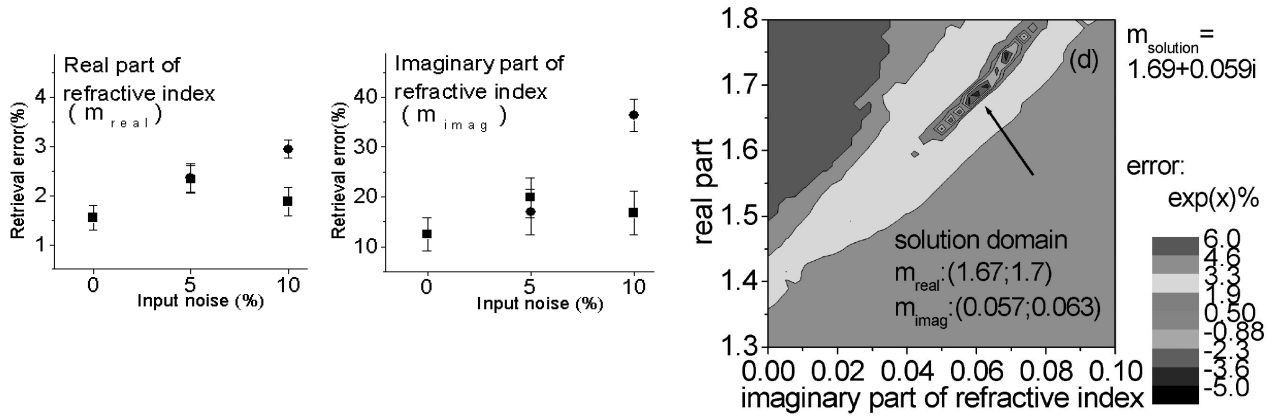

Figure 3.31: Retrieval errors for the additionally unknown refractive index (circles: 3+2 case, squares: 6+2 case): (a) real part, (b) imaginary part; (d) retrieval of the refractive index domain from LACE 98 measurements from 3.5-4 km, 2200-2400 UTC, for the 3+2 case.

vations. The measurement was characterized by an elevated biomass-burning particle layer between 3 and 6 km high. The orign was tracked back to intense forest fires in western Canada.
Firstly, the retrieved effective radius is in excellent agreement with the one from the *in situ* measurements whereas the volume and surface-area concentrations are slightly larger. There is a large deviation in particle number concentration. This value is critical in simulations, too. This is an ongoing work.
Secondly, comparing the results of the 3+2 case with the 6+2 case the first three parameters of Table 3.12 are in excellent agreement. Note that there was also very good agreement with a second inversion method, which was developed at the Institute for Tropospheric Research, see [Müller et al., 2001].
Thirdly, the real and imaginary part are slightly larger in the 3+2 case. This inaccuracy is caused by a larger possible solution domain, see Fig. 3.31(d), as in the 6+2 case, not shown here. Almost all simulation retrievals show the same behavior that the possible retrieved solution domain of the refractive index for the 3+2 case is larger. This fact reflects itself clearly in Fig. 3.31 (a),(b), too, and was discussed in the previous paragraph. However, the values of the refractive index are not directly comparable with the *in situ* data, see caption of Table 3.12.
Finally, the parameter set permits calculation of the SSA, which is a key parameter in climate impact studies.

Algorithm II (IfT): Improvements focused on the increase of the stability, and thus of the accuracy of the retrieved parameters. Narrow particle size distributions, or size distributions with a large amount of particles near or below a mean particle radius of 0.1 mm may cause large errors [Müller et al., 2000, Müller et al., 2002], because small particles become inefficient in their scattering properties. The necessity for reliable results in this size range was shown with the inversion of experimental data obtained with the institute's six-wavelength aerosol lidar during the Aerosol Characterization Experiment 2 (ACE 2; North Atlantic/Portugal, June/July 1997) [Müller et al., 2002], and the Indian Ocean Experiment (INDOEX; Indian Ocean/Maldives, February/March 1999) [Müller et al., 2001]. The retrieved microphysical parameters clearly indicated that anthropogenic pollution sources produce a significant amount of particles in this crucial size range.

For this reason several new tools were implemented or will be implemented in the near future. The

Parameter	*in situ* (A): $r \geq 1.5$ nm	*in situ* (B): $r \geq 50$ nm	case 3+2	case 6+2
r_{eff} (μm)	0.24±0.06	0.25±0.07	0.23 ±0.01	0.24±0.01
v_t (μm^{3}cm^{-3})	9±5	8±5	11±1	11±1
a_t (μm^{2}cm^{-3})	110±50	95±55	136±5	136±5
n_t (cm^{-3})	640±174	271±74	563±186	506±131
m_{real}	(1.56)	(1.56)	1.69±0.03	1.66±0.02
m_{imag}	(0.07)	(0.07)	0.059±0.005	0.053±0.004
$SSA(532$ nm)	0.78±0.02	0.79±0.02	0.78±0.01	0.79±0.01
$SSA(355$ nm)	-	-	0.72±0.01	0.74±0.01

Table 3.12: Microphysical particle properties retrieved from lidar data by regularized inversion in comparison with *in situ* measurements aboard the Falcon from 3.4-3.9 km. (A) airborne measurements on the basis of the complete particle size distribution, (B) under omission of the particle in the Aitken mode. The value in brackets is the volume-weighted complex refractive index of two internal components in contrast to two external detected components: 30-35% sootlike material: $1.75 + 0.45i$, 65-70% ammonium-sulfatlike material: $1.53 + 0i$, see [Müller et al., 2001]

data banks which are used for the inversion of the optical data were further extended. Before, a fixed number of eight base functions was used in the inversion. The rather crude resolution caused large errors for the microphysical parameters in particular for narrow particle size distributions. First studies with an additional data bank that uses twelve base functions showed an increased accuracy. The constraint of a negligible volume concentration below particle radii of 0.1 mm caused large errors for size distribution with a significant amount of particles in this size range. This constraint was modified. Now, results for different levels of decreasing or even increasing volume concentration with decreasing particle radius can be compared. Test simulations showed that such a comparison allows an easier identification of instabilities in the inversion and an overall improvement of the accuracy of the retrieved parameters.

Until now the inversion scheme searches for that specific solution which for a given data set complies best with the constraints imposed. In the future the scheme will be up-graded toward an averaging of individual solutions for a given data set. Simulations with a comparable inversion algorithm have shown a further increase of stability ([Veselovskii et al., 2002]). This approach will also provide additional error estimates for the retrieved parameters. Simulations with this scheme with reduced data sets of three backscatter and two extinction coefficients showed that the sought mean and integral parameter can be retrieved with comparable accuracy to the one obtained from a combination of six backscatter and two extinction coefficients. The necessary accuracy of the optical data was estimated in the range of 10%-15%, which is a little lower than an anticipated accuracy around 20% for the inversion of six backscatter and two extinction coefficients. The simulations were restricted to monomodal logarithmic-normal size distributions. Simulations on the basis of bimodal distributions have not started yet.

Microphysical particle properties from 3-wavelength aerosol Raman lidar
Case studies with experimental data continued with the IfT and the IMP algorithm. Emphasis was put on a selection of highly different aerosol conditions in order to test the range of applicability

of the inversion schemes. Previous studies dealt with particles from biomass burning and particles within a continental-polluted boundary layer [Wandinger et al., 2002]. Most recent examples deal with an aerosol layer observed in the free troposphere. On the basis of backward trajectory analysis this aerosol layer most likely originated from anthropogenic pollution sources in eastern and central parts of North America. Some results will be presented below. Another example treats the case of an aerosol layer in the stratosphere. The investigations for this example are still in progress.

In this context data sets from another lidar station, i.e., at the Institute for Atmospheric Physics (IAP; Kühlungsborn, Germany) for the first time were selected for the retrieval of microphysical particle properties. This approach presents a major step toward an operational retrieval of physical particle properties from other EARLINET stations, as soon as they provide three backscatter and two extinction coefficients. The experience gained with the inversion of data from the IAP instrument, which has performance capabilities different from the instrument at IfT allowed to develop a first protocol of data quality control, which is necessary for all lidar stations before any inversion of data is performed.

In the case of the aerosol layer in the free troposphere the results of the inversion are presented by [Eixmann et al., 2002]. In contrast to the IfT data, which showed errors below 20% for each data point, the IAP data were of high quality with respect to the backscatter coefficients, but showed large errors of more than 50% in both extinction channels. In the case of the IAP data extinction spectra with highly different spectral slopes within the error bounds of 50% were chosen for the inversion. Table 3.13 shows the final results found for the microphysical parameters derived with both inversion algorithms. r_{eff} is the effective radius, v is the volume concentration, s is the surface-area concentration, n is the number concentration, m_{real} is the real part of the complex refractive index, m_{imag} its imaginary part, and ssa is the single-scattering albedo at 532 nm. The parameters describe low-absorbing ammonium-sulfate-like material.

Parameter	UPIM	IfT
$r_{eff}(\mu m)$	0.15 ± 0.02	0.15 ± 0.01
$v(\mu m^3 cm^{-3})$	1.85 ± 0.01	2.5 ± 0.6
$s(\mu m^2 cm^{-3})$	38.5 ± 5.4	49.8 ± 8.6
$n(cm^{-3})$	573 ± 283	237 ± 61
m_{real}	1.56 ± 0.03	1.40 ± 0.05
m_{imag}	0.0088 ± 0.007	0.004 ± 0.004
ssa	0.95 ± 0.03	0.97 ± 0.03

Table 3.13: Inversion results

Algorithm III (IBNANB): Retrieving parameters of atmospheric aerosols by data of multi-frequency laser sounding with using a small number of working wavelengths: Retrieving atmospheric aerosol parameters by combining measurements of multi-wavelength lidar and sun sky-scanning radiometer (Intermediate Report).
Our investigations within the frame of WP17 were oriented towards equipment opportunities, which are available for many partners in EARLINET community. We consider a problem on retrieving optical and microphysical parameters of atmospheric aerosols by data of multi-frequency laser sounding with using a small number of working wavelengths. For this case, retrieval algorithms for lidar data

are constructed by utilizing a priori information on aerosol particle parameters. Thus, the problem is to gather the said additional information and to design optimal algorithms for assessing aerosol parameters by using lidar and the additional data.
During the second year period we consider the problem on retrieving atmospheric aerosol parameters by combining measurements of a multi-wavelength lidar and a spectral radiometer like CIMEL. The development is being made commonly with Dr. Dubovik and Dr. Holben from the NASA Goddard Space Flight Center.
The methodology is based on the following concept. The results of the Sun radiometer present fairly complete characteristics of aerosol properties over the whole atmospheric layer. The objective is to construct vertical distribution of aerosols by matching both the integrated aerosol properties observed by the ground-based radiometer and a vertically variable signal of a multi-wavelength lidar. From the mathematical point of view, the algorithm follows principles of the statistically optimal inversion. The equation set includes three following subsystems:
- multi-wavelength lidar equations containing information on vertical aerosol parameter profiles;
- optical parameters integrated over coordinate z, which are considered as a constraint on aerosol optical model parameters and determined on the basis of Sun radiometer data;
- smoothness constraints on vertical aerosol parameters distributions.
The values of aerosol parameters at specified altitudes are determined as a maximum of the likelihood function written down for this equation set. The iterative algorithms for aerosol parameters retrieve are constructed that use steepest descent method. Now we are working out this algorithms to solve the posed problem.

3.17.4 Socio-Economic relevance and policy implication

Microphysical properties of aerosols describe the particle's influence on the earth's radiation budget, on clouds and on precipitation, as well as their role in chemical processes of the troposphere and stratosphere. Warnings of climate change due to ozone depletion in the atmosphere have worried us for a number of years. One reason for the ozone depletion is the chlorine (Cl) in CFCs in the stratosphere. On the other side, polar stratospheric clouds (PSCs) are believed to play an active role in precursor stages of ozone depletion in the winter-cold stratosphere by catalyzing heterogeneous chemical reactions on their surface and by redistributing HNO_3 through sedimentation. Knowledge about the aerosol surface aera concentration is necessary to model processes involving ozone chemistry. The size distribution of these cloud particles is an important parameter for quantifying these mechanisms, because it relates the total surface to the total mass.
The investigations to the determination of microphysical parameters from a 3-wavelength aerosol Raman lidar (could be a standard lidar in future) are to our knowledge the first ones, therefore there will be significant interest in the science community to use these methods, for the improvement of global/regional atmospheric or of climate prediction models. Scientific publications and conference presentations, resulting from WP17, will give the opportunity to the science community to address the mechanisms of local aerosol formation, to study the trans-boundary transport processes of air pollution over Europe and to study the impact of aerosol loads in the earth's radiation budget and their link to Global Change. Finally, the investigations could be proposed for an air pollution abatement strategy in Europe, in compliance with the EU air pollution abatement/Climate Change policy.

3.17.5 Plan and Objectives for the next period

Important activities, in full accordance with the contract, were implemented right from the start of the project.
For the next period the groups UPIM and IfT will continue the investigations with respect to a minimum data set. This is planed especially by examinations with different noisy data. Further investigations are necessary concerning the determination of the imaginary part of the refractive index which is very sensitive in the inversion process.
Secondly, investigations towards the development of a two-dimensional inversion algorithm are going on.
Thirdly, further investigations will be done in the next time to continue the influence of spheroids and additionally to examine the influence of inhomogeneous particles on the inversion process.
Finally, the values of aerosol parameters at specified altitudes are determined as a maximum of the likelihood function by the IPNANB algorithms. The iterative algorithms for aerosol parameters retrieve are constructed that use steepest descent method. Now IPNANB is working out this algorithms to solve the posed problem.

3.18 General project assessment

As outlined in the previous sections the work within the individual work packages has made good progress and matches the expectations as laid down in the statement of work in the beginning of the project. As usual in a scientific project some adjustments had to be made, mainly leading to some extra work. The consortium is very happy that all the participating institutions have provided substantial extra resources to overcome the problems associated with this extra work. This evidences that high priority is given to the project in the institutions and that overall progress is considered sufficient, to say the least.

The main result of the project is the most comprehensive and systematically collected data base on the vertical distribution of aerosol that is presently available, and it is continuously growing. Apart from the individual studies that have been initialized on the basis of the growing data set, an important achievement of the project is the establishment of a real network with fairly homogeneous operation and evaluation procedures and with comparable and well assessed data quality, despite of the different starting conditions for the participating groups. It also has to be emphasized that very good cooperation has been achieved. It is now standard that several groups perform coordinated measurements for special purposes, and that data from several groups are used for joint analyses. Thus a new community has been formed that is truly European, spanning a major part of the continent.

The joint systematic effort has led to a clear advantage over attempts that have been made in other parts of the world in the same field of science. This is also reflected in the fact that EARLINET has received several requests for cooperation. This extends from formal requests for joining the project in the frame of the cooperation with the Newly Associated States of the EU, which hopefully will be approved, to more or less tightly coupled groups forming at the south rim of the Mediterranean, Latin America, and the former Soviet Union. Apparently the EARLINET approach has convinced at least major parts of the lidar community that the methods chosen for this project are addressing the problems appropriately, and the the organizational form is adequate. The group hopes that these planned connections can be established so that a global network for aerosol profiling is approached.

3.18.1 Plan for the next period

The last year of the current project will see continuous efforts to increase the data base by both regularly scheduled and special measurements. The routine and increased experience that has been achieved for all groups now will help to increase the number of measurements in parallel to the data analysis. Particular emphasis will be put on data interpretation in terms of, e.g., the quantification of the aerosol load in different areas, identification of source regions, studies of long range transport, changes in aerosol load during the overpass over Europe, and Saharan dust impact in the Mediterranean and other European regions.

In case that the extension of EARLINET to NAS-countries will be approved, three more stations will become operational which will follow the same measurement and evaluation procedures. This would enhance the value of EARLINET data in particular for the Eastern and South-Eastern regions, which are mostly downstrem from the industrialized areas of Europe, but are also close to probably important source regions in Eastern Europe. In addition a modelling group would be incorporated for further enhancing the analysis capabilities for Saharan dust outbreaks and possibly serving to generalize the results.

Bibliography

[Ansmann et al., 1997] Ansmann, A., Mattis, I., Wandinger, U., Wagner, F., Reichardt, J., and Deshler, T. (1997). Evolution of the Pinatubo aerosol: Raman lidar observations of particle optical depth, effective radius, mass, and surface area over central Europe at 53.4°N. *Appl. Opt.*, 31:7113–7131.

[Bais et al., 2002] Bais, A., Kazantzidis, A., Kazadzis, S., Balis, D., Zerefos, C., and Meleti, C. (2002). Effects of aerosol optical depth and single scattering albedo on surface UV irradiance. *SPIE proceedings*.

[Balis et al., 2002] Balis, D., Zerefos, C., Kourtidis, K., Bais, A., Hofzumahaus, A., Kraus, A., Schmitt, R., Blumthaler, M., and Gobbi, G. (2002). Measurements and modeling of photolysis rates during the PAUR II campaign. *J. of Geophys. Res.*, page in press.

[D.Hofman et al., 1985] D.Hofman, Rosen, J., and Grindel, W. (1985). Delayed production of sulfuric acid condensation nuclei in the polar stratosphere from El Chichon volcanic vapors. *J. of Geoph. Res.*, 90 D1:2341–2354.

[Eixmann et al., 2002] Eixmann, R., Böckmann, C., Fay, B., Matthias, V., Mattis, I., Müller, D., Kreipl, S., Schneider, J., and Stohl, A. (2002). Tropospheric aerosol layers after a cold front passage in January 2000 as observed at several stations of the German Lidar Network. *Atmos. Res.*, in press.

[Fernald, 1984] Fernald, F. G. (1984). Analysis of Atmospheric Lidar Observations: Some Comments. *Appl. Opt.*, 23:652–653.

[Ingold et al., 2001] Ingold, T., Mätzler, C., Kämpfer, N., and Heimo, A. (2001). Aerosol optical depth measurements by means of a Sun photometer network in Switzerland. *J. of Geoph. Res.*, 106:27537–27554.

[Jäger et al., 1995] Jäger, H., Uchino, O., Nagai, T., Fujimoto, T., Freudenthaler, V., and Homburg, F. (1995). Ground based remote sensing of the decay of the Pinatubo eruption cloud at three northern hemisphere sites. *Geoph. Res. Lett.*, 22:607–610.

[Kazantzidis et al., 2001] Kazantzidis, A., Balis, D., Bais, A., Kazadzis, S., Galani, E., Kosmidis, E., and Blumthaler, M. (2001). Comparison of model calculations with spectral UV mesurements during the SUSPEN campaign: the effect of aerosols. *J. Atm. Sciences*, 58:1529–1539.

[Kent and Hansen, 1998] Kent, G. and Hansen, G. (1998). Multiwavelength lidar observations of the decay phase of the stratospheric aerosol layer produced by the eruption of Mount Pinatubo in June 1991. *Appl. Opt.*, 37:3861–3872.

[Klett, 1981] Klett, J. D. (1981). Stable analytical inversion solution for processing lidar returns. *Appl. Opt.*, 20:211–220.

[Klett, 1985] Klett, J. D. (1985). Lidar inversion with variable backscatter/extinction ratios. *Appl. Opt.*, 24:1638–1643.

[Matthias et al., 2002] Matthias, V., Böckmann, C., Freudenthaler, V., Pappalardo, G., Bösenberg, J., Amiridis, V., Amodeo, A., Ansmann, A., Balis, D., Boselli, A., Chaykovski, A., Chourdakis, G., Comeron, A., Delaval, A., Tomasi, F. D., Eixmann, R., Frioud, M., Hågård, A., Iarlori, M., Komguem, L., Kreipl, S., Larchevêque, G., Matthey, R., Mattis, I., Papayannis, A., Persson, R., Rizi, V., Rocadenbosch, F., Rodriguez, J., Schneider, J., Schumacher, R., Shcherbakov, V., Simeonov, V., Wandinger, U., Wang, X., and Wiegner, M. (2002). Lidar intercomparison on algorithm and system level in the frame of EARLINET. MPI-Report in press, Max-Planck-Institut für Meteorologie, Hamburg.

[McCormick et al., 1995] McCormick, M. P., Thomason, M. L., and Trepte, C. (1995). Atmospheric effects of the Mt. Pinatubo eruption. *Nature*, 373:399–403.

[Müller et al., 2002] Müller, D., Ansman, A., Wagner, F., Franke, K., and Althausen, D. (2002). European Pollution Outbreaks During ACE 2: Microphysical Particle Properties and Single Scattering Albedo Inferred From Multiwavelength Lidar Observations. *J. Geophys. Res.*, in press.

[Müller et al., 2000] Müller, D., Wagner, F., Wandinger, U., and Ansmann, A. (2000). Microphysical particle parameters from extinction and backscatter lidar data by inversion with regularization: Experiment. *Appl. Opt.*, 39:1879–1892.

[Müller et al., 2001] Müller, D., Wandinger, U., Althausen, D., and Fiebig, M. (2001). Comprehensive particle characterization from three-wavelength Raman-lidar observations: case study. *Appl. Opt.*, 40:4863–4869.

[Rosen et al., 1994] Rosen, J., Kjoome, N., McKenzie, R., and J.Liley (1994). Decay of Mount Pinatubo aerosol at midlatitudes in the northern and southern hemispheres. *J. of Geoph. Res.*, 99:25733–25739.

[Veselovskii et al., 2002] Veselovskii, I., Kolgotin, A., Griaznov, V., Müller, D., Wandinger, U., and Whiteman, D. (2002). Inversion with regularization for the retrieval of tropospheric aerosol parameters from multiwavelength lidar sounding. *Appl. Opt.*, in press.

[Wandinger et al., 2002] Wandinger, U., Müller, D., Böckmann, C., Althausen, D., Matthias, V., Bösenberg, J., Weiß, V., Fiebig, M., Wendisch, M., Stohl, A., and Ansmann, A. (2002). Characterization of optical and microphysical particle properties from multiwavelength lidar and airborne in situ measurements in biomass-burning and industrial-pollution aerosols. *J. Geophys. Res.*, in press.

[Zuev. et al., 2001] Zuev., V. V., Burlakov, V., El'nikov, A., Ivamov, A., Chaikovski, A., and Scherbakov, V. (2001). Processes of long-term relaxation of stratospheric aerosol layer in northern hemisphere midlatitudes after powerful volcanic eruption. *Atm. Env.*, 35:5059–5066.